pH-Sensors Regulating Transcription, Metabolism, and Cancer Cell Biology

by
Kyle Kisor

DISSERTATION
Submitted in partial satisfaction of the requirements for degree of
DOCTOR OF PHILOSOPHY

in

Biomedical Sciences

in the

GRADUATE DIVISION
of the
UNIVERSITY OF CALIFORNIA, SAN FRANCISCO

Approved:

DocuSigned by:
Jeffrey Bush
367536768C42487...

Jeffrey Bush

Chair

DocuSigned by:
Diane Barber

Diane Barber

DocuSigned by:
Matthew Jacobson

Matthew Jacobson

DocuSigned by:
Todd Nystul
B55FB5CFA606452...

Todd Nystul

Committee Members

To my Uncle Earl and Aunt Marie, whose memories were my inspiration in choosing scientific research and motivate me to persevere through all the challenges.

To my grandparents, Helen Martinez, Nila Kisor, and Earl Kisor, whose love and encouragement are everlasting pillars of my life.

To my parents, Mercedes Kisor and Phillip Kisor, whose endless selflessness, support, and love have made everything possible.

Acknowledgments

I often describe completing a PhD, and science as a whole for that matter, as a lot of failure with just enough success sprinkled in to keep you going. However, making it through the inevitable rollercoaster of highs and lows that happen during a PhD would have been an even greater challenge without all my mentors, colleagues, friends, and family. To everyone that cheered me up after a bad day or celebrated with me in my successes, I could not have done any of this without you. I am truly grateful for all your support, kindness, and love. From the bottom of my heart, thank you all.

I first want to thank my incredible and brilliant mentor, Dr. Diane Barber. I will never forget the first time I met Diane at a seminar she gave at UC Irvine while I was still an undergraduate there. I remember thinking how unique and exciting the research in her lab was, and never did I think I could end up there. While at the time I did not realize I was capable of performing such exciting research, our conversation after her seminar gave me the confidence to apply to the UCSF Biomedical Sciences program. Even after interviews and throughout the process of deciding where to accept, Diane was the only faculty member at any school that personally called me to congratulate me and ease any concerns I had about coming to UCSF. I could immediately tell that she truly cared about her trainees and colleagues and it was the deciding factor for me coming to UCSF and I am forever grateful for it. While it was clear from the beginning I wanted to work with Diane, I have learned so much from her over the last six years. The invaluable lessons Diane has taught me have been transformative in how I approach science while also being remarkably applicable to life. First, to be fearless. Diane has always encouraged me to not be paralyzed by fear of failure as an excuse for not trying something new. There were many times during my PhD I had to dive right into something far out of comfort zone to move my project forward. Diane was always there to encourage me to try and if I failed, she was always there with kindness to pick me back up. Second, “but what is the question?”. As any Barber Lab member knows, “but what is the question?” is one of Diane’s many mantras. It is

often easy to get excited about new directions and lose sight of what is important, but Diane was always there with that one simple phrase to reel me back in. The thought of *the question* and the perspective of what is important will always stick with me. Third, and above all else, to be kind. Diane would start almost every one-on-one meeting with me by connecting on a personal level. Whether it was asking how I am doing, how my family is, or discussing our shared love of sports, she always knew how to best put me at ease. Her profound kindness during my PhD was essential to my experience and I hope to provide that for everyone in my professional and personal life. I am forever grateful to Dr. Diane Barber for being an outstanding scientist, mentor, and person and for guiding me through the most challenging times of my life.

I also would also like to thank all the faculty mentors I have had the pleasure of knowing and learning from over the years. First, to my thesis committee, Dr. Jeffrey Bush, Dr. Matthew Jacobson, and Dr. Todd Nystul for their enthusiastic support and direction during my PhD. I am extremely grateful for their time and advice, which guided much of the work during my thesis. I would also like to acknowledge the other faculty members who helped shape me as a researcher, including Dr. Torsten Wittman, Dr. Mathew Kutys, and Dr. Licia Selleri. And, I would like to thank my undergraduate mentor, Dr. Peter Kaiser, for his support early in my scientific career which was paramount to getting me to UCSF.

I would like to give a special thanks to everyone who I have worked with in the Barber Lab who has made my experience so overwhelmingly positive. Each Barber Lab member was pivotal in my growth as a scientist and a person, including Dr. Bradley Webb, Dr. Katharine White, Dr. Francesca Aloisio, Dr. Rae Sesanto, Dr. Yi Liu, Dr. Nathaniel Meyer, Dr. Burinrutt Thanasuwat, Dr. Christos Kougentakis, Dr. Sonia Infante, Joy Gittins, Cambria Chou-Freed, Harnoor Virk, Connie Phuong, and Annie Kingsland.

In addition to the Barber Lab, I have felt supported by the entire HSW6 community and all who have made coming to lab everyday so pleasant, including Dr. Jeffrey Van Haren, Dr. Rabab Caharfeddine, Dr. Alessandro Dema, Dr. Kevin Wilkins, Dr. Mageshi Kamaraj, Tiffany

Criger, Tania Singh, Kyle Jacobs, Lakyn Mayo, and Giulia Viola. I would also like to send a heartfelt thank you to those at UCSF who contributed to making UCSF a great place to be a graduate student beyond my everyday colleagues and mentors. I would especially like to thank Demian Sainz, Meredith Miner, Ned Molyneaux, Lisa Magaral, Dr. Mark Ansel, Dr. Anita Sil, Dr. Adrian Erlebacher and the entire BMS staff. I would also like to thank the UCSF Graduate Division and the Department of Cell and Tissue Biology. Lastly, thank you to the NIH F31 fellowship and NSF for funding both me and this work.

I would also like to sincerely thank every friend I have made during my time in San Francisco. I will always cherish the memories we made both at UCSF and outside the lab. I would like to thank my BMS friends Jennifer Umhoefer, Rachel Nakagawa, David Shin, and Dr. Irene Chen. I am so grateful for all your support and friendship over the years. I would especially like to thank Dr. Francesca Aloisio and Marcus Isaksson for being two of my closest friends for the entirety of my time in San Francisco, and for truly being there for me when I needed them most. Lastly, it is difficult to put into words how special, meaningful, and important my friendship with Dr. Kevin Wilkins has been. We came in together in 2017 as BMS cohort members and roommates and have achieved the rare feat of staying roommates for the entirety of our times here. We have both grown and changed together so much over the years, but the one constant has been you being my best friend. You once said I was the brother you never had, and I feel the same way. I am so grateful to have you in my life.

One of the most difficult parts of my PhD was being so far from the people I care about back home. Despite the physical distance, I have not only been able to maintain friendships but also cultivate new ones. Dr. Michael Emami, my best friend since grade school has never failed to make me laugh, share an adventure, or be there for me through everything. You also helped me rekindle my friendship with Dr. Jessica Navarez-Mejia and for all of this I am deeply grateful for you both. I would also like to thank my friend Charlie Luber for his 15+ years of friendship, positivity, and support. I will never forget on our drive back from his bachelor party he

encouraged me with his unwavering optimism to push through my lowest of lows during my PhD, and my biggest success followed the next week. I want to thank Charlie for being an incredible friend and for introducing me to Maggie Luber, a new friendship that I value sincerely. I would also like to thank Dane Nielsen for becoming a genuine friend and sharing such fun times with me at home, in San Francisco, and on our various ski trips. To all of you, I am so very grateful for everything, thank you.

While I enjoyed my time in San Francisco prior to 2021, it does not compare to the times since meeting Jane Fountain. Jane is without a doubt the most loving, supportive, smart, funny, and beautiful person I have ever met. I am so thankful to her for being so understanding of all the late nights in the lab, the times I could not make it out, and her being there for me to vent when I needed it most. In addition to all the fun we had together on our date nights, vacations, and just a simple night staying in, I am also profoundly grateful to everyone I have met through her. I would like to thank you for introducing me to friends Lena Jensen, Jordan Gentry, Daniel Krueger, Mia Eikani, and Hayley Miller who made San Francisco so much fun. I also want to thank Jane for introducing me to the entire Fountain family. I want to especially thank Jane's parents, Linda and Larry Fountain for welcoming me so openly to their home and including me in all of the special times in their family's lives these last few years. There were many times they both provided me with a sense of home when I was most homesick, thank you both so very much for everything. I also want to thank Jane's sisters and brothers-in-laws Annie Hawkinson, Kate Fountain, Cole Hawkinson, and Adam Lamar for being so kind and welcoming. Lastly, I would like to thank Jane for the memories we built together in San Francisco that I will cherish forever. I could not have asked for a more perfect person than Jane to enrich my life in every single way. I cannot wait to see what is next for us, I love you.

I want to also thank my extended family, who have always been there for me my whole life and have played a large role in shaping who I am. I am forever grateful and would like to thank every aunt, uncle, and cousin from both the Martinez and Kisor sides of my family for

loving and supporting me in everything I do. I especially want to acknowledge the memories of my Uncle Earl and Aunt Marie. Losing both to cancer at a young age was a major catalyst in my pursuit of understanding disease to help those similarly affected, deciding my career path. In my toughest times, remembering they are the reason I started this journey helped motivate me to push on. I want to thank them for the time we did share together. I love them and miss them greatly.

I also want to thank my Nana, Grandma, and Grandpa for being the most loving grandparents I could ever ask for. I am exceptionally grateful to Nana for immigrating to the United States from Colombia to give the future generations of our family a better life. Without the sacrifices Nana has made for the last 60 years, I would not be where I am today. I also want to thank Grandma and Grandpa for being my second set of parents and for the unconditional love they show me every day. Some of my fondest memories include all the times I was able to visit them at home and hearing Grandpa make Grandma laugh in her most iconic way. Their enduring love and support for each other and all of my family inspires me to do the same. I am incredibly fortunate to have all of them in my life, and I love them endlessly.

I also want to sincerely thank my first best friends, my two amazing sisters Helena and Natalie. We have grown, laughed, and loved each other since they were born and I am so grateful for the relationship we have today. I want to thank them for all the love and support they have always shown me no matter what. I am also profoundly thankful for all the times they both visited me and the time we spent together when I came home; it was much needed. I am so proud of who you have both become, and I am honored to be your brother. I love you.

Most of all, I want to thank my Mom and Dad for their love and support in everything I have ever done. Leaving home to pursue my PhD was one of the hardest decisions I had to make, and they both wholeheartedly supported my decision. My parents have also been my greatest role models in how to be loving, supportive, selfless, and hardworking, which I am so grateful for. Thank you for always putting Helena, Natalie, and I first, and for the sacrifices you

both made to make us feel happy and loved. Thank you for instilling in me the priority of education over everything else, even at a young age. I also want to thank you for teaching me my faith, and for the years of prayers you sent on my behalf that were much needed to get through my PhD. Nobody was more excited about my successes or comforting in my failures than either of you, both of which I am forever grateful. I am so lucky to be your son. I love you both.

Contributions to this work

The work presented in this thesis was performed under the supervision of Diane L. Barber, PhD. Additional guidance and support were provided by my thesis committee members Jeffrey Bush, PhD, Matthew Jacobson, PhD, and Todd Nystul, PhD.

Chapter 2 is adopted from a manuscript being submitted for publication:

Kisor, K., Garrido Ruiz, D., Jacobson, M.P. and Barber, D.L. (2024) pH-dynamics regulates transcription factor DNA binding selectivity. *In preparation*.

Chapter 3 was performed as a collaborative effort with Bradly Webb, PhD, a former postdoctoral fellow in the Barber laboratory who is currently an Assistant Professor at West Virginia University.

Chapter 4 was performed as a collaborative effort with Dr. Emil Alexov's group at Clemson University with experimental contributions by Connie Phuong in the Barber laboratory.

pH-Sensors Regulating Transcription, Metabolism, and Cancer Cell Biology

Kyle P. Kisor

Abstract

Dynamic changes in intracellular pH (pHi) regulate myriad cell behaviors, including proliferation, cell-substrate adhesion, cell migration, dysplasia and tumorigenesis, and stem cell differentiation for lineage specification. Previous work revealed how the reversible protonation of endogenous pH sensitive proteins, collectively termed “pH sensors,” is a mechanism whereby pHi dynamics regulates these cell behaviors. Often, these proteins contain a structurally or functionally critical histidine that can titrate between protonated and unprotonated within the narrow physiological range depending on the protein landscape. This in turn can affect protein electrostatics both in cis and with binding partners. My thesis research focused on three predicted pH sensors, transcription factors regulating gene expression, the muscle isoform of the enzyme phosphofructokinase (PFKM) regulating glycolysis, and a charge changing mutant p53-R273H promoting cancer progression. For transcription factors, we identified 65 in distinct families, including FOX, SOX and MITF/Myc that contain a conserved histidine in their DNA binding domain (DBD) that in available structures forms a direct hydrogen bond with nucleotides. Focusing on FOX family transcription factors, we identified pH-regulated binding affinities for a canonical FkhP binding motif sequence with higher affinity at pH 7.0 compared with pH 7.5 for FOXC2, FOXM1, and FOXN1. For FOXC2, we determined greater activity at lower pHi in cells and confirmed that pH-dependent binding and activity is mediated by a conserved histidine (His122) in the DBD. Additionally, using an unbiased *in vitro* screen (SELEX) we identified differences in binding DNA motif preferences between pH 7 and 7.8. For PFKM, we determined that His242 is required but not sufficient for a pH-sensing mechanism of allosteric relief of ATP inhibition of enzyme activity. For p53-R273H, we screened bioactive compounds from three commercially available libraries to identify two compounds that restore DNA binding, which we previously showed is decreased at the higher pHi of cancer cells.

Collectively, these data reveal how pH broadly regulates protein electrostatics at titratable histidine residues to regulate diverse behaviors including gene expression, metabolism, and cancer. Moreover, our current findings establish a previously unreported mode of regulation for transcription factors across diverse families and confirm the feasibility of targeting charge changing mutations in disease by using small molecules to restore protein function.

TABLE OF CONTENTS

List of Figures

List of Tables

CHAPTER 1: INTRODUCTION

Intracellular pH (pHi) dynamics is increasingly being recognized as a critical regulatory signal for myriad cell behaviors, including cell proliferation, migration, and differentiation. Although changes in pHi were previously viewed as a mechanism to maintain homeostasis, we now know that changes in pHi occur and are necessary for normal cell processes such as cell cycle progression for proliferation (Flinck et al., 2018a; Putney & Barber, 2003; Spear & White, 2023), actin filament and cell-substrate adhesion remodeling for directed cell migration (Choi et al., 2013; Clement et al., 2013; Denker & Barber, 2002; Frantz et al., 2008; Martin et al., 2011; Srivastava et al., 2008), and stem cell differentiation and lineage specification (Benitez et al., 2019; Liu et al., 2023; Ulmschneider et al., 2016). Moreover, it is now established that pHi dynamics is dysregulated in human diseases, including cancer (Swietach et al., 2023; Webb et al., 2011; White, Grillo-hill, et al., 2017), diabetes (Gillies et al., 2019; Hayata et al., 2014), and neurodegeneration (Harguindey et al., 2017; Majdi et al., 2016). The molecular mechanisms by which pHi dynamics regulates normal and pathological cell behaviors, however, remains poorly understood and is a focus of my thesis research.

In contrast to a limited understanding of how pHi dynamics regulates cell behaviors, the upstream signals that change pHi are more resolved (Casey et al., 2010; Putney et al., 2002) **(Fig. 1).** Extracellular cues that change pHi include growth factors activating receptor tyrosine kinases, hormones activating G-protein coupled receptors, and extracellular matrix ligands activating integrin receptors. Changes in mechanical force and osmotic balance, most notably hypertonic conditions, as well as activated oncogenes also change pHi. These extracellular and intracellular cues mostly act through canonical signaling pathways to change the activity of Solute Carrier (SLC) plasma membrane ion transport proteins, including acid extruders Na-H exchanger 1 (NHE1), Na-HCO3 exchanger (NBC), and Na-dependent Cl-HCO3 exchanger (NDBC), and acid loaders of the Cl-HCO3 anion exchanger family (AE1-3) as well as V-ATPase proton pumps. Changes in the activity of acid extruders and loaders is predominantly, although not exclusively, regulated by phosphorylation of serine or threonine residues in intracellular

domains. For example, NHE1 is a substrate for several serine-threonine kinases, including Akt (Meima et al., 2009), the Sterile 20 kinase MAP4K4 (Yan et al., 2001), and the p160-Rho-associated kinase (ROCK) (Tominaga et al., 1998), with phosphorylation increasing H+ efflux by NHE1 and increasing pHi.

To better understand how pHi dynamics regulates cell behaviors, recent work bridges protein electrostatics and cell biology with a focus on the reversible protonation state of endogenous pH sensitive proteins termed “pH sensors” (Schönichen et al., 2013a). Dynamic protonation/deprotonation often occurs at a histidine residue, which is the only amino acid with a near neutral pKa of 6.5 in solution. However, the pKa of histidine, aspartic acid, glutamic acid and buried lysines can be upshifted or downshifted depending on the protein landscape to enable titration within the cellular pH range of 7.0-7.8 (Isom et al., 2011; Karp et al., 2010; Srivastava et al., 2008). These changes in amino acid charge can rapidly alter protein structure and function, including activity, ligand binding, and stability (Schönichen et al., 2013b). For example, focal adhesion kinase (FAK), a key regulator of focal adhesions, is a pH-sensor with increased activity at higher pHi (Choi et al., 2013). In quiescent cells at pHi ~ 7.3-7.4, FAK is in an inactive “closed” conformation in part because of interdomain electrostatic interactions mediated in part by a protonated His58. During cell-substrate attachment, pHi increases to ~ 7.7 at focal adhesions, FAK-H58 is deprotonated to release an *in cis* autoinhibited conformation, and a conformational change exposes an autophosphorylation Tyr397 site necessary for kinase activity and efficient cell spreading (Choi et al., 2013). The design principles of additional pH-regulated endogenous proteins have been identified for cell behaviors driven by pH-dynamics, including talin binding of actin filaments for focal adhesion remodeling (Srivastava et al., 2008), activity of the actin filament regulatory protein cofilin for cell migration (Frantz et al., 2008), and β-catenin stability for WNT signaling (White et al., 2018). To further understand molecular mechanisms whereby pHi dynamics regulates cell behaviors, my thesis research included three projects. First, and my major focus, was identifying a previously unrecognized mechanism of pH

sensing by transcription factors for DNA binding selectivity in the context of how pHi dynamics can regulate gene expression. Second, I identified a molecular mechanism for pH sensing by the muscle isoform of the glycolytic enzyme phosphofructokinase-1 (PFKM) that resolves how pHi dynamics regulates PFKM inhibition by ATP. Third, I built on previous findings that a recurrent Arg273His mutation in the tumor suppressor protein p53 confers a gain of pH-sensing at the higher pHi typically seen in cancer cells (White, Ruiz, et al., 2017), and identified small molecules that target the p53-R273H site to modulate pH sensing. In addition to these 3 projects, I also contributed data and co-authored two publications: one on how pHi regulates oxidative phosphorylation and mitochondrial morphology (Manoli et al., 2021) and a review on intracellular pH dynamics and charge-changing somatic mutations in cancer (White et al., 2019). The abstracts of these publications are included in my thesis after my Discussion for Chapter 4 on small molecules regulating DNA binding by p53-R273H. Findings from my thesis research provide new insights on how pHi dynamics regulate the electrostatics of pH-sensitive proteins to regulate cell behaviors and mechanisms that can be targeted in disease.

Figures

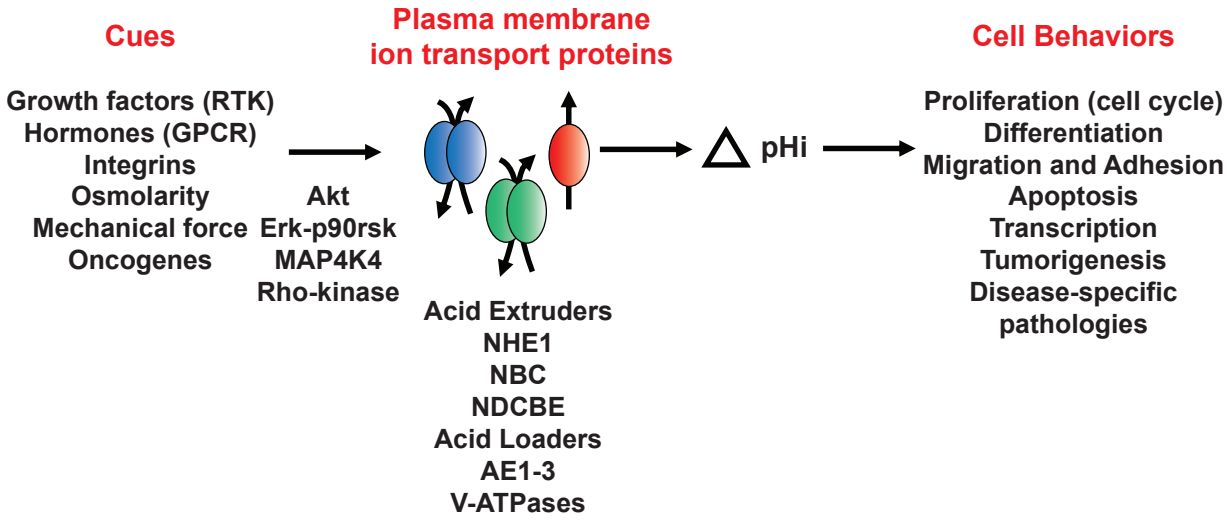

Figure 1.1. pHi regulates cell behaviors.
Changes in intracellular pH (ΔpHi) can be regulated by the indicated cues and serine-threonine kinases to modify activity of plasma membrane ion transport proteins, including acid extruders, acid loaders, and V-ATPases. Also shown are some of the cell behaviors known to be regulated by ΔpHi.

CHAPTER 2: pH-DYNAMICS REGULATES TRANSCRIPTION FACTOR DNA BINDING SELECTIVITY

Introduction

Changes in intracellular or cytosolic pH (pHi) were previously viewed as a compensatory mechanism to maintain homeostasis. It is now established, however, that changes in pHi occur during and are necessary for myriad normal cell processes such as cell cycle progression for proliferation (Flinck et al., 2018a; Putney & Barber, 2003; Spear & White, 2023), actin filament and cell-substrate adhesion remodeling for directed cell migration (Choi et al., 2013; Clement et al., 2013; Denker & Barber, 2002; Frantz et al., 2008; Martin et al., 2011; Srivastava et al., 2008), and stem cell differentiation and lineage specification (Benitez et al., 2019; Liu et al., 2023; Nikolovska et al., 2022; Oginuma et al., 2020; Ulmschneider et al., 2016) Moreover, pHi dynamics is dysregulated in human diseases, including cancer (Swietach et al., 2023; Webb et al., 2011; White, Grillo-hill, et al., 2017), diabetes (Gillies et al., 2019; Hayata et al., 2014), and neurodegeneration (Harguindey et al., 2017; Majdi et al., 2016). The molecular mechanisms for how pHi dynamics regulates normal and pathological cell behaviors, however, remain understudied. We report testing a new idea to understand how pHi dynamics can directly regulate gene expression.

To better understand how pHi dynamics regulates cell behaviors, recent work bridges protein electrostatics and cell biology with a focus on the reversible protonation state of endogenous pH sensitive proteins termed “pH sensors” (Schönichen et al., 2013a; Sun et al., 2022). Dynamic protonation and deprotonation of titratable amino acids in response to changes in pHi can rapidly alter protein structure and function, including activity (Choi et al., 2013; Kazyken et al., 2023; Morales Rodríguez et al., 2023; Webb et al., 2016) and ligand binding (Frantz et al., 2008; Johnston et al., 2019; Lu et al., 2023; Onufriev & Alexov, 2013; Srivastava et al., 2008) as well as stability (Malevanets et al., 2017; Wang et al., 2019; White et al., 2018) and aggregation (Westermark et al., 2011; Xiang et al., 2015).

Many cell behaviors regulated by pHi dynamics include changes in gene expression (Putney & Barber, 2004; Spear & White, 2023; Ulmschneider et al., 2016), and although nuclear

and cytosolic pH are similar, how pHi can regulate transcription factor target gene specificity remains understudied and unclear. In addressing this question, we find that at least 65 transcription factors in diverse families, including FOX, SOX, and Myc/MITF, have a conserved histidine in their DNA-binding domain (DBD), which in available crystal structures forms a hydrogen bond with nucleotides. Additionally, beyond a conserved histidine in multiple families, histidine occurs in DNA binding domains of transcription factors more frequently than predicted (Ahmad & Sarai, 2004; Baker & Grant, 2007). With the ability of histidine to titrate within the narrow pHi range of 7.0-7.8, we predicted that protonation and deprotonation of a conserved DNA-binding histidine in transcription factors could change affinities for binding different nucleotides; for example, when protonated at a lower pHi being a hydrogen bond donor for thymine and when deprotonated at a higher pHi being a hydrogen bond acceptor for adenine. We confirmed this prediction by showing pH regulated DNA binding by three FOX family transcription factors, FOXC2, FOXM1, and FOXN1. Further, for FOXC2 we show pHi regulated activity in cells as well as the critical importance of a conserved histidine, His122, for pH-sensitive DNA binding. Our findings fill gaps in our current understanding not only for how pHi dynamics can regulate gene expression and target gene selectivity but also for how transcription factors with highly similar DNA-binding domains can regulate diverse genes and functions reiteratively for developmental programs that include changes in pHi (Liu et al., 2023; Oginuma et al., 2020).

Results

Transcription factors contain predicted pH-sensors in the DBD

We previously described the design principles of several pH-sensors that are generally regulated by titration of a histidine within the cellular pH range of 7.0 to 7.8 (Choi et al., 2013; Frantz et al., 2007, 2008; Srivastava et al., 2008; Webb et al., 2016; White et al., 2018). In asking whether some transcription factors might function as pH sensors, we searched for conserved histidine residues important for DNA binding across transcription factor families. We first performed sequence alignments of all known major transcription factor family members expressed in humans. We found that all FOX family members contain a histidine residue in a highly conserved N(S/A)IRH motif within Helix 3 of the DBD (**Fig. 2.1A**). In all available crystal structures of FOX transcription factors in complex with DNA, the conserved histidine aligns in the major groove of DNA and forms a hydrogen bond with nucleotides. Our structural overlay shows the side chain of conserved histidine residues is also spatially conserved (**Fig. 2.1B**). We also noted that all members of the SOX transcription factor family except Sry and SOX30 (**Fig. 2.2A**) and all members of the MITF/Myc/Max family except AP4 (**Fig. 2.2B)** contain a conserved histidine in the DBD, which in available structures in complex with DNA forms a hydrogen bond with nucleotides. Additionally, a hydrogen bond between a histidine and DNA nucleotides is reported for the ETS transcription factor ETV6 (**Fig. 2.2C**) (Vo et al., 2017), the STAT transcription factor STAT6 (**Fig. 2.2D**) (J. Li et al., 2016), and ARNT, the DNA-binding subunit of the HIF1 complex (**Fig. 2.2E**) (Schulte et al., 2017; Wu et al., 2015). Hence, at least 65 transcription factors in diverse families contain a histidine in the DBD that in available structures forms a hydrogen bond with nucleotides.

Given the conservation of a histidine in the DBD of many transcription factors with direct hydrogen bonds to nucleotides, coupled with the well-established ability of histidine to titrate within the cellular pH range, we hypothesized that a pH-dependent titration of the conserved histidine may regulate DNA binding specificity through hydrogen bonding preferences with

nucleotides. For example, a protonated histidine may serve as hydrogen bond donor for a hydrogen bond accepting thymine. However, when deprotonated at higher pH a deprotonated histidine may serve as a hydrogen bond acceptor for an adenine donor (**Fig. 2.1C**). Guanine and cytosine can serve as either a hydrogen bond donor or acceptor depending on the orientation of the nucleotide relative to the protein binding residue. We first tested these predictions *in silico* in collaboration with Diego Garrido Ruiz in the Matthew Jacobson lab at UCSF by using constant pH molecular dynamic simulations (CpHMD) with FOXC2 because it is the only FOX family member with a crystal structure shown in complex with DNA that contains a single histidine (His122) in the DBD. We found that when FOXC2 is bound to the canonical Forkhead primary (FkhP) sequence (GTAAACA), His122 is predicted to be doubly protonated in 91% of the simulations. However, when singularly protonated at the delta or epsilon nitrogen, FOXC2 is predicted to be in the bound state in only 0.01% and 0.08% of the simulations, respectively. In contrast, when FOXC2 is in the unbound state His122 is predicted to be singularly protonated at the delta or epsilon nitrogen in 81% and 14% of the simulation while only doubly protonated in 5% (**Fig. 2.1D**). Together, these data suggest that FOXC2-H122 is a putative pH-sensing residue predicted to bind the canonical FkhP sequence when protonated at low pH.

FOX family transcription factors have high affinity for FkhP at low pH

We next asked whether binding of FOX family proteins to the canonical FkhP sequence has higher affinity at low pH as predicted by our CpHMD simulations. We first tested this prediction for FOXC2 (**Fig. 2.3A**), using fluorescence anisotropy with a purified recombinant DBD expressed as a GST fusion protein and a 5'6FAM labeled FkhP sequence. A pH titration of FOXC2 at 2.3 μM reveals that the overall affinity for the FkhP sequence decreases linearly within the cellular range between pH 7.0 to 7.6 with no observable change in binding above pH 7.8 at this protein concentration (**Fig. 2.3B**). We next determined the association constant (K_A)

for FOXC2 to the FkhP sequence at pH 7 and 7.5 and found that the binding affinity of FOXC2 for the FkhP sequence is significantly greater at pH 7 (K_A of 0.75 ± 0.12 μM) compared with 7.5 (0.18 ± 0.02 μM) (**Fig. 2.3C,F**). We also asked whether other FOX family members have higher affinity binding to the FkhP sequence at lower pH. Using GST fusions of DBD sequences, we confirmed higher affinity binding for FOXM1 at pH 7 (K_A 1.1 ± 0.11 μM) compared with pH 7.5 (0.54 ± 0.08 μM) (**Fig. 2.3D,F**) and for FOXN1 at pH 7 (K_A 1.4 ± 0.31 μM) compared with pH 7.5 (0.19 ± 0.01 μM) (**Fig. 2.3E,F**). These data confirm that binding of three FOX family members, FOXC2, FOXM1, and FOXN1, to the FkhP sequence is pH-dependent, with higher affinity binding at pH 7.0 compared with pH 7.5.

His122 of FOXC2 is necessary for pH-dependent binding to the FkhP sequence

To determine the significance of the conserved histidine for pH-regulated binding to the FkhP sequence we focused on FOXC2-His122 because it is the only histidine in the FOXC2 DBD. We used site-directed mutagenesis, first testing a His122Lys substitution with the reasoning that lysine with a predicted pKa of > 10 would be constitutively charged within the cellular pH range and a hydrogen bond donor like a protonated histidine. We observe that FOXC2-H122K has strong relative binding affinity compared with wild-type FOXC2 for the FkhP sequence between pH 6.8-8 (**Fig. 2.4A**). Further, when we performed a FOXC2-H122K protein titration, we find that the affinity is pH-independent with no difference in binding affinity at pH 7.0 (K_A 0.86 ± 0.15 μM) compared with pH 7.5 (K_A 0.91 ± 0.08 μM) (**Fig. 2.4B,D**). We also tested a His122Asn substitution, with the prediction that an asparagine might mimic a deprotonated histidine and have lower affinity and pH-independent binding to the FkhP sequence. Moreover, a naturally occurring FOXC2-H122N is reported in lung cancers (Forbes et al., 2017a). Our data confirm that the binding affinity of a FOXC2-H122N DBD is lower compared with WT at pH 7.0 and similar to WT at pH 7.5, but also pH-independent with no difference in affinity at pH 7.0 (K_A 0.14 ± 0.03 μM) compared with pH 7.5 (K_A 0.10 ± 0.01 μM) at pH 7.5 (**Fig. 2.4C,D**). Additionally, we

tested the importance of the conserved His287 in FOXM1 for pH-dependent DNA binding by using a His287Lys substitution. While affinity at pH 7 (K_A 4.1 ± 0.81 μM) and pH 7.5 (K_A 1.8 ± 0.27 μM) is greater compared with WT, binding is still pH-dependent (**Fig. 2.5A,B)**. To determine why FOXM1-H287K is not sufficient for pH-independent binding, we used CpHMD simulations to sample five histidine residues in FOXM1-DBD. Our results predict that the protonation state of His269 (blue), His275 (cyan), and His311 (green) does not affect DNA binding. In contrast, both His287 (orange) and the proximal His292 (yellow) are predicted to prefer the DNA bound state when protonated and unbound when neutral (**Fig. 2.5C**). Together, these data indicate that His122 is necessary for pH-dependent binding of FOXC2, but in FOX family proteins with more than one histidine in the DBD, the conserved histidine may contribute to but not exclusively confer pH-dependent DNA binding**.**

FOXC2 has pH-dependent activity in cells with higher activity at lower pH for an FkhP reporter

We next asked whether pHi regulates FOXC2 activity for an FkhP sequence in cells, using a luciferase assay with MDA-MB-436 clonal human breast cancer cells. Imaging MDA-MB-436 cells loaded with the pH-sensitive dye SNARF, we confirmed a relatively high pHi of 7.62 ± 0.21 that is decreased to pHi 7.42 ± 0.04 in the presence of 5-(N-Ethyl-N-isopropyl)-Amiloride (EIPA) (10 μM, 24 h), a selective pharmacological inhibitor of the plasma membrane H+ extruder NHE1 (**Fig. 2.6A**). Imaging also revealed that pHi and nuclear pH are similar in control cells and cells treated with EIPA (**Fig. 2.6A**). In MDA-MB-436 cells transfected with a 6x-FkhP repeat luciferase reporter with a minimal promoter (minP) (**Fig. 2.6B**) but not FOXC2, there is minimal basal reporter activity with no significant difference between controls and cells treated with 10 μM of EIPA. However, in cells transfected with WT FOXC2, there is a significant 1.65-fold relative greater reporter signal in the presence compared with the absence (control) of EIPA (**Fig. 2.6B**). We also tested activity of mutant FOXC2-H122K and FOXC2-H122N in MDA-MB-

436 cells with the 6x-FkhP repeat luciferase reporter. We find that the activity of both mutant proteins is pH-independent (**Fig. 2.6B**), consistent with their pH-independent binding affinities for the FkhP sequence determined *in vitro* by fluorescence anisotropy (**Fig. 2.4**). Although we found pH-independent luciferase activity in cells expressing FOXC2-H122K and FOXC2-H122N, the overall activity of FOXC2-H122K was lower than WT and lower than expected based on the observed high affinity *in vitro*. This may be due to changes to tertiary structure of the full-length mutant protein compared with the shorter DBD used for *in vitro* binding measurements.

To lower pHi, we added EIPA 8h after transfecting with FOXC2 and the luciferase reporter. As an alternative approach to eliminate a time delay, we generated MDA-MB-436 cells with CRISPR/Cas9 silencing of NHE1 expression. Using cells loaded with the pH-sensitive dye BCECF, we confirmed a lower pHi in NHE1-null cells of 7.39 ± 0.03 compared with a pHi of 7.71 ± 0.03 in control parental cells (**Fig. 2.6C**). With this approach we confirmed that in the absence of FOXC2 the reporter signal is minimal and pH-independent (**Fig. 2.6D**). Additionally, like with EIPA-treated parental cells, co-expression of the reporter and FOXC2 in NHE1-null cells results in a 2.17-fold increase in activity compared with activity in parental controls (**Fig. 2.6D**). Together, these data using two different approaches to lower pHi, pharmacological and genetic, show pH-dependent FOXC2 activity for an FkhP reporter in cells, with higher activity at lower pHi likely mediated by His122.

FOXC2 prefers FHL-like sequences at higher pH

After confirming our first prediction of higher affinity binding to thymine in the canonical FkhP motif at lower pH for FOXC2, FOXM1, and FOXN1, we tested our second prediction that binding to adenine would have a higher affinity at higher pH, with a deprotonated histidine as a hydrogen bond acceptor. However, using recombinant FOXC2 DBD and published DNA consensus motifs we were unable to obtain binding to several sequences with AGC rich His recognition sites (data not shown). We therefore used SELEX-SEQ as an unbiased approach

to identify DNA binding motifs for a given transcription factor from a randomized library (**Fig. 2.7A**). We performed SELEX-SEQ using GST-FOXC2 at pH 7 and pH 7.8 to identify a potential sequence with high affinity binding at high pH. We chose pH 7.8 to minimize binding to a predicted low pH sequence preferences such as FkhP where binding is attenuated after pH 7.6 (**Fig 2.3B**). After four rounds of selection at pH 7 we find that the most enriched sequence is the canonical FkhP motif (**Fig. 2.7B**). In contrast, at pH 7.8 the three most enriched sequences are different than those at pH 7 (**Fig. 2.7C**). All three sequences are similar to the reported FOX family consensus FHL motif (Nakagawa et al., 2013).

We used a used a 5'6FAM labeled FHL sequence to measure binding of purified recombinant FOXC2 DBD expressed as a GST fusion protein and fluorescence anisotropy. We made a 2x-FHL 5-mer repeat with a single nucleotide adenine spacer (11-mer) to be consistent with the molecular weight of the 11-mer FkhP sequence previously described. Additionally, we generated a 9-mer FHL with "GC" nucleotides flanking the 5-mer core FHL sequence (9-mer) for the minimal length needed for anisotropy signal. We were unable to measure binding to the 11-mer FHL sequence nor to a subsequently generated 9-mer oligo. Hence, to further confirm our findings with SELEX-seq, in future studies we plan to determine FOXC2 activity in MDA-MB-436 cells with a 6x-FHL repeat luciferase reporter, with the prediction that activity will be greater at pH 7.7 compared with pH 7.4.

Biological Significance of pH dependent FOXC2 activity

To determine the effect that pHi-regulated FOXC2 activity has on gene expression, we are analyzing bulk RNA-seq data as suggested by thesis committee members. We collected RNA from three separate preparations of MDA-MB-436 parental and NHE1-null cells with heterologous expression of full-length FOXC2 WT or pH-independent mutants His122Lys and His122Asn. We are currently performing differential gene expression analysis of sequencing

data generated on a NovaSeq6000 to identify selectivity of FOXC2 target genes at pHi 7.4 compared with pHi 7.7. (see Fig. 2.6C).

Figures

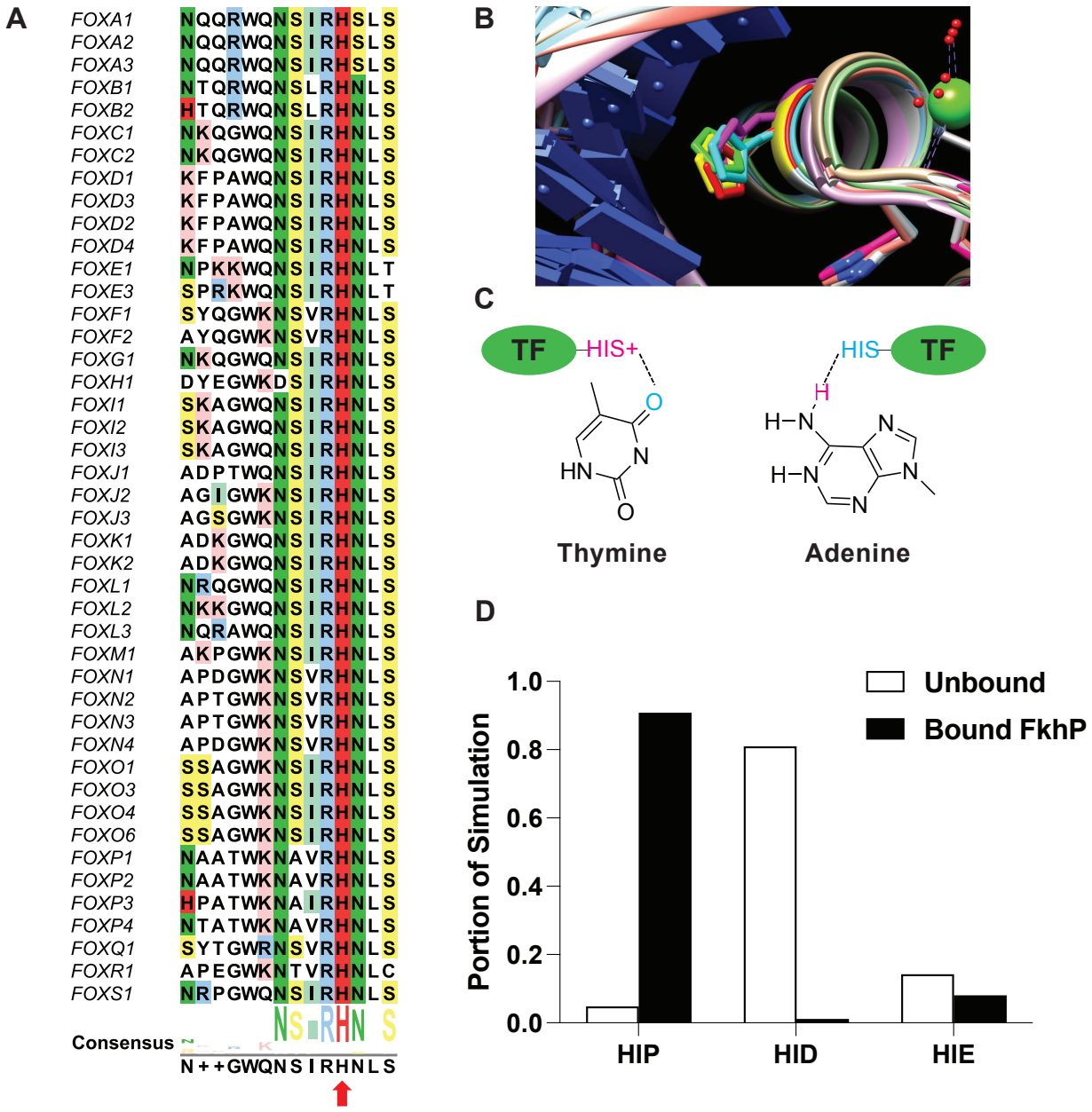

Figure 2.1. FOX family proteins are predicted pH sensors for pH-dependent binding to DNA.

A. Sequence alignment of all FOX family member proteins DBD Helix H3 with conserved histidine highlighted in red and denoted by red arrow. B. In available structures of FOX proteins in complex with DNA, the conserved histidine is also spatially aligned. C. A protonated transcription factor histidine is a predicted hydrogen donor for thymine acceptor while a neutral histidine is a predicted hydrogen bond acceptor for adenine donor. D. CpHMD portion of simulation in which double protonated (HIP), protonated at delta nitrogen (HID), protonated at epsilon nitrogen (HIE) are predicted to be unbound (white bars) or bound FkhP (black bars).

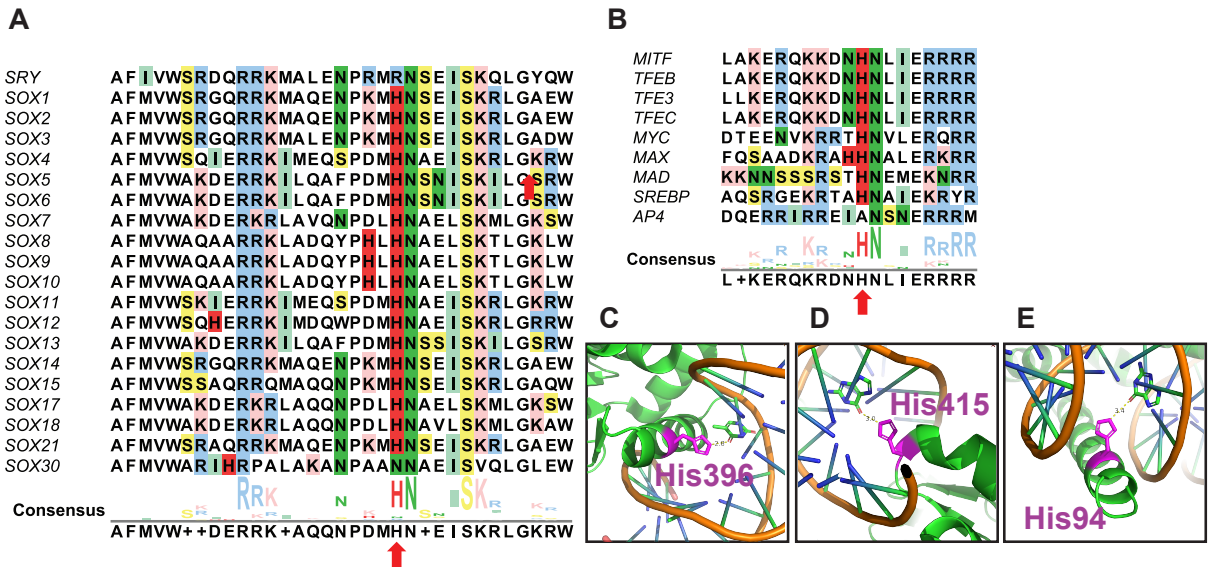

Figure 2.2. Transcription factors across families contain a histidine in the DBD.
A, B. Sequence alignment of all (A) SOX family members proteins DBD Helix 1 and 2 (B) MITF/MYC/MAX family members with conserved histidines highlighted in red and denoted by red arrows. C-E. Select transcription factors in other families with a nucleotide recognizing histidine (magenta) in the DBD. (C) ETV6-His396 hydrogen bond to a thymine (PDB: 4MHG). (D) STAT6-H415 hydrogen bond to a guanine (PDB:4Y5W). (E) ARNT-His94 hydrogen bond to a guanine (PDB: 4ZPK).

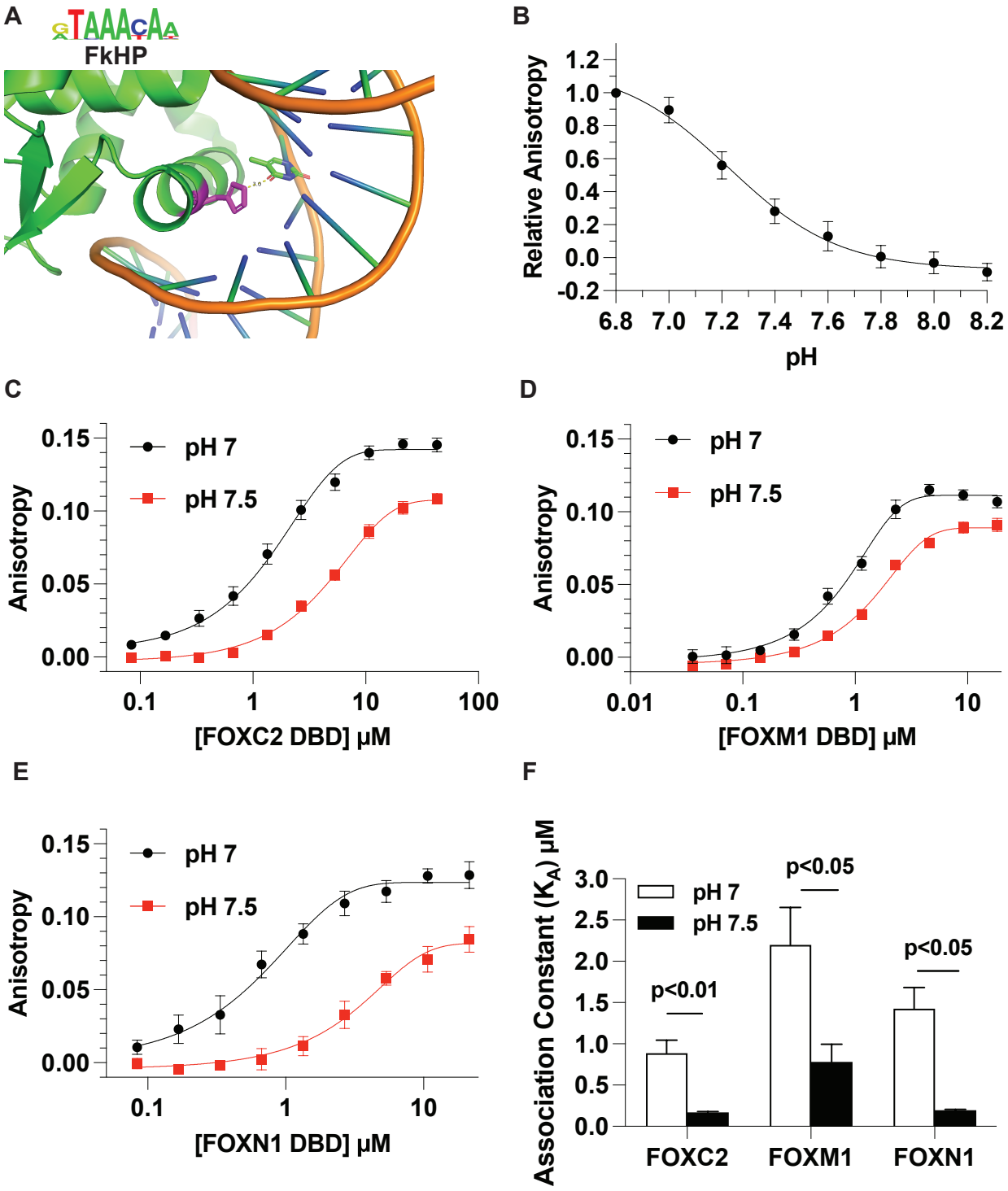

Figure 2.3. Binding of FOX family proteins to the FkhP sequence is pH-dependent with high affinity at low pH.

A. FOXC2 single histidine in DBD bound to the FkhP sequence making a hydrogen bond with thymine (PDB: 6AKO). B. pH titration of FOXC2 to the FkhP sequence. C-D. Binding curves at pH 7 and 7.5 for FOXC2 (C), FOXM1 (D), and FOXN1 (E). F. Association constants calculated from binding curves. Data are means ± s.e.m. of at least three separate measurements with two separate protein preparations.

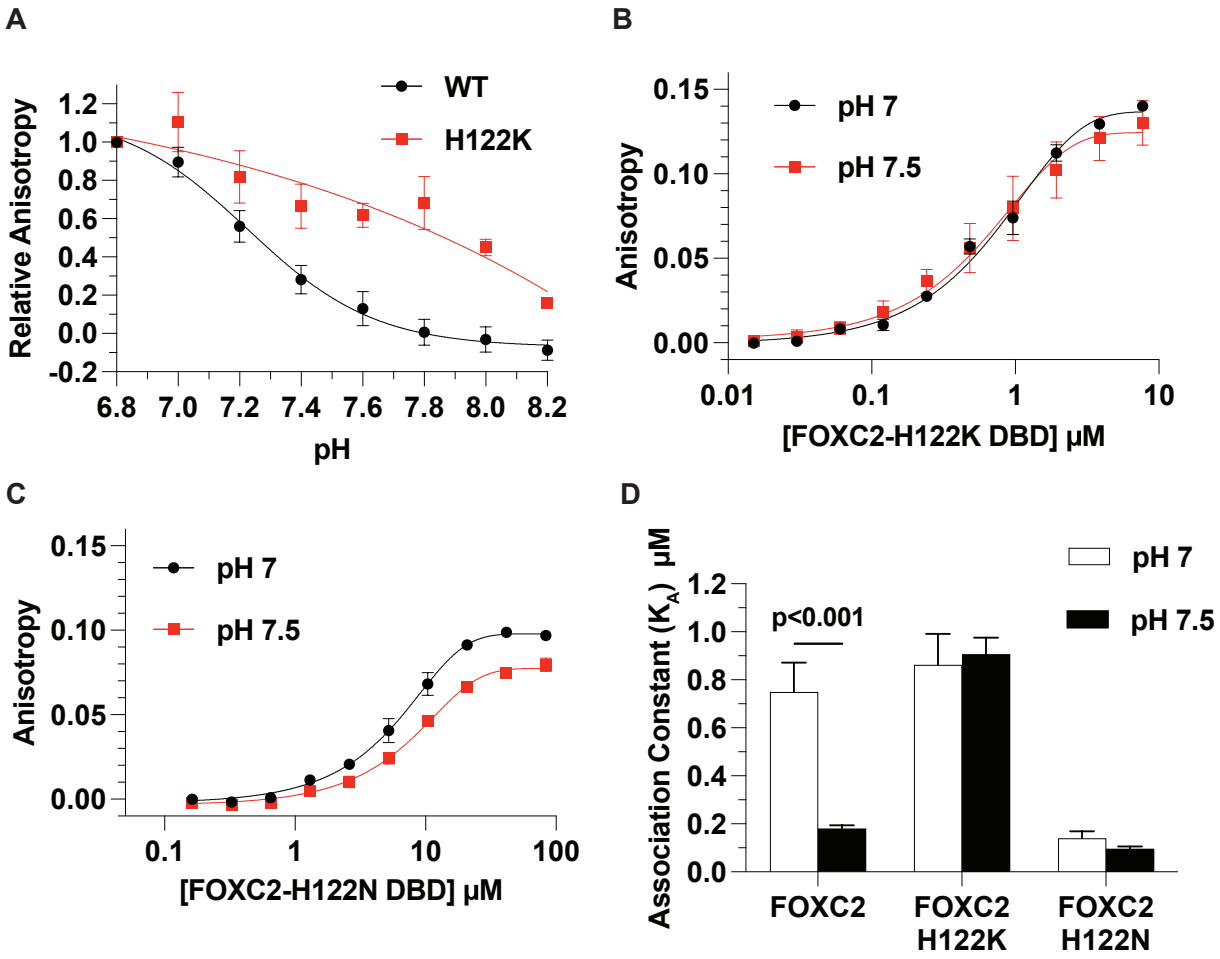

Figure 2.4. pH-dependent binding of FOXC2 to the FkhP sequence is dependent on His122.

A. pH titration of FOXC2-H122K compared to WT. B, C. Binding curves of pH-independent mutants H122K (B) and H122N (C). D. Association constants for FOXC2 WT and pH-independent mutants. Data are means ± s.e.m. of at least three separate measurements with two separate protein preparations.

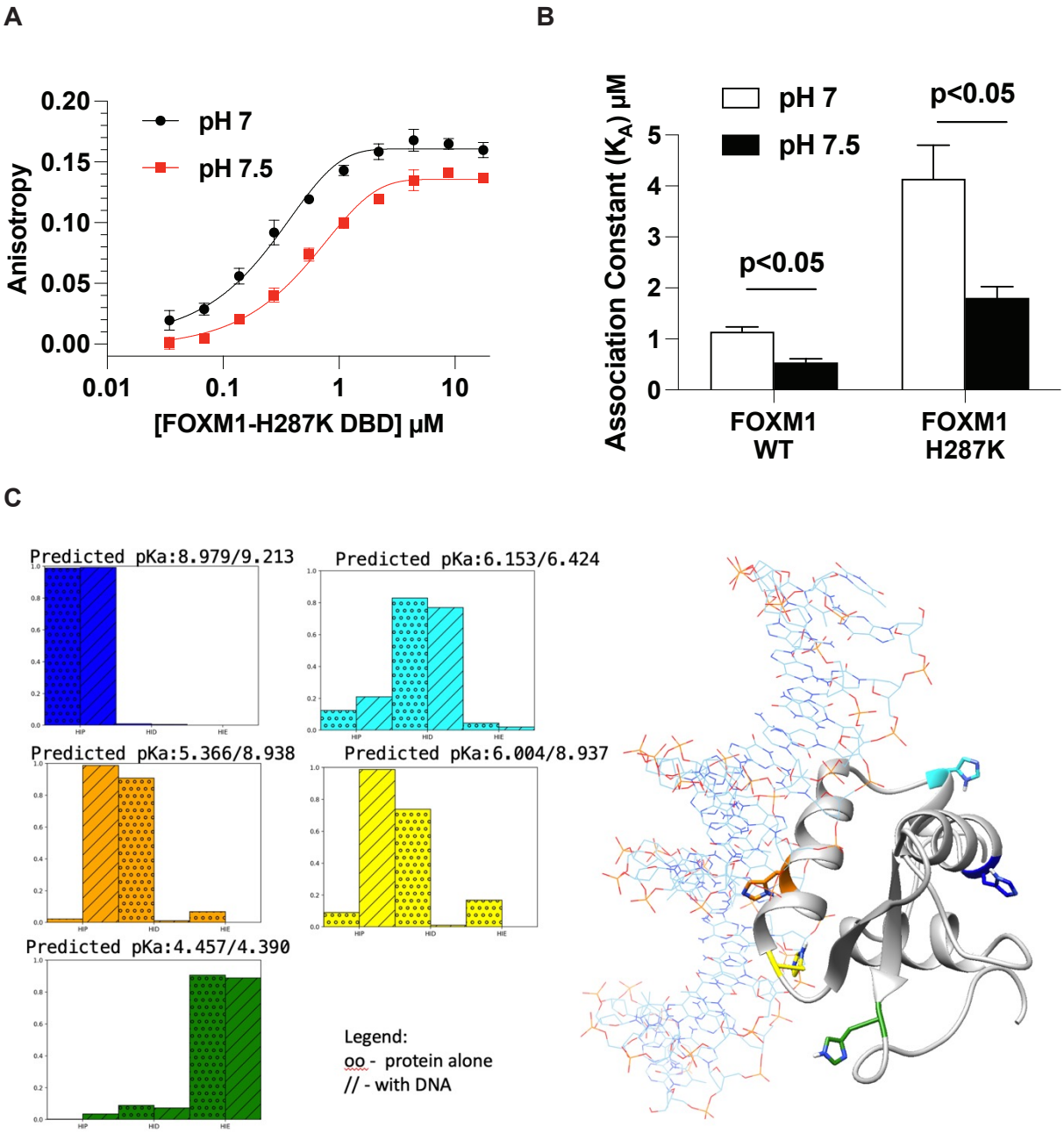

Figure 2.5. FOXM1-H287K is not sufficient for pH-dependent binding to the FkhP sequence.

A. Binding curves at pH 7 and 7.5 for FOXM1-H287K. B. Association constants calculated from binding curves. Data are means ± s.e.m. of at least three separate measurements with two separate protein preparations C. FOXM1 HIS protonation states for protein alone and in complex with DNA for five of six histidines in the DBD. HIS287(orange) and HIS292(yellow) exhibit a strong preference for the doubly protonated, charged state in the context of the DNA complex, while other His residues do not. Error bars are not calculated because we only produced one set of simulations.

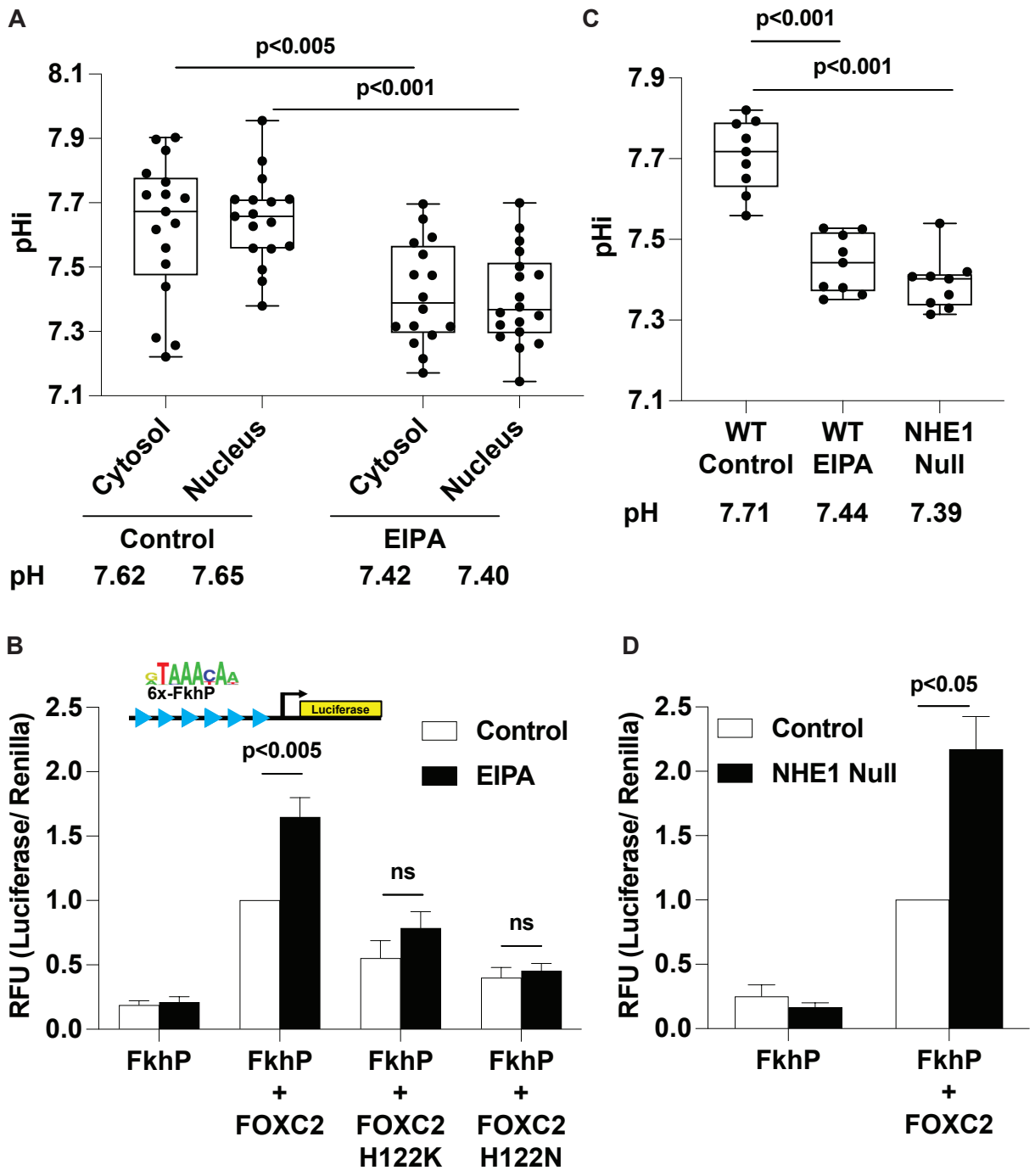

Figure 2.6. FOXC2 has pH-dependent transcriptional activity in cells that is dependent on His122.

A. pHi measurements of MDA-MB-436 cells in cytosol and nucleus with and without EIPA. Data are means of three independent measurements ± s.e.m. B. Luciferase assay for FOXC2 activity for an FkhP sequence in control (pHi ~7.65) and EIPA treated (pHi ~7.4) cells with inset design of reporter. C. pHi measurements of MDA-MB-436 control (pHi ~7.7), EIPA treated (pHi ~7.4), and NHE1 null (~pHi 7.4). D. Luciferase assay for FOXC2 activity at FkhP sequences in control (pHi ~7.7) and NHE1-null cells (pHi ~7.4). All data are from at least three independent measurements and were analyzed by Tukey-Kramer HSD with a significance level of $p<0.05$.

A

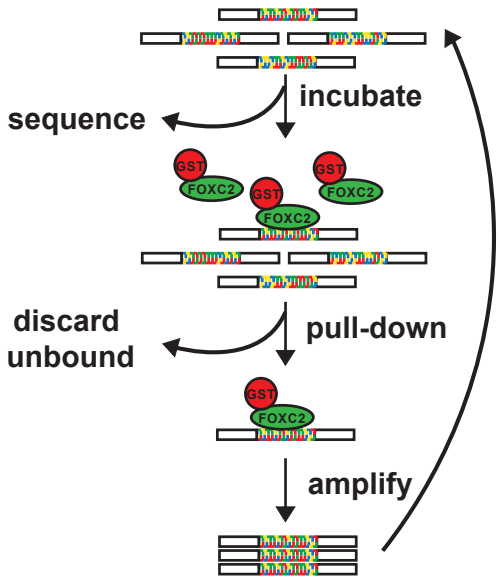

B

pH 7

Kmer	Affinity
ATAAAC	1
AAATAA	0.891104628
AATAAA	0.838538756

C

pH 7.8

Kmer	Affinity
CCACC	1
GACGC	0.932969423
GACCC	0.929438943

Figure 2.7. SELEX reveals DNA binding differences for FOXC2 between pH 7 and pH 7.8.
A. Design of SELEX assay. B,C. Top three enriched sequences in SELEX-seq after four rounds of enrichment at pH 7 (B) and pH 7.8 (C).

Discussion and Future Directions

How different co-expressed members of transcription factor families with highly conserved DNA-binding domains recognize distinct DNA sequences to regulate diverse target genes and disparate cell behaviors remains an important question for understanding developmental processes. DNA-binding selectivity is in part determined by multiple mechanisms, including co-factor association, post-translational modifications such as phosphorylation, and DNA accessibility through epigenetic modifications (Lambert et al., 2018). Our current findings add new mechanistic insight on pHi dynamics being a previously unrecognized regulator of DNA-binding selectivity that we predict is applicable to at least 65 transcription factors in diverse families that contain a conserved titratable histidine that forms hydrogen bonds with nucleotides. We do not predict that pHi dynamics function as binary switch for DNA binding preference but rather acts as a coincidence regulator with other established mechanisms.

Here we show that FOX family member transcription factors bind the canonical FkhP DNA sequence with higher affinity at lower pH *in vitro* and in cells, FOXC2 has higher activity for the FkhP sequence at lower pHi. Further, our data indicate that for FOXC2, pH-dependent DNA binding and activity is conferred by the conserved His122. In addition to high affinity binding of FOX family members to the canonical FkhP motif at low pH, our SELEX-seq data with FOXC2 identified distinct DNA sequences that bind at pH 7.0 compared with pH 7.8. Although sequences identified by SELEX-seq at pH 7.8 are like the known FOX FHL-N consensus motif, we were unable observe significant binding to these sequences *in vitro*, regardless of pH. While it is possible that FOXC2 prefers to bind these FHL-N like sequences relative to FkhP at higher pH, PCR amplification steps in SELEX-seq may overrepresent overall binding affinity of FOXC2. Further, it is possible that these short 5 base pair sequences enable different FOXC2 binding without flanking nucleotides present in the SELEX library. However, we also observed poor binding *in vitro* by adding FHL-N core flanking sequences found in known FOX target gene promoters or successive FHL-N repeats. Another possible caveat is that fluorescence

anisotropy requires the molecular weight of the ligand to be markedly higher than the probe for a sufficient signal (Moerke, 2009). To circumvent these *in vitro* limitations, ongoing studies to validate DNA sequences binding at higher pH obtained with SELEX-seq include using reporter assays in cells. We predict that 6x repeats of these FHL-N like sequences driving luciferase expression may reveal higher FOXC2 activity at higher pHi. Additional future studies include testing the activity of FOXN family members that are known to bind the FHL-N motif with high affinity (Newman et al., 2020; Rogers et al., 2019).

We are also determining the functional significance of pHi regulated FOXC2 activity in cells. While increased pHi is known to promote EMT (epithelial to mesenchymal transition) (Amith et al., 2016) and FOXC2 directly regulates N-cadherin and p120-catenin expression in cancer (Mani et al., 2007; Mortazavi et al., 2010; Ren et al., 2014), we were unable to observe significant pH-dependent differences in expression of these target genes with overexpression of FOXC2, despite testing multiple cell types including breast cancer MDA-MB-436, colorectal cancer HCT116, and lung cancer H1299. It is possible that overexpression of FOXC2 is not sufficient to either repress p120 or activate N-cadherin expression in these cell contexts. While our findings indicate that pH is a previously unrecognized regulator of DNA binding selectivity of transcription factors, pHi is also known to regulate chromatin accessibility where pH-sensors have been identified in select epigenetic readers and writers (McBrian et al., 2013; Tencer et al., 2017). With gene expression regulated by multiple mechanisms, including chromatin accessibility, co-factors, post-translational modifications, and cell context dependency, study of FOXC2 pH-dependent gene regulation of specific candidates is a limited approach. To resolve these limitations, our ongoing studies include using RNA-seq in cells overexpressing WT FOXC2 with changing pHi to determine transcriptome wide and pH-dependent gene expression differences. Because pHi can broadly affect chromatin and upstream signaling for gene expression changes, our RNA-seq studies also include cells overexpressing pH-independent mutants FOXC2-H122K and FOXC2-H122N to filter significantly different transcripts in cells

expressing WT but not mutants. These different conditions will also allow us to determine FOXC2-H122 dependency of differentially expressed genes. A future direction would be to use this bulk RNA-seq approach with other FOX family transcription factors known to regulate cell behaviors that are also regulated by pHi dynamics. For example, FOXM1 is known to regulate multiple cell cycle stages, (Wierstra, 2013), which are also regulated by pHi dynamics (Flinck et al., 2018a; Putney & Barber, 2003), FOXD3 promotes exit from naïve self-renewing mouse embryonic stem cells (Respuela et al., 2016), with exit also being dependent on increased pHi (Ulmschneider et al., 2016), and overexpression of several FOX transcription factors promote cancer cell behaviors (Katoh et al., 2013; Zhu et al., 2023), as does increased pHi (Swietach et al., 2023; Webb et al., 2011; White, Grillo-hill, et al., 2017). Additionally, FOXN1 is known as the master regulator of thymic epithelial development (Romano et al., 2013). Although pH dynamics regulates differentiation and specification of embryonic and specific adult stem populations, whether it plays a role in thymic development has not been reported (Liu et al., 2023; Ulmschneider et al., 2016). Future studies are necessary to establish cell behaviors directly regulated by pHi-dependent FOX target gene specificity.

An additional future direction is to apply our approach with FOX transcription factors to determine whether DNA binding by SOX transcription factors is also regulated by pH. In contrast to FOX family members, a nucleotide-binding histidine is not completely conserved in SOX family members but does occur in 18 of 20 SOX family transcription factors. Sry and SOX30 are the exception and contain an arginine and asparagine, respectively. These differences will allow using Sry and SOX30 and swapping DBD as an additional approach not available with FOX proteins. Further, which cell behaviors require invariant charged amino acids such as arginine or asparagine at nucleotide recognizing residues will help us better understand the significance of a nucleotide-binding histidine in the DBD of transcription factors.

Of note, there are two previous reports using selective FOX family members that suggest pH regulated functions. Using FOXP2, Blane and Fanucchi (Blane & Fanucchi, 2015)

show that the protonation state of the conserved histidine in the DBD regulates protein tertiary shape and DNA-binding affinity for a known DNA motif, although their study included non-physiological pH values as low as pH 5 and as high as pH 9. Using FOXP1, Medina and colleagues (Medina et al., 2019). show that the protonation state of a less conserved histidine exclusive to the FOXM/O/P subfamilies modulates domain swapping stability to regulate its DNA-binding affinity. Although these studies reveal pH-regulated functions of FOXP2 and FOXP1, they offer limited insight on the mechanisms and broader scope of pH dynamics being a regulator of DNA binding by transcription factors across distinctly different families.

Taken together our findings suggest that pH dynamics is a broadly conserved mechanism regulating the activity of myriad transcription factors, and they also address how highly conserved transcription factors can regulate diverse target genes and functions reiteratively. Additionally, our findings further establish how pHi regulated electrostatics can affect protein function to regulate cell behaviors for a more complete understanding of both development and disease.

Methods

Amino acid sequence and structural alignment

For sequence alignment of FOX, SOX, and MITF/MYC/MAX family proteins, FASTA sequences were downloaded from UniProt and uploaded to Jalview software. For each family, sequences were aligned using ClustalO default settings. Amino acids were arbitrarily colored with red used to highlight the conserved DNA-binding His residues in each family. For structural alignment, available FOX crystal structures in complex with DNA were downloaded from the Protein Data Bank (PDB), which included FOXM1 (3G73), FOXO4 (3L2C), FOXC2 (6AKO), FOXN1 (6EL8), FOXO3a (2UZK), FOXP2 (2AS5), and FOXO1 (3CO7). Structures were uploaded to UCSF ChimeraX and structurally aligned using 3G73 as a reference structure.

Constant pH Molecular Dynamics Simulations

Constant pH molecular dynamics were used to sample protonation state distributions for defined titratable histidine residues using explicit solvent representation and an atomistic description of the protein-DNA complex. Shifts in expected pKa of histidine residues were estimated within the simulation pH range to inform how DNA-protein interaction is modulated as a function of changes in pH. All CpHMD simulations were run for 100ns at pH 7.0, with protonation state change attempts every 100fs.

Cloning, Expression, and Purification

The GST-fusion protein plasmid pGEX-6P-2 was digested with BamHI and EcoRI enzymes and the DBD of FOXC2 (amino acids 72-172), FOXM1 (amino acids 222-360), and FOXN1 (amino acids 270-366) were PCR amplified with BamHI and EcoRI multiple cloning site overhangs. FOX templates were obtained from Addgene (Moparthi & Koch, 2020) and FOX-DBD DNA sequences were ligated and cloned into the pGEX-6P2 using Gibson Assembly Master Mix (NEB: E2611L). Point mutants were generated with the QuikChange Lightning site-directed

mutagenesis kit (Agilent: 210515) according to the manufacturer protocol. Each construct was transformed into and expressed in BL21-DE3 *E. coli* competent cells using heat shock (Thermo EC0114). For expression, cells were grown in 1L of Luria broth with ampicillin (100 µg/mL; 37°C with shaking at 225 rpm) until cells reached log-phase growth at OD_{600} = ~0.6. Expression was induced with 1 mM isopropyl-β-D-1-thiogalatapyranoside for 6 hours at 37°C with shaking at 225 rpm. Cells were pelleted (7000g; 15 min at 4°C) and either frozen at -80°C or used directly for protein purification.

GST-FOX DBD Protein Purification

Bacterial cell pellets were resuspended in 50mL of lysis buffer (50 mM Tris-HCl pH 8, 1 mM DTT, 5% glycerol, protease inhibitor cocktail [Roche: 1183615300]). Cells in pellets were lysed by sonication on ice with 10 sec pulses of maximum setting followed by 1 min cooling period, repeated 12 times. The supernatant was clarified by centrifugation (12,000g; 30 min at 4°C) and mixed 1:1 with wash buffer (50mM Tris, 150mM NaCl, pH 8.0) from the GST purification kit (Pierce: 16105). 12.5mL of lysate was loaded on pre-equilibrated 3mL glutathione agarose spin columns, incubated end over end for 30 min at 4°C and repeated until all lysate was used. The flowthrough was collected by centrifugation (700g; 2 min at 4°C) and columns were washed with 6 mL of wash buffer three times. GST-FOX DBD was eluted with 3mL of wash buffer + 10mM reduced glutathione three times. Each fraction was collected, separated on a 10% SDS-PAGE gel, and coomasie stained to determine molecular size and purity. Eluate fractions were pooled, divided in half, concentrated, and exchanged in two separate anisotropy buffers (20mM Hepes, 140mM KCl, 0.05mM TCEP-HCl, pH 7 or 7.5) using Amicon Ultra-15 Filters with a 10 kDa molecular weight cutoff (MilliporeSigma: UFC901008). The protein concentration was determined by A_{280} using NanoDrop spectrophotometer (Thermo: ND-1000), aliquoted, flash frozen in liquid nitrogen, and stored at -80°C.

GST-FOX DBD Anisotropy Assay

GST-FOX DBD protein aliquots were thawed at room temperature and diluted to a final volume of 120µL in anisotropy buffer pH 7 and 7.5 to the highest concentration of each protein (FOXC2- 50µM, FOXM1- 21µM, FOXN1- 50µM, FOXC2-H122K- 9µM, FOXC2-H122N- 97µM, FOXM1-H287K- 21µM) needed to reach binding saturation which was empirically determined. Protein was serially diluted ten times to a volume of 60µL and 10µL of 6'FAM labeled duplex FkhP (ccaTAAACAac) (IDT) was added to each protein dilution and one blank for a final concentration of 7.5nM DNA and 70µL reaction volume. PCR strip tubes were capped and incubated at RT in the dark for 30 min. Following incubation, 20µL of each dilution and blank was loaded in triplicate to a 384-well black plate (Greiner: 784076) using a multichannel pipette. Fluorescence anisotropy measurements were made using a SpectraMax M5 plate reader (Molecular Devices). Sigmoidal curve fits were generated using GraphPad Prism and association constants determined using Mathematica software to solve for K_D in equation $A_{obs} = A_0 + (\Delta A * T)/(K_D + T)$ where A_{obs} is observed anisotropy, A_0 is anisotropy of initial unbound probe, ΔA is difference in anisotropy between unbound and fully bound populations, and T is concentration of titrant protein. K_A was determined as ($1/K_D$). Data are represented as averages of at least three independent measurements from two separate protein preparations and error bars are ± s.e.m. Binding affinities of FOX WT proteins were analyzed by two-tailed unpaired Student's t-test and with a significance level of $p<0.05$. Comparison of WT FOXC2 and FOXM1 to His mutants were analyzed by Tukey-Kramer HSD with a significance level of $p<0.05$.

GST-FOX DBD pH Titration

Anisotropy buffer was prepared in increments of 0.2 pH units from pH 6.8-8.2 and 7.5nM final concentration of labeled FkhP oligo was added to each. Either 2.3µM final concentration GST-FOXC2 or buffer alone was added to a final reaction volume of 70µL. Reactions were incubated

and measured as described above. Data are represented as average anisotropy values of [(FOXC2+DNA) – (DNA alone)] set relative to maximal binding at pH 6.8 ± s.e.m.

Cell Culture and Luciferase Assay

For determinations with EIPA to lower pHi, MDA-MB-436 cells obtained from ATCC were maintained in atmospheric conditions at 37°C in Leibovitz's L-15 medium (Cytiva: SH30525.01) supplemented with insulin (10µg/mL), Penicillin/Streptomycin (100U/mL each), and 10% FBS. For determinations with NHE1-null conditions, MDA-MB-436 cells were maintained at 37°C and 5% CO_2 in RPMI 1640 (Gibco:11875085) supplemented with Penicillin/Streptomycin (100U/mL each), and 10% FBS. For luciferase assays, 3.5 x 10^5 cells were plated in 6-well plates and grown overnight to 80% confluency prior to transfection. Cells were transfected with a total of 1µg DNA using lipofectamine 3000 (Invitrogen: L3000001) according to manufacture protocol. Cells received either 500ng 6x-FkhP obtained from Addgene (Moparthi & Koch, 2020) or 500ng 6x-FkhP and 500ng pCS2 Flag-FOXC2 WT from Addgene (Moparthi & Koch, 2020) or mutant FOXC2 generated as described above. Each transfection also included control pRL-TK renillla plasmid obtained from the L. Selleri Lab (University of California San Francisco) at a ratio of 1:10 of reporter plasmid (50ng). At 8 hours after transfection, cells were washed once with PBS and medium added in the absence or presence of 10 mM EIPA. Cells were then maintained for an additional 40 hours and collected for Dual-Luciferase assays (Promega: E2920). In brief, cells were washed once with PBS and lysed in 500µL of Dual-Glo luciferase buffer with shaking on a nutator for 10 min at 4°C. Lysates were collected in microfuge tubes and clarified by centrifugation for 5 min at 13,000 rpm at RT. From supernatants, 100µL was loaded in quadruplicate in separate wells in a 96-well opaque white plate (Costar: 3917). Luciferase signal was read on a SpectraMax M5 plate reader and Dual-Glo Stop & Glo Buffer was then added to quench the luciferase signal and activate renilla for 10 min. The renilla signal was read and the

Luciferase/Renilla ratio was normalized to control with 6x-FkhP + WT FOXC2. Data were analyzed by Tukey-Kramer HSD with a significance level of $p<0.05$.

pHi Determinations

For imaging pHi (cytosolic) and nuclear pH, MDA-MB-436 cells plated on 35 mm glass bottom MatTek dishes for 48 h were washed 2X and incubated for 15 min in pHi buffer (110mM NaCl, 5mM KCl, 10 mM glucose, 25mM $NaHCO_3$, 1mM KPO_4, 1mM $MgSO_4$, 2mM $CaCl_2$, pH 7.4) containing 10 mM of the dual emission pH-sensitive dye 5-(and-6)-carboxylic acid, acetoxymethyl ester (SNARF) as previously described (Grillo-Hill et al., 2014). For measurements with EIPA, a final concentration of 10 mM was included in cell medium 24 h before measurements and in all wash and dye-loading buffers. After dye loading and washing 2X in pHi buffer, ratiometric determinations at Ex490 were made at pH-sensitive and -insensitive emissions of 580 nm and 640 nm, respectively, using a Plan Apo 40 0.95 NA objective on an inverted Nikon spinning disc microscope system (Nikon Eclipse TE2000 Perfect Focus System; Nikon Instruments; Nikon Instruments) equipped with a CoolSnap HQ2 cooled charge-coupled camera (Photometrics) and camera-triggered electronic shutters controlled with NIS-Elements Imaging Software (Nikon). For measuring pHi in cell populations, parental and NHE1-null MDA-MB-436 cells plated in standard 24-well dishes for 48 h were washed 2X and incubated for 15 min in pHi buffer containing 1 mM of the dual excitation pH-sensitive dye 2',7'-Bis-(2-Carboxyethyl)-5-(and-6)-carboxyfluorescein, acetoxymethyl ester (BCECF) as previously described (Meima et al., 2009). After dye loading and washing 2X in pHi buffer, ratiometric determinations were made at Em 535 nm and pH-sensitive and -insensitive excitations of 490 nm and 440 nm, respectively, using a SpectraMax M5 plate reader. To calibrate ratiometric measurements to pHi values for both pHi imaging and cell population pHi, at the end of each determination cells were incubated sequentially for 5 min each with a Na^+-free, K^+ buffer

containing the ionophore nigericin at pH 7.5 and then at pH 6.6 to equilibrate intracellular and extracellular pH, as previously described (Grillo-Hill et al., 2014; Meima et al., 2009).

SELEX-seq Identification of High pH High Affinity Sequences

For SELEX-seq, a previously reported protocol (Riley et al., 2014) was used with modifications. We designed our library with a 16 base pair randomized region flanked by PCR sites GTTCAGAGTTCTACAGTCCGACGATCTGG**NNNNNNNNNNNNNNNN**TCGTATGCCGTCTTC TGCTTG. For each round of selective enrichment, final concentrations of 0.25μM DNA library with 2.5μM GST-FOXC2 were incubated for 30 min at RT in either binding buffer (20mM Hepes, 140mM KCl, 0.05mM TCEP-HCl) at pH 7 or 7.8. Next, 30μL of 50% pre-equilibrated glutathione Sepharose beads (Cytiva: 17075601) were added and incubated end over end for 30 min at RT and DNA-FOXC2-bead complexes were pelleted by centrifugation at 5000 rpm for 4 min. DNA-FOXC2-bead complexes were washed twice with 300μL binding buffer and resuspended in 100μL binding buffer prior to heat dissociation for 5 min at 95°C. Eluate DNA was clarified by centrifugation (10,000 rpm for 5 min) and PCR amplified with forward ($SELEX_F$) and reverse ($SELEX_R$) primers complementary randomized region flanking nucleotides (Table 2.1). PCR products were cleaned using the MinElute PCR purification kit (Qiagen: 28004) and the selection process was repeated four times with PCR products from prior rounds used as the starting library. 5' and 3' adapter overhangs were added by PCR (Table 2.1) to the initial starting library (R_0) with all four rounds of selection (R_{1-4}) used to prepare for addition of barcoded indexes. Indexes were added by PCR (Table 2.2) using the Nextera IDT UD Set D (Illumina: 20027213) for multiplex sequencing. Sequencing was performed at the University of California, San Francisco Genomics CoLab using a Miniseq high output 150 cycles kit for paired end reads (Illumina: FC-420-1002). Samples were demultiplexed and analysis performed using the University of California, Davis Bioinformatics Core according to the protocol outlined in (Riley et

al., 2014) using their published ‘R’ “SELEX” package which is publicly available at: (bioconductor.org/packages/release/bioc/html/SELEX.html).

Tables

Table 2.1. Primers used in SELEX-seq.

Step	Primer	Sequence 5'>3'
Library Amplification	$SELEX_F$	GTTCAGAGTTCTACAGTCCGACGATCTGG
	$SELEX_R$	CGAAGTCAAGCAGAAGACGGCATACGA
Adapter Overhangs	$Overhang_F$	TCGTCGGCAGCGTCAGATGTGTATAAGAGACAGGTTCAGAGTTCTACAGTCCGACGATC
	$Overhang_R$	GTCTCGTGGGCTCGGAGATGTGTATAAGAGACAGCGAAGTCAAGCAGAAGACGGCATAC
Barcoded Indexes	$Barcode_F$	AATGATACGGCGACCACCGAGATCTACACNNNNNNNNTCGTCGGCAGCGTC
	$Barcode_R$	CAAGCAGAAGACGGCATACGAGATNNNNNNNNGTCTCGTGGGCTCGG

Table 2.2. Indexes from Nextera IDT UD Set D used for each sample.

Sample	Index ID	Index 5'	Index 3'
R_0 Initial Library	UDP0337	TGTAAGGTGG	AAGGCCTTGG
R_1 FOXC2 pH 7	UDP0338	CAACTGCAAC	TGAACGCAAC
R_1 FOXC2 pH 7.8	UDP0339	ACATGAGTGA	CCGCTTAGCT
R_2 FOXC2 pH 7	UDP0340	GCAACCAGTC	CACCGAGGAA
R_2 FOXC2 pH 7.8	UDP0341	GAGCGACGAT	CGTATAATCA
R_3 FOXC2 pH 7	UDP0342	CGAACGCACC	ATGACAGAAC
R_3 FOXC2 pH 7.8	UDP0343	TCTTACGCCG	ATTCATTGCA
R_4 FOXC2 pH 7	UDP0344	AGCTGATGTC	TCATGTCCTG
R_4 FOXC2 pH 7.8	UDP0304	CCGCTCCGTT	TACGGCGAAG

CHAPTER 3: MOLECULAR MECHANISM OF pH-DEPENDENT RELIEF OF ALLOSTERIC ATP INHIBTION BY HUMAN PFKM

Introduction

Phosphofructokinase-1 (PFK-1), the “gatekeeper of glycolysis,” catalyzes first committed step of the glycolytic pathway by converting fructose-6-phosphate to fructose 1,6-bisphosphate. As the reaction is irreversible, PFK-1 has evolved to be allosterically activated or inhibited by over 10 metabolites and in response to hormone signaling to fine-tune glycolytic flux for ATP production to meet energy requirements (Schöneberg et al., 2013). For example, PFK-1 activity is allosterically inhibited by a high ATP/AMP ratio and when this ratio decreases, the activity of PFK-1 increases to stimulate glycolysis to restore ATP production (Zheng & Kemps, 1992). Also, allosteric inhibitors include citrate and phosphoenolpyruvic acid, which are downstream messengers of high energy production (Colombo et al., 1975; Icard et al., 2012). In contrast, the allosteric activator fructose 2,6-bisphosphate (F2,6bP) is produced in response to insulin by fructose-6-phosphate (F6P), which is a PFK-1 substrate and creates a feedforward loop to increase glycolysis by increasing PFK-1 affinity for F6P (Depre et al., 1993). However, regulation of PFK-1 activity is not limited to molecular substrates. PFK-1 activity is also regulated by its assembly into filamentous polymers (Webb et al., 2017) and by changes in pH (Trivedi & Danforth, 1966), although the molecular mechanisms mediating these regulatory effects on PFK-1 activity remain unresolved.

PFK-1 is expressed in humans as three isoforms; liver (PFKL), muscle (PFKM), and platelet (PFKP), although the expression of each isoform is not limited to specific tissues. Moreover, each isoform has distinct sensitivities to different modes of regulation (Mor et al., 2011). PFKM activity is more sensitive to pH than the other two isoforms. A substantial >10-fold increase in PFKM activity between pH 7.0 to 7.5 was first shown nearly 50 years ago using enzyme isolated from rabbit muscle (Trivedi & Danforth, 1966). This work revealed that a higher pH relieves allosteric inhibition of enzyme activity by ATP. Subsequent work broadly inferred that pH-regulated activity is likely due to unspecified histidine residue(s) because histidine can titrate within this pH range (Carpenter & Hand, 1986; Webb et al., 2015). Until recently,

however, there were two limitations for resolving the molecular mechanism of pH sensing by PFKM. First was lack of recombinant PFK-1 as a tetrameric active enzyme. Previous studies relied on PFK-1 purified from tissues or cells, which precludes using targeted mutagenesis to test candidate pH-sensing residues. To overcome this limitation, the Barber group generated all three human PFK-1 isoforms as recombinant proteins with post-translational modifications by using baculovirus expression (Webb et al., 2015a). A second limitation was the lack of a mammalian PFK-1 tetrameric structure. The Barber lab determined two structures of recombinant human PFKP, one in complex with ATP and Mg^{2+} and another in complex with ADP, which revealed significant conformational differences and detailed interactions with substrate (Webb et al., 2015a).

A second project of my thesis research addressed the long-standing question of what molecular mechanism mediates pH sensitive relief of allosteric ATP inhibition of PFKM activity. This project was aided by a collaboration with Brad Webb, a former postdoc in the Barber lab who resolved the structure of PFKP (Webb et al., 2015b) and is currently an Assistant Professor at West Virginia University. I used sequence differences between PFKM compared with PFKP and PFKL, homology modeling of the PFKP structure, baculovirus-expressed recombinant PFK-1 isoforms, and site-directed mutagenesis to identify PFKM-His242 as a critical residue for mediating the pH-regulated relief of ATP inhibition. Moreover, I found that although His242 is necessary for pH regulated PFKM activity, it is not sufficient to confer pH sensing by PFKL. These findings elucidate a critical mechanism of the most highly regulated enzyme in glycolysis, PFKM, further highlighting how pHi can serve as a robust mechanism to regulate protein activity.

Results

The pH-dependent relief of allosteric ATP inhibition by PFKM is predicted to be mediated by His242

Previous work using PFKM isolated from frog (Trivedi & Danforth, 1966) and rabbit (Pettigrew & Frieden, 1979) muscle established that increasing pH from 7.0 to 7.8 relieved allosteric inhibition of enzyme activity by ATP. To identify the molecular mechanisms mediating pH-regulated PFKM activity, we used recombinant human PFKM generated in a baculovirus expression system and purified with a 6xHis-tag, as previously described (Webb et al., 2015a, 2017b) We first confirmed relief of ATP-inhibited activity with increasing pH, determined with 0.5mM fructose 6-phosphate (F6P), an inhibitory concentration of ATP (4mM), and a pH titration from pH 6.8 to 8.2 by using an auxiliary enzyme assay linking F1,6bP production to NADH oxidation as previously reported (Webb et al., 2015a) (**Fig. 3.1A**). To identify putative pH-sensor sites of PFKM, which had previously been suggested but not experimentally validated to be a histidine (Carpenter' And & Hand, 1986; Webb et al., 2015), we determined which histidine(s) are exclusive to the PFKM isoform and may confer pH sensing. In the crystal structure of PFKM purified from rabbit skeletal muscle (Banaszak et al., 2011) (PDB:3O8L), His242 is located in the ATP inhibitory pocket and in part coordinates the negative charge of phosphate groups on ATP (**Fig. 3.1B**). Further, amino acid sequence alignment of PFKM, PFKL, and PFKP (**Fig. 3.1C**) reveals that His242 is exclusive to the muscle isoform, suggesting its importance as a putative pH-sensor site for the pH sensitive activity of PFKM but not PFKL or PFKP (Webb et al., 2017a). In contrast, the uncharged side chains of phenylalanine and glutamine in PFKL and PFP, respectively are not predicted to coordinate the negative charge of ATP at this position. (**Fig. 3.1C**). Taken together, these observations predict that His242 is a pH-sensor site that may be protonated and bind the negatively charged inhibitory ATP and inhibit enzyme activity at low pH. In contrast, we predicted at higher pH, His242 may be deprotonated to attenuate the electrostatic binding of inhibitory ATP for relief of allosteric inhibition.

His242 is necessary for pH-dependent relief of allosteric ATP inhibition by human PFKM

To experimentally test our prediction that His242 mediates pH-dependent relief of allosteric inhibition of PFKM, we generated a PFKM-H242F substitution by site directed mutagenesis, selecting a Phe based on the residue at this site in the liver isoform (**Fig. 3.1C**). For WT PFKM, we found that at pH 7 there is a roughly 3-fold decrease in overall activity at 4mM ATP (3.5 μmol F1,6bp min^{-1} mg^{-1}) compared with maximal activity at 1mM ATP (10.9 μmol F1,6bp min^{-1} mg^{-1}). In contrast, at pH 7.5, maximal activity is achieved at 2mM ATP (13.8 μmol F1,6bp min^{-1} mg^{-1}) and maintained with 4mM ATP (11.8 μmol F1,6bp min^{-1} mg^{-1}) (**Fig. 3.2A**). While PFKM-H242F also reaches maximal activity at 2mM ATP, overall activity is markedly reduced to 1.6 and 1.4 μmol F1,6bp min^{-1} mg^{-1} at pH 7 and 7.5, respectively (**Fig. 3.2B**). Because of the low overall activity of PFKM-H242F, to better assess whether His242 is necessary for pH-dependent relief of allosteric ATP inhibition we also determined relative activity at pH 7 and 7.5 for both WT and His242Phe. For WT, we find relief of allosteric ATP inhibition at pH 7.5 where 89% of maximal activity is retained at 4mM ATP as opposed to only 21% at pH 7 (**Fig. 3.2C**). In contrast, His242Phe retains 78% and 99% of activity at 4mM ATP for pH 7 and 7.5, respectively (**Fig. 3.2D**). Together these data suggest that His242 is necessary for efficient overall activity and for pH-dependent relief of allosteric inhibition of PFKM by ATP.

His242 is not sufficient for pH-dependent relief of allosteric ATP inhibition by human PFKL

To determine whether His242 is sufficient for a gain of pH-dependent relief of allosteric inhibition, we generated recombinant WT PFKL and PFKL-F242H. For WT PFKL, we found at pH 7.5 there is a roughly 6-fold reduction in overall activity at 0.5mM ATP (0.28 μmol F1,6bp min^{-1} mg^{-1}) compared with maximal activity at 0.125mM ATP (1.69 μmol F1,6bp min^{-1} mg^{-1}). PFKL-F242H also reaches maximal activity at 0.125 mM at both pH 7 (8.05 μmol F1,6bp min^{-1} mg^{-1}) and pH 7.5 (195 μmol F1,6bp min^{-1} mg^{-1}) but activity is reduced at least 4-fold by 0.5 mM

ATP at either pH. However, the overall activity of PFKL-F242H is markedly greater than WT at both pH 7 and 7.5. (**Fig. 3.3A**). Because overall activity of PFKL-F242H is greater than WT, we also determined the relative activity for each condition at 0.125 mM ATP. We found no difference in relief of allosteric ATP inhibition by PFKL-F242H at either pH 7 or pH 7.5 compared to WT PFKL at pH 7.5 (**Fig. 3.3B)**. Taken together, these data suggest that a histidine substitution for Phe242 increases the overall activity of PFKL but is not sufficient for a gain of pH-dependent relief of allosteric ATP inhibition.

Figures

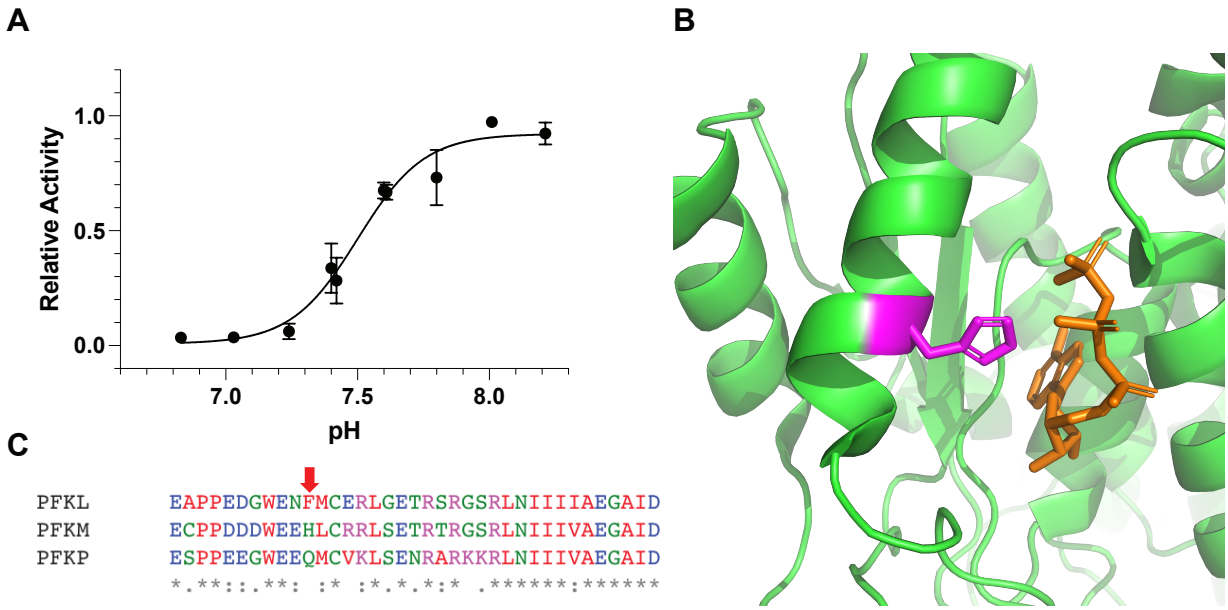

Figure 3.1. The pH-dependent relief of allosteric ATP inhibition by PFKM is predicted to be mediated by His242.

The pH-dependent activity of recombinant human PFKM at 4mM ATP and 0.5 mM fructose 6-phosphate. Data are means ± s.e.m. of seven independent measurements with two separate protein preparations. B. His242 (magenta) is positioned in the inhibitory ATP pocket and in part coordinates the inhibitory ATP (orange) negative charge (PDB:3O8L). C. Amino acid sequence alignment of the three human isoforms PFKL, PFKM, and PFKP where His242 is exclusive to the muscle isoform at this position (red arrow).

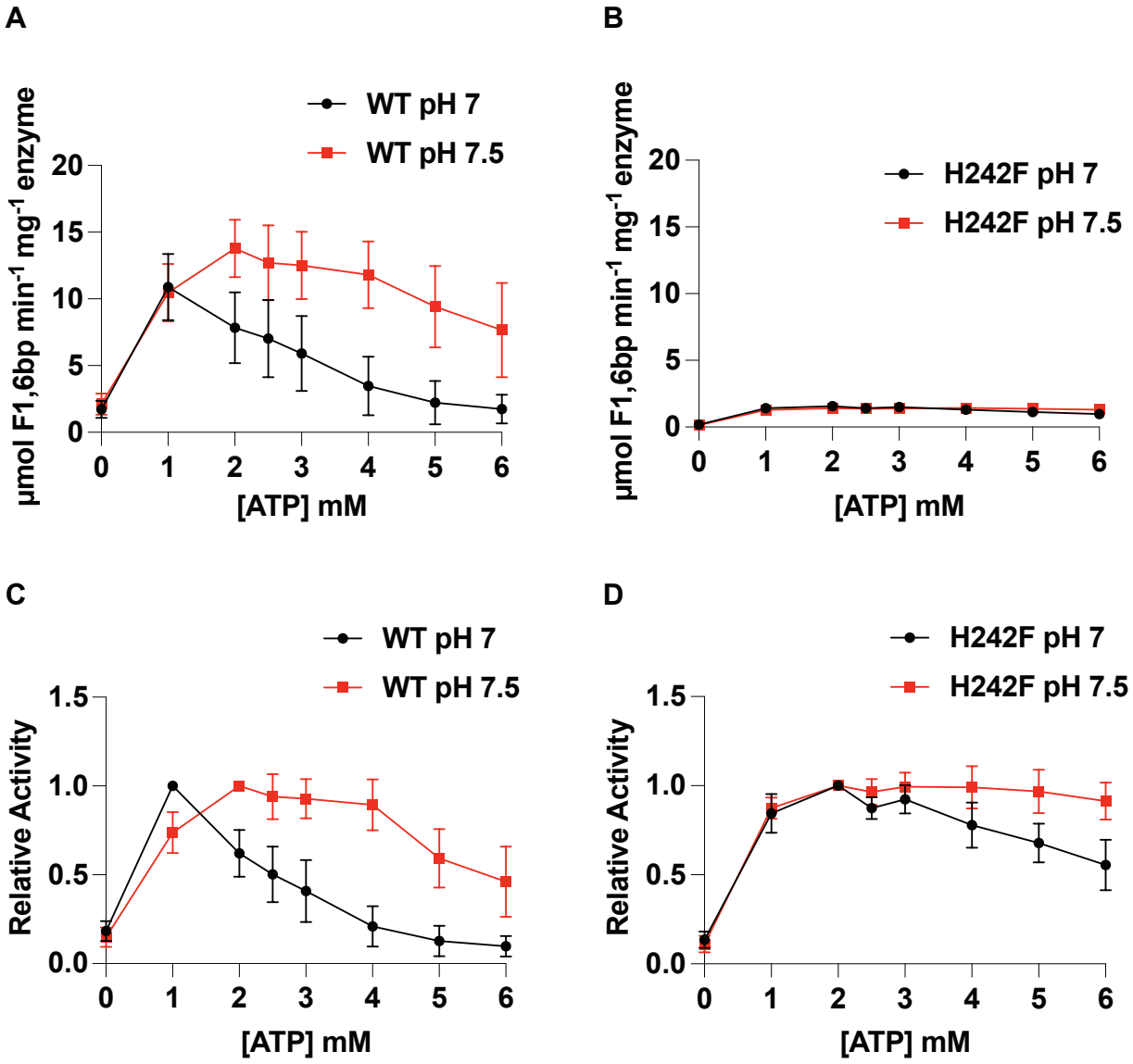

Figure 3.2. His242 is necessary for pH-dependent relief of allosteric ATP inhibition by human PFKL.

A,C. For WT PFKM, allosteric ATP inhibition is relieved at pH 7.5 compared with pH 7 for overall activity (A) and relative activity (C). PFKM-H242F has decreased overall activity (B) but relative activity has pH-independent relief of allosteric ATP inhibition (D) Data obtained at 1mM fructose 6-phosphate and expressed as µM F1,6bp min^{-1} mg^{-1} of enzyme (A,C) or relative to maximal activity (B,D). Data are means ± s.e.m. of six independent measurements with two separate protein preparations.

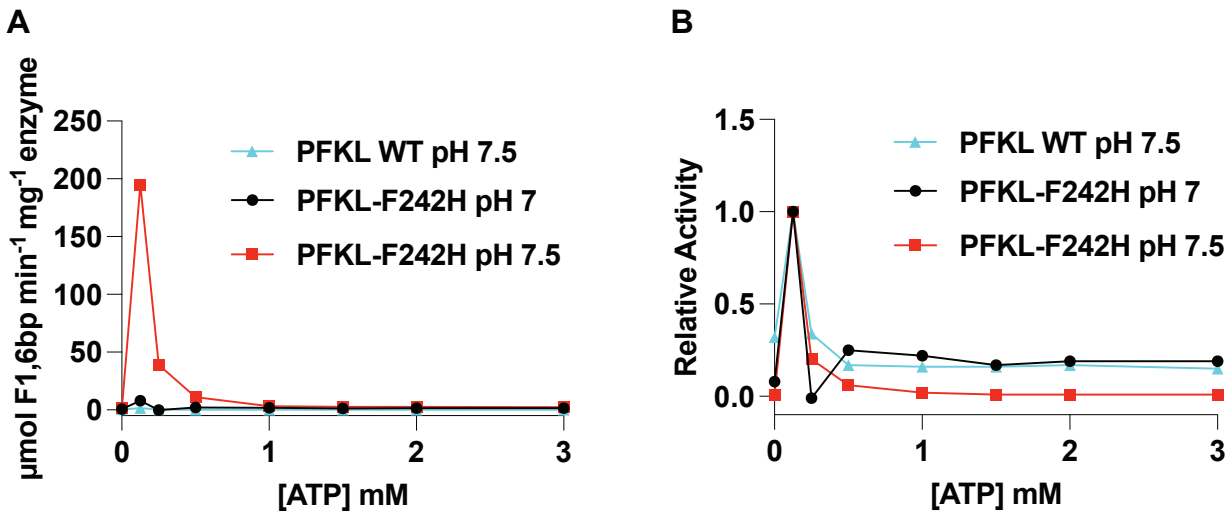

Figure 3.3. His242 is not sufficient for pH-dependent relief of allosteric ATP inhibition by human PFKL

A,B. Activity of PFKL WT at pH 7 (cyan), PFKL-F242H at pH 7 (black), and PFKL-F242H at pH 7.5 (red). (B) Overall activity expressed in µM F1,6bp min^{-1} mg^{-1} of enzyme. (C) Activity set relative to maximal at 0.125 mM ATP. Data are from one measurement and future independent measurements to be performed in future experiments.

Discussion and Future Directions

Although mechanisms regulating PFK-1 isoforms have been extensively studied and characterized (Colombo et al., 1975; Depre et al., 1993; Icard et al., 2012; Trivedi & Danforth, 1966; Webb et al., 2017a; Zheng & Kemps, 1992), how pH regulates PFKM activity is incompletely understood. Building on findings made nearly 50 years ago that increasing pH relieves allosteric ATP inhibition of PFKM activity (Trivedi & Danforth, 1966) and homology modeling with a recently resolved crystal structure of human PFKP (Webb et al., 2015b), we identified human PFKM-His242 as a critical pH-sensing residue. However, despite being necessary for pH regulated PFKM activity, it is not sufficient to confer pH-dependent relief of allosteric ATP inhibition of PFKL. We predict this may be due to a proximal Arg245 in PFKM upshifting the pKa of His242 and allowing titration of His242 in the physiological range. Future studies using PFKM-Arg245 mutants are necessary to confirm these predictions.

Why PFKM but not PFKP or PFKL evolved for pH-dependent relief of ATP inhibition remains an open question. While high glycolytic rate results in accumulating ATP, muscle cells must override a negative feedback of increased cellular ATP concentrations to limit glycolytic flux during times of anaerobic metabolic need. Previous work showed that during the first few seconds of muscle contraction, myocyte pHi rapidly increases from phosphocreatine hydrolysis (Adams et al., 1990). Further, with extended muscle contraction lactic acid accumulates and decreases pHi as a byproduct of anaerobic metabolism (Robergs et al., 2004). With high PFKM expression in muscle relative to other PFK-1 isoforms, it is plausible that pH-dependent relief of allosteric ATP inhibition of PFKM activity is a means to maintain or increase glycolysis during exercise despite accumulating cellular ATP. Further, we speculate that ATP inhibition of PFKM activity at low pH may inhibit glycolysis to protect cells from further lactic acid damage during acidification and thus fine tune the balance of high glycolytic flux.

Whether pH-dependent relief of allosteric inhibition by PFKM plays a role in cell behaviors regulated by pHi dynamics is unknown. While mouse embryonic stem cells (mESCs)

require a transient increase in pHi to differentiate to the epiblast (EpiSC) state (Ulmschneider et al., 2016), they also require metabolic reprogramming. In the naïve state, mESCs have a bivalent (glycolysis and oxidative phosphorylation) metabolism but there is metabolic shift to a reliance on glycolysis upon differentiation to EpiSCs (Mathieu & Ruohola-Baker, 2017; Zhou et al., 2012). Additionally, a hallmark of cancer cells is metabolic reprogramming to a glycolytic phenotype and have dysregulated constitutively increased pHi, which enables several cancer cell behaviors (Webb et al., 2011; White et al., 2018, 2019; White, Grillo-hill, et al., 2017; White, Ruiz, et al., 2017). Both in mESCs differentiation and cancer, this metabolic shift provides a distinct advantage where amino acid, lipid, and nucleotide synthesis are in high demand and can be fueled by glycolytic intermediates (Shyh-Chang & Ng, 2017). However, while previous work has focused on changes in metabolites and isoform expression in these contexts, a role for pH dynamics in regulating metabolic reprogramming has been reported (Chen et al., 2023; Designed Research; A, 2021; Inaishi et al., 2022; Ishfaq et al., 2022; Lim et al., 2022; Mahmoud, 2023; Moon et al., 2011; Rani et al., 2020; Tsogtbaatar et al., 2020) but remains incompletely resolved. It is possible that the high pHi during mESC differentiation and in cancer cells enables pH-dependent relief of allosteric ATP inhibition of PFKM activity to bypass the negative feedback loop of increased cellular ATP. Future studies to determine whether there is a shift in PFK-1 isoform expression to primarily PFKM for a pH-dependent increase in glycolysis during mESC differentiation or cancer progression would provide insights on how pHi can directly regulate metabolism in distinct cell behaviors.

Methods

Cloning, expression, and purification of recombinant human PFK-1

Homo sapiens PFKM and PFKL cDNA was cloned into the pFastBac HTb vector and site directed mutagenesis was performed for PFKM-H242F and PFKL-F242H using a commercially available mutagenesis kit (QuikChange Lightning, Aligent). Primers for mutagenesis were designed using ApE OSX Mavericks+ software and were obtained from Elim Biopharmaceuticals. Successful mutagenesis was confirmed by sequencing (QuintaraBio). PFKM WT and His242Phe baculovirus were generated according to the Bac-to-Bac Expression systems protocol (Invitrogen). 1 x 10^8 SF21 cells (*S. frugiperda)* were infected for 48 hours with baculovirus to generate recombinant enzyme. Cells were pelleted by centrifugation at 800xg for 5 minutes and re-suspended in 25 mL of lysis buffer (20mM Tris-HCl pH 7.5; 10mM imidazole; 10% glycerol; 1 mM 2-mercaptoethanol; 80mM potassium phosphate; one half tablet of cOmplete Protease Inhibitor Cocktail tablet [Roche]) and lysed with 15 passes of a dounce homogonizer. To remove cellular debris, lysed samples were centrifuged for 30 minutes at 11500 rpm and the pellet discarded. The supernatant was incubated with 3 mL of 50% slurry of TALON Superflow resin (GE Healthcare) and washed with 10 bed volumes of lysis buffer three times. Protein was eluted three times with 1 mL each time of elution buffer (lysis buffer with 100mM imidazole). Protein concentration was calculated using the BCA assay and elutions with greater than 100ng/µl were pooled and dialyzed in 2 liters of dialysis buffer (20mM Hepes pH 7.5; 1mM DTT; 1mM ATP; 5% Glycerol) using 10,000 MWCO SnakeSkin dialysis tubing (Thermo Scientific) for one hour and then with fresh dialysis buffer overnight at 4˚C. Dialyzed purified protein final concentration was calculated by the BCA assay and aliquots were flash-frozen in liquid nitrogen and stored at -80 ˚C.

Sequence Alignment of PFK-1 Isoforms and Structural Analysis of PFKM Inhibitory ATP pocket

PFKM, PFKL, and PFKP amino acid sequences, downloaded from NCBI, were aligned using the publicly available ClustalOmega online software (https://www.ebi.ac.uk/Tools/msa/clustalo/). Residues 232-268 are shown for PFKM and PFKL and residues 241-277 are shown for PFKP.

Enzyme Activity Assay

A previously described auxiliary enzyme assay was used as a measure of PFKM activity (Brüser et al., 2012; Webb et al., 2015a). The assay was performed in a 200µL reaction containing 100µL 2XE buffer (50mM Hepes at pH 7.0 and 7.5; 200mM KCl; 2mM DTT; 0.675 units/ml aldolase; 5 units/ml triosephosphate isomerase; and 2 units/ml glycerol phosphate dehydrogenase; 0.45mM NADH added after desalting of auxiliary enzymes). PFKM concentrations were normalized at 10x concentrations in H_2O for a total of 3.125ng for WT and 18.8ng for PFKM-H242F per reaction. Fructose-6-phosphate was used at a final concentration of 1mM and ATP was used as indicated. The reaction volume was made to 180µL with H_2O and plates were incubated at 25 ˚C for 10 minutes before addition of 20µL 100mM $MgCl_2$ to start the reaction. Absorbance at 340 nm was measured using a SpectraMax M5 microplate reader (Molecular Devices). Overall activity was determined as the amount of enzyme that catalyzed the formation of 1mmol of fructose 1,6-bisphoshate per minute at 25˚C. Relative activity was normalized to the ATP concentration with maximal activity for each condition; 1 mM ATP for WT at pH 7, 2 mM ATP for WT at pH 7.5, and 2 mM ATP for PFKM-H242F at both pH 7 and 7.5.

PFKM Activity pH titration

The activity of recombinant WT PFKM was determined using a modification of the auxiliary enzyme assay described above. The maximal inhibitory concentration of 4mM ATP at pH 7 in the presence of 0.5mM fructose 6-phosphate was determined empirically and used for these

assays. MOPS and HEPES buffers were used for pH 6.8–7.6 and 7.4–8.2, respectively. Activity was determined at pH 7.4 and 7.6 in both MOPS and HEPES buffer to confirm the buffer system does not affect activity. All other experimental parameters remained consistent. Data are expressed relative to maximal activity and are means ± s.e.m of seven separate measurements with two different protein preparations.

CHAPTER 4: SMALL MOLECULES INCREASE MUTANT p53-R273H BINDING TO DNA

Introduction

Most cancer cells, regardless of their tissue origin or mutational signature, have a constitutively higher cytosolic intracellular pH (pHi) of >7.5 than untransformed cells. A higher pHi can enable cancer progression through multiple mechanisms, including increasing cell proliferation (Flinck et al., 2018b; Parks et al., 2017; Putney & Barber, 2003; Spear & White, 2023), tumorigenesis (Grillo-Hill et al., 2015; Parks et al., 2013), metabolic reprogramming.(Counillon et al., 2016; Hardonnière et al., 2016; Man et al., 2022; Manoli et al., 2021), and metastasis (X. Li & Fliegel, 2022; Toft et al., 2021; Zhang et al., 2022). Recent findings revealed an additional previously unreported mechanism of a higher pH enabling cancer progression - by promoting the tumorigenic function of proteins with charge-changing somatic mutations (De Oliveira et al., 2022; Luna et al., 2020; White, Ruiz, et al., 2017)

Although not widely acknowledged, charge-changing somatic mutations are highly recurrent in cancers (Alexandrov et al., 2020) and occur independently of codon bias and CpG-site frequency (Szpiech et al., 2017). Moreover, cancer types dominated by charge changing mutations were revealed by categorizing cancers by amino acid mutations, in contrast to classifications by tissue origin or nucleotide mutation (Anoosha et al., 2016; Szpiech et al., 2017). For example, melanoma and bladder and cervical cancers are enriched in glutamic acid to lysine mutations, which substitute a negatively charged amino acid for a positively charged amino acid. In contrast, pancreatic and prostate cancers are dominated by arginine to histidine mutations, which substitute a positively charged amino acid to titratable amino acid. Whereas arginine (pKa ~12) should always be protonated, histidine (pKa ~6.5) can titrate within the cellular pH range. Hence Arg>His mutations have the potential to confer a gain in pH sensing compared with wild-type proteins being pH-insensitive within the cellular pH range. Examples confirming a gain in pH sensing with a higher pH enabling tumorigenic behaviors include EGFR-R776H (White, Ruiz, et al., 2017), IDH1-R132H (Luna et al., 2020), and p53-R273H (White, Ruiz, et al., 2017).

Targeting these electrostatic changes as a therapeutic approach to restore wild-type protein function has received limited attention (Sun et al., 2022; Tsuber et al., 2017). Our current study focused on the tumor suppressor protein p53 and identifying small molecules that could restore transcriptional activity of mutant p53-R273H that is attenuated at the higher pHi of cancer cells. Amino acid substitutions at Arg273 are the most frequent point mutations in p53, and 40% of these are Arg>His (Forbes et al., 2017b). In wild type p53, positively charged Arg273 binds the negatively charged phosphate backbone of DNA. Although protonated His273 can retain DNA binding, albeit at a lower affinity than wild type, deprotonated His273, which can occur at the higher pHi of cancers, substantially decreases DNA binding and transcriptional activity (White, Ruiz, et al., 2017). We used *in silico* modeling, *in vitro* protein biochemistry, and luciferase assays in cells to identify two bioactive compounds from commercial libraries that increase DNA binding affinity of p53-R273H at higher pH, with promise as a cancer therapeutic. Additionally, this work paves a new direction in therapeutics targeting charge-changing mutations broadly. In addition to a high incidence in cancers, recurrent Arg>His mutations are associated with other diseases, including ACVR1-R206H in fibrodysplasia ossificans progressiva (Kaplan et al., 2012), CFTR-R117H in cystic fibrosis (Yu et al., 2016), TCF4-R578H in Pitts-Hopkins syndrome (Whalen et al., 2012), and βB2-crystallin in cataracts (Xi et al., 2014), which highlights the value of our approach using small molecules targeting histidine substitutions to restore protein function.

Results

p53-R273H confers a gain of pH-dependent binding to DNA in vitro.

Our previous work established a gain of pH-sensing by p53-R273H, with decreased DNA-binding and transcriptional activity at the higher pHi of cancer cells (White, Ruiz, et al., 2017). To test for small molecules that might restore p53-DNA binding at high pH, we first developed an *in vitro* DNA-binding assay with recombinant p53 wild type (WT) and mutant p53-R273H. We expressed and purified thermostable WT and Arg273His 6x-His-p53 and determined association constants (K_A) to an established 6'FAM labeled GADD45 promoter sequence by using fluorescence anisotropy (Ang et al., 2006). We confirmed that high affinity binding of WT p53 to DNA is pH-independent and not different at pH 7 (K_A of 8.38 ± 1.13 μM) compared with pH 7.6 (K_A of 6.54 ± 1.74 μM) (**Fig. 4.1A,C**). In contrast, we found that p53-R273H binding to DNA is pH sensitive. Binding of p53-R273H at pH 7.0 (K_A of 0.541 ± 0.06 μM) is markedly less than WT and at pH 7.6 is significantly less than at pH 7.0 (K_A of 0.137 ± 0.03 μM) (**Fig. 4.1B,C**). Although previous work in cells determined that at pH 7.1 p53-R273H retained more than 50% of WT activity (White, Ruiz, et al., 2017), our *in vitro* DNA binding data suggest a 10-fold lower affinity of the mutant compared with WT p53 at pH 7.0. However, we concluded that our *in vitro* binding protocol would be adequate to test bioactive compounds as putative small molecules that rescue the reduced DNA binding by p53-R273H at high pH.

In silico identification of putative compounds for restoring DNA binding of p53-R273H.

Although there are on the order of millions of bioactive compounds commercially available, we applied increasingly more stringent filters to a select relatively few putative compounds that might rescue of DNA binding of p53-R273H at higher pH based on 1) molecular properties and 2) *in silico* docking predictions (**Fig. 4.2A**). In collaboration with the Emil Alexov group at Clemson University, we started from a database of 3.5 x 10^6 compounds pooled from ChemBridge, ChemDiv, and Life Chemicals libraries (**Fig. 4.2B**). With an objective to restore a

positive charge at residue His273 at high pH, our first pass filter was any molecule with an overall +1 charge, which yielded 6 x 10^5 potential compounds (**Fig. 4.2A,C**). We next defined the search space of 20 x 20 x 20 Å specifically surrounding residue H273 and used AutoDock Vina to determine predicted distance from the center of a compound to His273 and its predicted affinity. We filtered results for cutoffs of <10 Å distance and <-8kcal/mol predicted binding affinity, the latter being a stringent cutoff consistent with currently FDA approved targeted drugs (Akinlalu et al., 2021). To filter for residue specificity, we next defined the search space as 53x54x59 Å surrounding the entire p53-DBD, performed docking, and compounds predicted to bind any other residue <-8kcal/mol were eliminated (**Fig. 4.2D,E**). With these *in silico* data, we identified 48 compounds (**Table 5.1**) predicted to restore a positive charge specifically at His273 and possibly restore higher affinity binding to DNA (**Fig. 4.2F**). Taken together, these data generated a feasible number of candidate compounds to test for increasing DNA binding by p53-R273H.

Initial DNA binding reveals 10μM K788-8393 and F2636-0583 rescue at least 50% p53-R273H DNA binding at pH 7.6

All 48 compounds were commercially available, which we obtained and tested using fluorescence anisotropy as described above. For an initial screen we determined which compounds at a single p53-R273H concentration of 1.84 μM could increase by 50% DNA binding at pH 7.6. We found that 46 compounds at 10, 1, and 0.5 μM do not reach the 50% rescue threshold. In contrast, we found that two compounds, K788-8393 and F2636-05, at 10μM rescue at least 50% binding at pH 7.6 compared with pH 7 controls (**Fig. 4.3A,B**)

K788-8393 and F2636-0583 increase binding affinity of p53-R273H to DNA at pH 7.6.

We next determined DNA binding affinities for these two compounds by using protein titrations with DMSO controls or 10 μM of each compound. We found that binding of p53-R273H in

DMSO controls is pH-dependent and greater at pH 7 (K_A of 0.541 ± 0.06 μM) compared with 7.6 (K_A of 0.137 ± 0.03 μM) as expected (**Fig. 4.4A-C**). In contrast, binding at pH 7.6 is significantly greater with10 μM K788-8393 (K_A of 0.322 ± 0.04 μM) (**Fig. 4.4A,C**). Binding at pH 7.6 is also greater with 10 μM F2636-0583 (K_A of 0.415 ± 0.21 μM) (**Fig. 4.4B,C**); however data with F2636-0583 are from 2 determinations and further biological replicates are needed to determine whether there is a significant increase. Taken together these data suggest that these two compounds partially restore binding to DNA at pH 7.6 and warranted determining whether either can rescue pH-independent transcriptional activity.

Small molecules increase DNA binding of p53-R273H in cells.

To determine whether K788-8393 and F2636-0583 rescue p53-R273H transcriptional activity at the high pHi (~7.7) of cancer cells, we used the previously established luciferase assay (White, Ruiz, et al., 2017) with MDA-MB-436 human breast cancer cells and lowering pHi to 7.4 with the selective NHE1 inhibitor EIPA. MDA-MB-436 cells lack p53 and we generated lines stably expressing either p53-WT or p53-R273H. Previous work by White et al. (White, Ruiz, et al., 2017) showed that for cells expressing WT p53, reporter activity is not different at pHi 7.0 compared with 7.6. In contrast, we confirmed that cells expressing p53-R273H have significantly lower transcriptional activity at pHi 7.7 compared with pHi 7.4, and overall activity is reduced compared with WT at both pH values (**Fig. 4.5A**). We then determined whether K788-8393 and F2636-0583 can increase activity of p53-R273H. For DMSO controls we confirmed previous findings of pH-dependent p53 activity and find roughly 3-fold decreased activity at pH 7.7 compared with pH 7.4. However, in cells treated with 10 μM K788-8393, activity is increased at both pHi 7.4 and at pHi 7.7 where there is roughly 80% transcriptional activity compared with DMSO controls at pHi 7.4 (**Fig. 4.5B**). Further, cells treated with 10 μM F2636-0583 also have increased p53-R273H activity at pH 7.7 compared with DMSO controls at pH 7.7. However, with F2636-0583 p53-R273H activity at pHi 7.4 is decreased compared with DMSO controls at pHi

7.4 (**Fig. 4.5B**). Taken together, these data suggest that K788-8393 increases p53-R273H activity in cells at both pH 7.4 and 7.7, which warrants further studies to determine promise as a therapeutic to increase tumor suppressor function in cancer cells with a p53-R273H mutation.

Figures

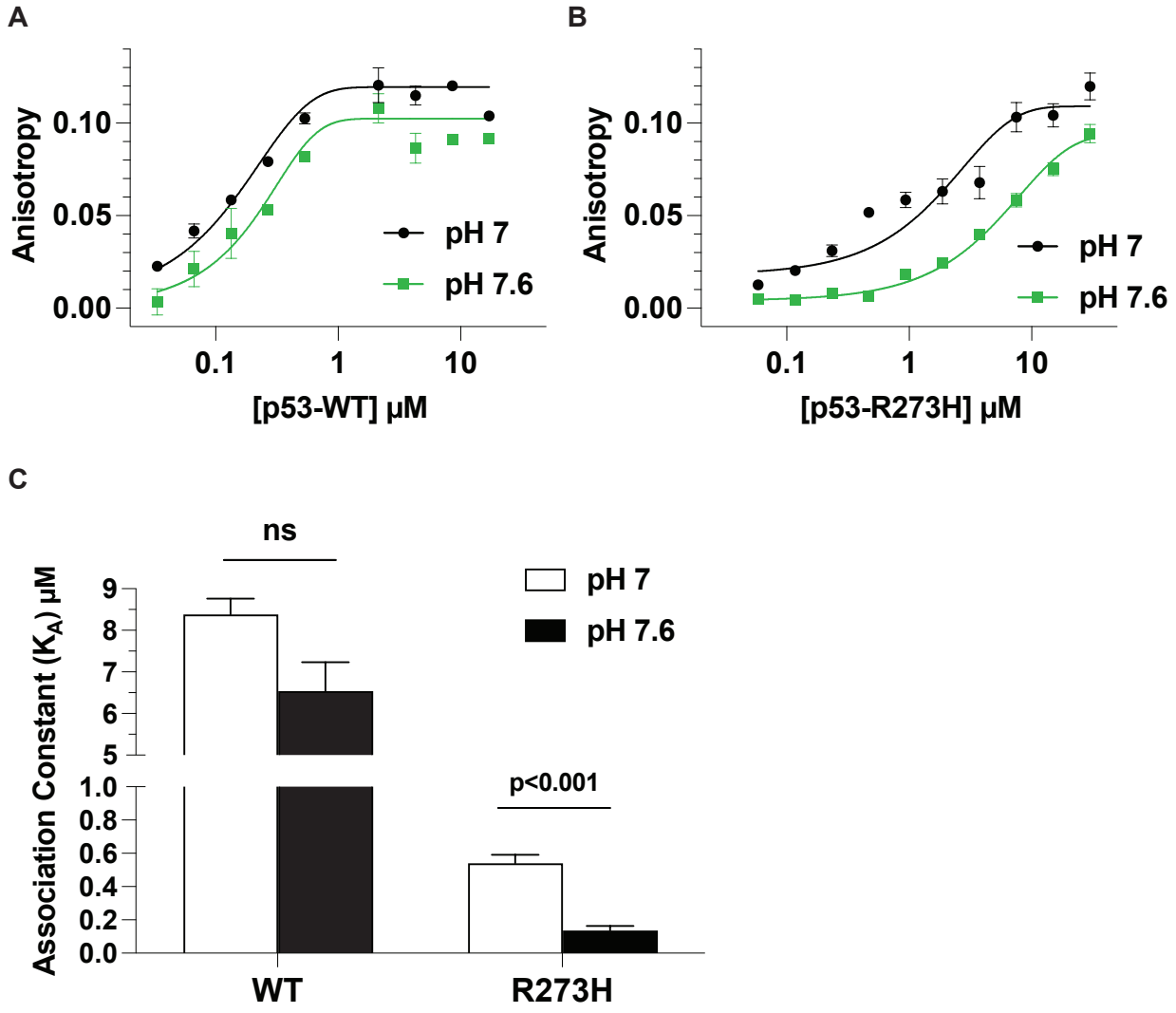

Figure 4.1. p53-R273H confers a gain of pH-dependent binding to DNA in vitro.
A,B. Binding curves for p53 to a 6'FAM labeled GADD45 promoter DNA at pH 7 and 7.6 for (A) WT and (B) Arg273His. C. Association constants calculated from binding curves. For WT p53, data are averages of two independent measurements ± s.e.m. For p53-R273H, data are averages of seven independent measurements from two separate protein preparations ± s.e.m. Binding affinities were analyzed by two-tailed unpaired Student's t-test.

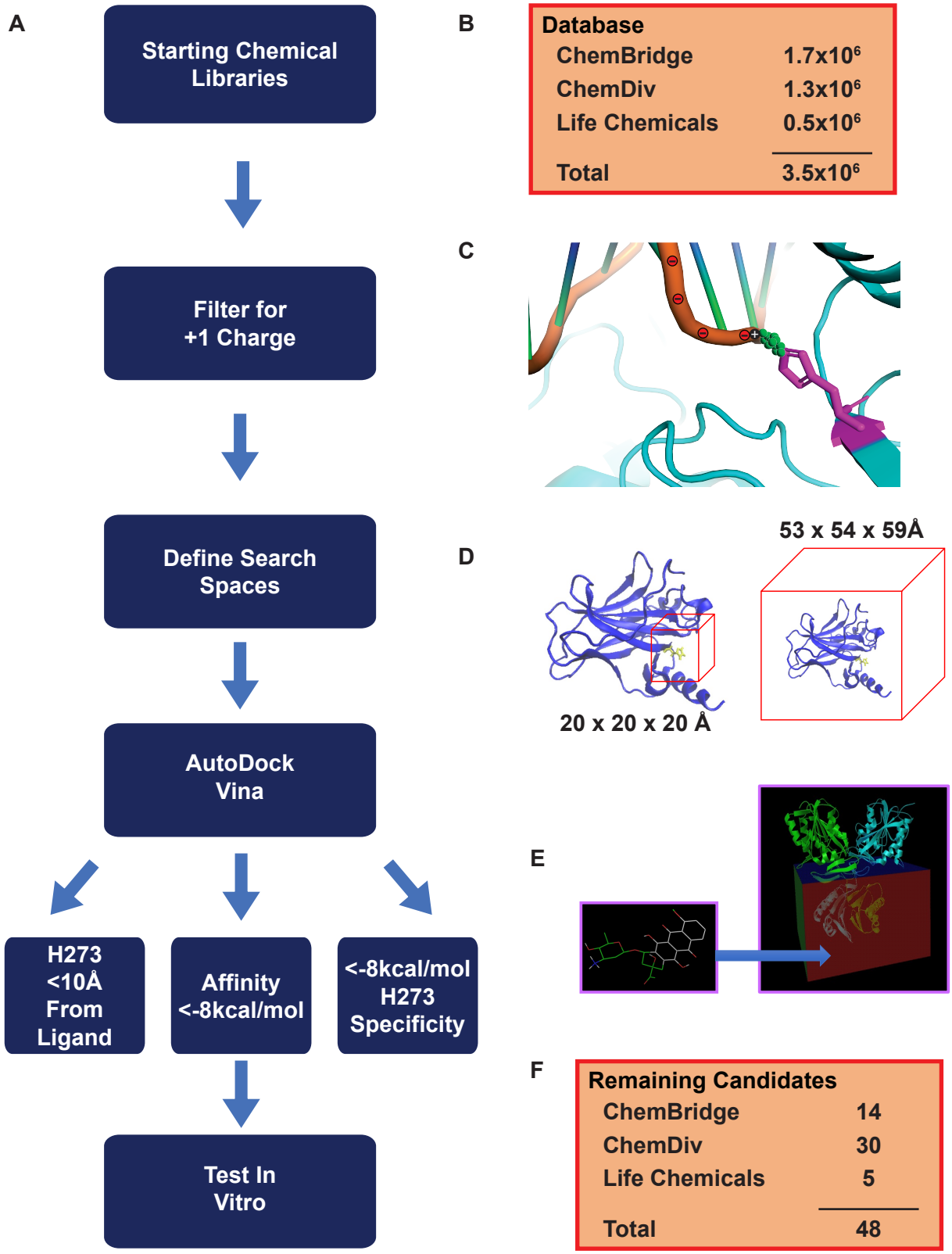

Figure 4.2. In silico identification of putative compounds for restoring DNA binding of p53-R273H. Figure caption continued on the next page.

Figure caption continued from the previous page. A. Schematic of workflow for filtering compounds from bioactive compound libraries. B. Starting number of compounds from three different compound libraries. C. Filter for compounds with a +1 charge necessary to restore electrostatic binding to DNA phosphate backbone. D. Search space defined to 20 $Å^3$ surrounding p53-R273H or the entire p53- DBD at 53 x 54 x 59 Å. E. +1 charge compounds docked to p53-DBD using AutoDock Vina and filtered for predicted distance, affinity, and specificity. F. Compounds remaining (48) for testing *in vitro* DNA binding.

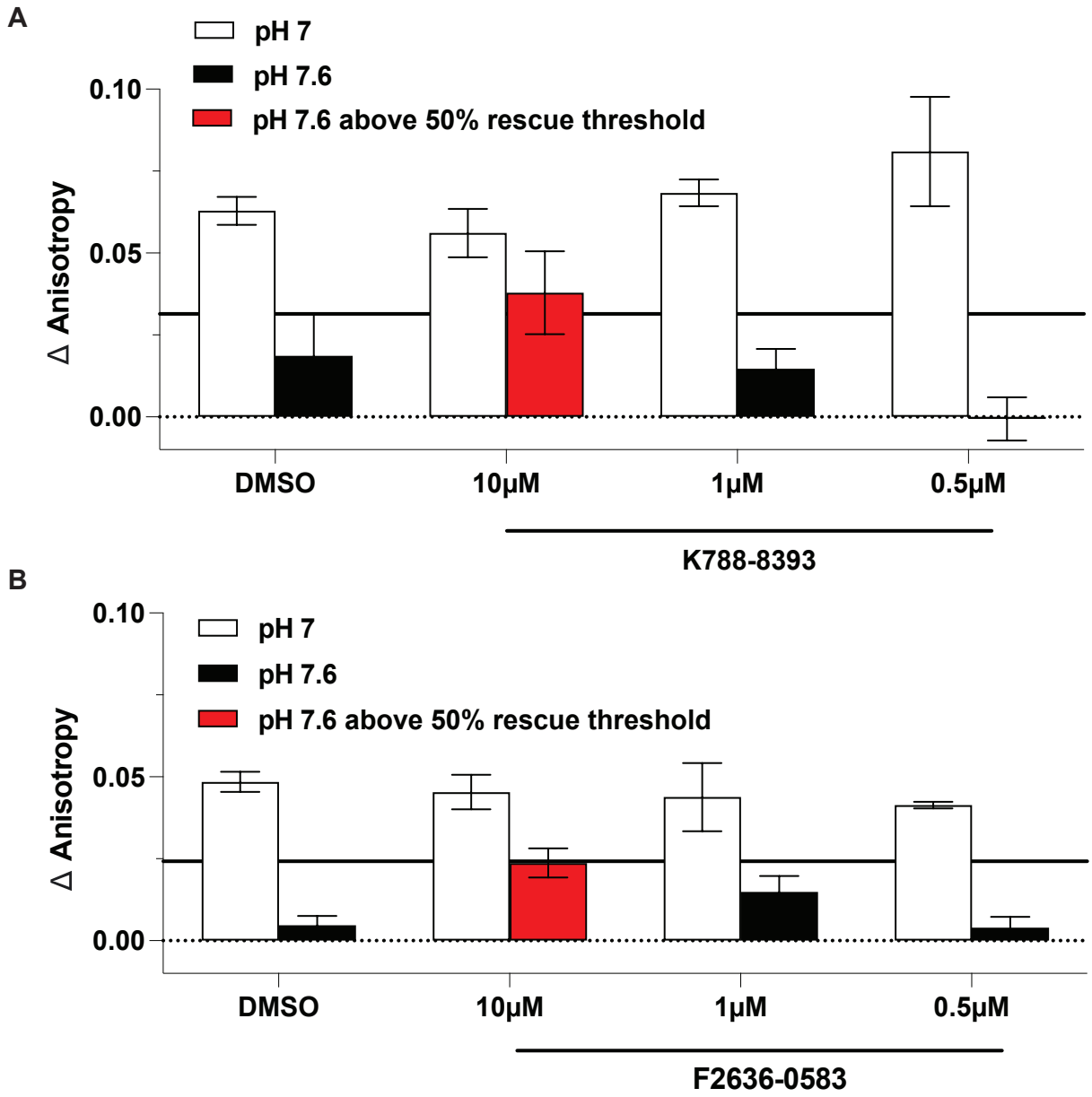

Figure 4.3. Initial DNA binding reveals 10μM K788-8393 and F2636-0583 rescue at least 50% p53-R273H DNA binding at pH 7.6.

A,B. Δ Anisotropy of p53-R273H to a 6'FAM labeled GADD45 promoter DNA with DMSO or 10μM, 1μM, or 0.5μM of compounds for (A) K788-8393 and (B) F2636-0583. Black line represents 50% threshold of pH 7 binding. Red columns are compounds and concentrations that cross the 50% threshold for further analysis. Data are averages of three independent measurements ± s.e.m.

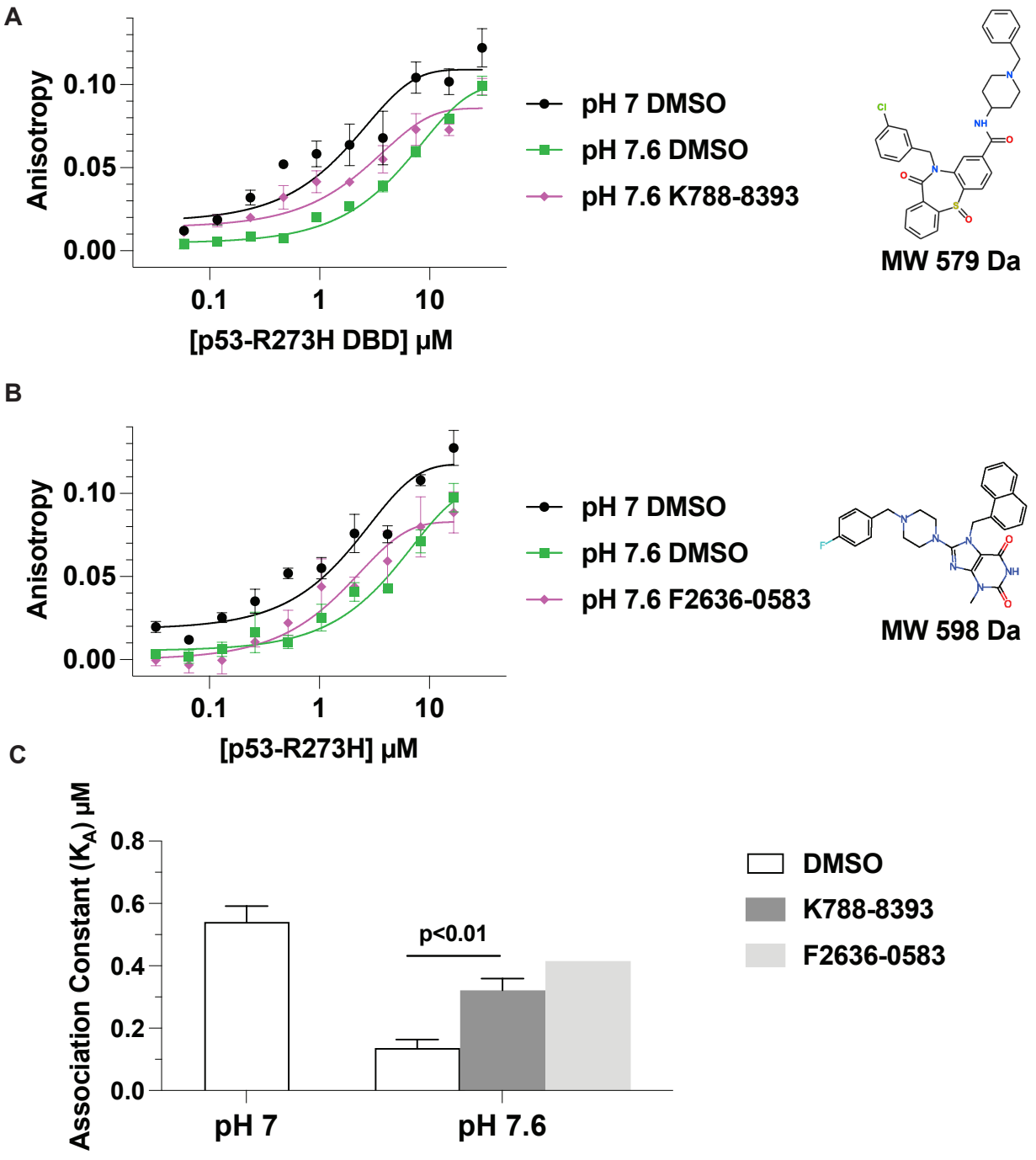

Figure 4.4. 10μM K788-8393 and F2636-0583 increase binding affinity of p53-R273H to DNA at pH 7.6.

A,B. Binding curves for p53-R273H to a 6'FAM labeled GADD45 DNA with DMSO or 10μM compounds for (A) K788-8393 with structure and molecular weight and (B) F2636-0583 with structure and molecular weight. C. Association constants calculated from binding curves. For K788-8393 data are means ± s.e.m of four independent measurements from two protein preparations. For F2636-0583 data are means of two independent measurements from two protein preparations. Binding affinities were analyzed by two-tailed unpaired Student's t-test and with a significance level of $p<0.05$

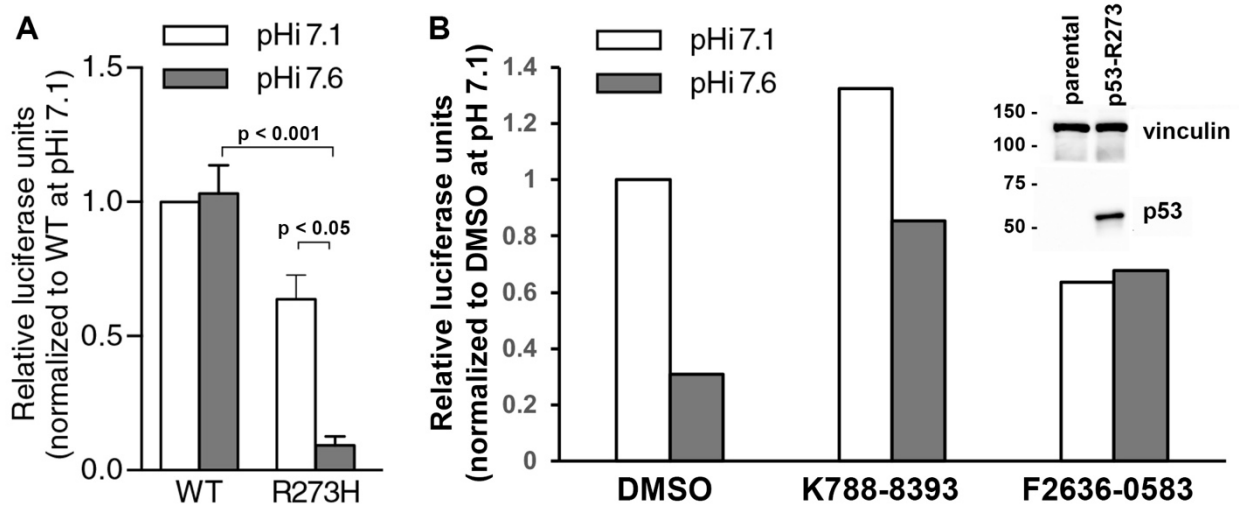

Figure 4.5. Small molecules increase DNA binding of p53-R273H in cells.
A. Luciferase assay with p53 WT or R273H at indicated pHi. Data are from White et al., 2017 Sci Signaling 10(495). pii: eaam9931. B. New data with luciferase assay in MDA-MB-436 cells stably expressing p53-R273H (immunoblot insert) at indicated pHi in the absence (DMSO) or presence of indicated small molecules at 10 μM for 48h. MDA-MB-436 cells have a steady-state pHi of 7.6 that was lowered to pHi 7.1 by treating for 48h with EIPA. Data are averages of quadruplicate measurements of a single assay.

Tables

Table 4.1. List of compounds identified from in silico screen.

Compound Library	ID	Molecular Weight (Da)
ChemBridge	68508566	390
	75075515	534
	93916792	452
	97197044	418
	33299690	422
	45907527	574
	56509142	372
	18553682	362
	22203565	374
	49075262	405
	49843984	383
	57265621	395
	67836493	525
	7741492	364
ChemDiv	3389-2657	438
	5629-0128	474
	6165-0040	496
	8013-0340	579
	8013-2585	503
	8015-0610	426
	8015-5759	478
	8015-5860	527
	8016-7906	467
	8017-8776	426
	8017-9097	476
	C094-2369	447
	C529-0553	570
	C529-0817	554
	C529-1046	627
	C620-0716	505
	D447-0399	480
	E239-0316	517
	F486-0998	468
	F486-1201	454
	G281-2538	515
	G768-0187	488
	G768-0613	492
	K788-8393	584
	L679-0465	473

Continued from the previous page.

Compound Library	ID	Molecular Weight (Da)
ChemDiv	S733-0399	449
	SB80-0440	449
	SB80-1052	453
	SB80-1349	465
Life Chemicals	F0843-0035	490
	F2925-0640	484
	F6548-3610	492
	F2636-0583	499
	F2925-0109	480

Discussion and Future Directions

Charge changing somatic mutations are overrepresented in several cancers and can confer a gain or loss of pH-sensing at the higher pHi of cancer cells (Szpiech et al., 2017; White, Ruiz, et al., 2017). We previously reported that the recurrent p53-R273H mutant but not WT p53 has pH-dependent DNA binding, with decreased binding and tumor suppressor activity at higher (7.6) compared to lower (7.0) pH ((White, Ruiz, et al., 2017). Of relevance for therapeutic promise, we asked whether Arg>His substitutions can be targeted by small molecules to restore a pH-independent protein function, with a current focus on restoring DNA binding by p53-R273H. We describe a pipeline with computational docking to identify putative small molecules from bioactive compound libraries that might confer a positive charge to p53-R273H at the higher pHi of cancer cells and use biochemical assays to reveal two compounds that increase DNA binding of p53-R273H at high pH.

The two compounds, K788-8393 and F2636-0583 that increase binding of p53-R273H to DNA are both small molecules (< 1000 Da) and have relatively small total polar surface areas (Matsson & Kihlberg, 2017). However, compound efficacy (EC_{50} and IC_{50}), off-target effects, and general cytotoxicity, although possible to evaluate empirically (Brooks et al., 2019), remain to be determined in cells. While our *in vitro* and cell reporter data show that each compound increased p53-R273H binding and transcriptional activity at the higher pHi of cancer cells, our future objective is to determine whether each compound rescues a cellular functional response such as tumor suppression. Additionally, we will determine whether compounds increase percent cell death in response to double strand DNA breaks in cells expressing p53-R273H like p53 WT to determine functional rescue of apoptosis (White, Ruiz, et al., 2017).

While lowering pHi by inhibiting plasma membrane ion transport proteins such as NHE1 attenuates cancer cell behaviors (Grillo-Hill et al., 2015; White, Grillo-hill, et al., 2017; White, Ruiz, et al., 2017), there remain concerns about specificity and disrupting critical homeostatic mechanisms that require pHi dynamics (Choi et al., 2013; Denker & Barber, 2002; Frantz et al.,

2007, 2008; Gao et al., 2014; Jensen et al., 2019; Li et al., 2009; Magalhaes et al., 2011; Srivastava et al., 2008). Our proposed therapeutic approach with small molecules provides an alternative that we predict would have greater specificity with effects only in cells expressing p53-R273H but not WT. Future studies *in vitro* are needed to confirm AutoDock Vina predictions that compounds are specific to a His but not an Arg at the 283 site, which we are currently testing by using FOXC2-DNA binding as described in Chapter 2. We predict small molecule rescue of charge can be applied to other charge changing mutations that enable cancer and other diseases. For example, the recurrent mutation in EGFR-R776H confers a gain in pH-sensing at high pHi where His776 deprotonation promotes the active receptor conformation leading to hyperactive growth factor signaling (White, Ruiz, et al., 2017). Additionally, we predict several other recurrent charge-changing somatic mutations including SMAD4-R361H, DDX3X-R534H, and FBXW7-R465H may confer a gain in pH-sensing for a functional advantage at the higher pHi of cancer cells. However, disease-promoting charge changing mutations are not exclusive to cancer and include ACVR1-R206H for fibrodysplasia ossificans progressive (Kaplan et al., 2012), CFTR-R117H for cystic fibrosis (Yu et al., 2016), and TCF4-R578H for Pitts-Hopkins syndrome (Whalen et al., 2012). Hence, our approach to target charge-changing mutations to restore wild-type protein function could be applied broadly. Taken together our findings address rescue of one of the most mutated genes in cancer, and also broadly open new directions in targeted therapeutics for pathologies caused by charge changing mutations.

Methods

Cloning and Protein Expression

Thermostable tetrameric recombinant p53 was generated as previously described (Ang et al., 2006). In brief, we ordered a synthesized gBlock (IDT) coding for the DNA binding and tetramerization domains (94-361) with thermostabilizing mutations M133L/V203A/N239Y/N268D (Ang et al., 2006; Joerger et al., 2004; Nikolova et al., 1998). The gBlock was amplified for Gibson assembly and inserted in a XhoI and EcoRI predigested N-terminal 6x-His tag coding pET28a plasmid using Gibson Assembly Master Mix (NEB: E2611L). The p53-R273H point mutation was generated using a QuikChange Lightning site-directed mutagenesis kit (Agilent: 210515) was used according to the manufacturer protocol. Each construct was transformed into BL21-DE3 *Escherichia coli* competent cells using heat shock (Thermo EC0114). For expression, cells were grown in 1L of Luria broth with kanamycin (50 µg/mL; 37°C with shaking at 225 rpm) until cells reached log-phase growth at OD_{600} = ~0.4. Expression was induced with 1 mM isopropyl-β-D-1-thiogalatapyranoside for 16 hours at 18°C with shaking at 225 rpm. Cells were pelleted (7000g; 15 min at 4°C) and either frozen at -80°C or continued directly to protein purification.

6x-His-p53 Protein Purification

Bacterial cell pellets were resuspended in 50mL of lysis buffer (50mM HEPES, 500mM NaCl, 5% glycerol, 20mM Imidazole, protease inhibitor cocktail [Roche: 1183615300) as previously described (Guiley & Shokat, 2023). Cells were lysed by two passes through a microfluidizer at 10,000 PSI with coils on ice (Microfluidics LM10). The supernatant was clarified by centrifugation (12,000g; 30 min at 4°C) and mixed 1:1 with equilibration buffer (20mM sodium phosphate, 300mM NaCl, 10mM imidazole, pH 7.4) from 6x-His purification kit (Thermo: 88229). 12.5mL of lysate was loaded on pre-equilibrated 3mL Ni-NTA resin spin columns, incubated end over end for 30 min at 4°C and repeated until all lysate was used. The flowthrough was

collected by centrifugation (700g; 2 min at 4°C) and columns were washed with 6 mL of wash buffer (20mM sodium phosphate, 300mM NaCl, 25mM imidazole, pH 7.4) three times. 6x-His-p53 was eluted with 3mL of elution buffer (20mM sodium phosphate, 300mM NaCl, 250mM imidazole, pH 7.4). Each fraction was collected, run on a 10% SDS-PAGE gel, and coomasie stained for purity analysis. Eluate fractions were pooled, split in half, concentrated, and buffer exchanged in two separate anisotropy buffers (20mM Hepes, 140mM KCl, 0.05mM TCEP-HCl, pH 7 or 7.5) using Amicon Ultra-15 Filters with a 10 kDa molecular weight cutoff (MilliporeSigma: UFC901008). The protein concentration was determined by A_{280} using NanoDrop spectrophotometer (Thermo: ND-1000), aliquoted, flash frozen in liquid nitrogen, and stored at -80°C.

p53 Anisotropy Assay

6x-His-p53 protein aliquots were thawed at room temperature and diluted to 20μM in a final volume of 120μL in anisotropy buffer pH 7 and 7.6. Protein was serial diluted in PCR strip tubes ten times to a volume of 60μL. Then, 10μL of previously described 6'FAM labeled duplex *Gadd45* promoter p53 recognition element (GTACAGAACATGTCTAAGCATGCTGGGGAC) (IDT) (Ang et al., 2006) was added to each protein dilution and one blank for a final concentration of 7.5nM DNA and 70μL reaction volume. PCR strip tubes were capped and incubated at RT in the dark for 30 min. Following incubation, 20μL of each dilution and blank was loaded in triplicate to a 384-well black plate (Greiner: 784076) using a multichannel pipette. Fluorescence anisotropy measurements were made using a SpectraMax M5 plate reader (Molecular Devices). Sigmoidal curve fits were generated using GraphPad Prism and association constants determined using Mathematica software to solve for K_D in equation $A_{obs} = A_0 + (\Delta A * T)/(K_D + T)$ where A_{obs} is observed anisotropy, A_0 is anisotropy of initial unbound probe, ΔA is difference in anisotropy between unbound and fully bound populations, and T is

concentration of titrant protein. K_A was determined as ($1/K_D$). Binding affinities were analyzed by two-tailed unpaired Student's t-test and with a significance level of $p<0.05$.

In silico docking of p53 with compound libraries for putative hits

Bioactive compound libraries from ChemBridge, ChemDiv, and Life Chemicals were downloaded and filtered for an overall +1 charge using Python. Remaining compounds were docked to 20 $Å^3$ surrounding p53-R273H or the entire DBD at 53 x 54 x 59 Å using AutoDock Vina (Eberhardt et al., 2021; Trott & Olson, 2009). Compounds predicted to bind His2273 <10Å from molecular centers and binding affinities <-8kcal/mol specific to His273 were kept in the list for testing *in vitro*.

p53 Anisotropy Assay Initial Screen

To determine compounds from putative hits identified *in silico* for further analysis, we performed a modification of the anisotropy assay described above. Briefly, 3x final concentrations p53-R273H (6μM), 6'FAM-*Gadd45* (22.5nM), and DMSO or compound dilutions (30μM, 3μM, 1.5μM) were made up separately in anisotropy buffer pH 7 or 7.6. Then, 3x compound dilutions and 3x +/- protein were pre-incubated 1:1 for 15 min at RT to avoid potential compound binding directly to DNA probe. Following pre-incubation, 3x 6'FAM-*Gadd45* was added 1:1:1 for final concentrations of p53-R273H (2μM), 6'FAM-Gadd45 (7.5nM), DMSO or compound (10μM, 1μM, or 0.5μM) for 15 min at RT in the dark. Then, 20μL of each dilution and blank was loaded in triplicate to a 384-well black plate (Greiner: 784076) using a multichannel pipette. Fluorescence anisotropy measurements were taken on SpectraMax M5 plate reader. Binding for each condition was defined as Δ Anisotropy [(Anisotropy p53+DNA)- (Anisotropy DNA alone)]. Compounds at concentrations which restored pH 7.6 binding to at least 50% of pH 7 DMSO controls were kept for further binding analysis. All data are averages of three independent measurements from two separate protein preparations ± s.e.m.

p53 Anisotropy Assay to determine p53-DNA binding affinity with compounds

Compounds K788-8393 and F2636-058 identified in the initial binding screen were further characterized by fluorescence anisotropy for effects on p53 binding to 6'FAM-Gadd45 DNA. p53-R273H was made to a 3x final concentration (60μM) in a final volume of 60μL in anisotropy buffer pH 7 and 7.6. Protein was serial diluted in PCR strip tubes ten times with one blank to a volume of 30μL and 3x compound or DMSO was added 1:1 (30μM) and incubated for 15 min at RT. Then, 3x 6'FAM-Gadd45 (22.5nM) was added 1:1:1 and incubated for 15 min at RT. Plates were loaded, samples read, and binding analysis was performed as described above, with binding affinities analyzed by two-tailed unpaired Student's t-test and with a significance level of $p<0.05$.

Cell Culture and Luciferase Assay

For determinations with EIPA to lower pHi, MDA-MB-436 cells obtained from ATCC were maintained in atmospheric conditions at 37°C in Leibovitz's L-15 medium (Cytiva: SH30525.01) supplemented with insulin (10μg/mL), Penicillin/Streptomycin (100U/mL each), and 10% FBS. For luciferase assays, 3.5×10^5 cells were plated in 6-well plates and grown overnight to 80% confluency prior to transfection. Cells were transfected with a total of 1μg DNA using lipofectamine 3000 (Invitrogen: L3000001) according to manufacture protocol. Cells received 1 μg p53-luc (El-Deiry et al., 1993) 100 ng control pRL-TK renillla plasmid obtained from the L. Selleri Lab (University of California San Francisco) at a ratio of 1:10 of reporter plasmid. At 8 hours after transfection, cells were washed once with PBS and medium added in the absence or presence of 10 mM EIPA. Cells were then maintained for an additional 40 hours and collected for Dual-Luciferase assays (Promega: E2920). In brief, cells were washed once with PBS and lysed in 500μL of Dual-Glo luciferase buffer with shaking on a nutator for 10 min at 4°C. Lysates

were collected in microfuge tubes and clarified by centrifugation for 5 min at 13,000 rpm at RT. From supernatants, 100µL was loaded in quadruplicate in separate wells in a 96-well opaque white plate (Costar: 3917). Luciferase signal was read on a SpectraMax M5 plate reader and Dual-Glo Stop & Glo Buffer was then added to quench the luciferase signal and activate renilla for 10 min. The renilla signal was read and the Luciferase/Renilla ratio was normalized to control DMSO at pH 7. Data is from one independent experiment with future replicates to be performed.

CHAPTER 5: ADDITIONAL PUBLICATIONS FROM THESIS WORK

Intracellular pH dynamics and charge-changing somatic mutations in cancer

An unresolved question critical for understanding cancer is how recurring somatic mutations are retained and how selective pressures drive retention. Increased intracellular pH (pHi) is common to most cancers and is an early event in cancer development. Recent work shows that recurrent somatic mutations can confer an adaptive gain in pH sensing to mutant proteins, enhancing tumorigenic phenotypes specifically at the increased pHi of cancer. Newly identified amino acid mutation signatures in cancer suggest charge-changing mutations define and shape the mutational landscape of cancer. Taken together, these results support a new perspective on the functional significance of somatic mutations in cancer. In this review, we explore existing data and new directions for better understanding how changes in dynamic pH sensing by somatic mutation might be conferring a fitness advantage to the high pH of cancer.

Cancer and Metastasis Reviews (2019) 38:17–24
https://doi.org/10.1007/s10555-019-09791-8

Intracellular pH dynamics and charge-changing somatic mutations in cancer

Katharine A. White[1,2] · Kyle Kisor[2] · Diane L. Barber[2]

Published online: 13 April 2019

Abstract
An unresolved question critical for understanding cancer is how recurring somatic mutations are retained and how selective pressures drive retention. Increased intracellular pH (pHi) is common to most cancers and is an early event in cancer development. Recent work shows that recurrent somatic mutations can confer an adaptive gain in pH sensing to mutant proteins, enhancing tumorigenic phenotypes specifically at the increased pHi of cancer. Newly identified amino acid mutation signatures in cancer suggest charge-changing mutations define and shape the mutational landscape of cancer. Taken together, these results support a new perspective on the functional significance of somatic mutations in cancer. In this review, we explore existing data and new directions for better understanding how changes in dynamic pH sensing by somatic mutation might be conferring a fitness advantage to the high pH of cancer.

Keywords Intracellular pH dynamics · Oncogenes · pH sensing · Somatic mutations

1 Introduction

Most cancer cells have a constitutively higher intracellular pH (pHi) of 7.4–7.6 compared with normal cells (7.2). The increased pHi of cancer, as several previous reviews described [1–4], enables multiple cancer cell behaviors, including proliferation, metastasis, metabolic adaptation, and evasion from apoptosis. Increased pHi is also reported to be an early event in cancer development [5] and can induce dysplasia in the absence of activated oncogenes [6]. In this review, we present an emerging view on somatic charge-changing mutations altering pH sensing by proteins as an additional mechanism for how increased pHi in conjunction with somatic mutations can enable disease progression.

2 Charge-changing mutations in cancer

The incidence of recurrent somatic mutations in cancer is in part determined by fitness advantages to a dynamic microenvironment [7–9], including changes in metabolism [10], oxygen availability [11, 12], extracellular matrix composition [13], and pH dynamics [1]. While extensive work has characterized cancer heterogeneity based on tissue origin [14], driver mutations [15], or nucleotide mutational signatures [16–18], recent analyses highlight cancer heterogeneity by amino acid mutational signatures [19–21]. Fitness advantages are generally conferred by alterations in protein function, and analysis of amino acid signatures may be more representative of selection effects from tumor or microenvironment pressures in cancer evolution. Work from Szpiech and colleagues identified six amino acid mutational signatures in a tumor-normal paired database [16], and the signatures are dominated by charge-changing amino acid substitutions (arginine (Arg)>histidine (His) and glutamate (Glu)>lysine (Lys) (Fig. 1a) [19]. These same signatures are recapitulated when the analysis is performed at the level of the individual patient (Fig. 1b). These substitution signatures are independent of both underlying nucleotide mutation signature [16] and codon bias. Importantly, the Arg>His and Glu>Lys signatures are mutually exclusive (i.e., cancers that were dominated by patients with high Glu>Lys had very few patients with an Arg>His signature and *vice versa*). Anoosha and colleagues independently identified similar charge-changing amino acid mutational signatures in an analysis of the entire COSMIC dataset [20]. Moreover, the Anoosha analyses suggested that the Arg>His mutational signature is enriched in driver genes whereas the Glu>Lys signature has no preference for driver genes over passenger genes [20]. These same amino acid signatures have not been identified in

✉ Diane L. Barber
diane.barber@ucsf.edu

[1] Harper Cancer Research Institute, Department of Chemistry and Biochemistry, University of Notre Dame, South Bend, IN 46617, USA

[2] Department of Cell and Tissue Biology, University of California San Francisco, San Francisco, CA 94143, USA

Ethyl isopropyl amiloride decreases oxidative phosphorylation and increases mitochondrial fusion in clonal untransformed and cancer cells

Many cancer cells, regardless of their tissue origin or genetic landscape, have increased expression or activity of the plasma membrane Na-H exchanger NHE1 and a higher intracellular pH (pHi) compared with untransformed cells. A current perspective that remains to be validated is that increased NHE1 activity and pHi enable a Warburg-like metabolic reprogramming of increased glycolysis and decreased mitochondrial oxidative phosphorylation. We tested this perspective and find it is not accurate for clonal pancreatic and breast cancer cells. Using the pharmacological reagent ethyl isopropyl amiloride (EIPA) to inhibit NHE1 activity and decrease pHi, we observe no change in glycolysis, as indicated by secreted lactate and intracellular pyruvate, despite confirming increased activity of the glycolytic enzyme phosphofructokinase-1 at higher pH. Also, in contrast to predictions, we find a significant decrease in oxidative phosphorylation with EIPA, as indicated by oxygen consumption rate (OCR). Decreased OCR with EIPA is not associated with changes in pathways that fuel oxidative phosphorylation or with mitochondrial membrane potential but occurs with a change in mitochondrial dynamics that includes a significant increase in elongated mitochondrial networks, suggesting increased fusion. These findings conflict with current paradigms on increased pHi inhibiting oxidative phosphorylation and increased oxidative phosphorylation being associated with mitochondrial fusion. Moreover, these findings raise questions on the suggested use of EIPA-like compounds to limit metabolic reprogramming in cancer cells.

AMERICAN JOURNAL OF PHYSIOLOGY
CELL PHYSIOLOGY

Am J Physiol Cell Physiol 321: C147–C157, 2021.
First published May 26, 2021; doi:10.1152/ajpcell.00001.2021

RESEARCH ARTICLE

Advances in Mitochondrial Biology: Mitochondria as Regulators of Health and Longevity

Ethyl isopropyl amiloride decreases oxidative phosphorylation and increases mitochondrial fusion in clonal untransformed and cancer cells

Sagar S. Manoli,[1] Kyle Kisor,[1] Bradley A. Webb,[2] and Diane L. Barber[1]

[1]*Department of Cell and Tissue Biology, University of California, San Francisco, California and* [2]*Department of Biochemistry, West Virginia University, Morgantown, West Virginia*

Abstract

Many cancer cells, regardless of their tissue origin or genetic landscape, have increased expression or activity of the plasma membrane Na-H exchanger NHE1 and a higher intracellular pH (pHi) compared with untransformed cells. A current perspective that remains to be validated is that increased NHE1 activity and pHi enable a Warburg-like metabolic reprogramming of increased glycolysis and decreased mitochondrial oxidative phosphorylation. We tested this perspective and find it is not accurate for clonal pancreatic and breast cancer cells. Using the pharmacological reagent ethyl isopropyl amiloride (EIPA) to inhibit NHE1 activity and decrease pHi, we observe no change in glycolysis, as indicated by secreted lactate and intracellular pyruvate, despite confirming increased activity of the glycolytic enzyme phosphofructokinase-1 at higher pH. Also, in contrast to predictions, we find a significant decrease in oxidative phosphorylation with EIPA, as indicated by oxygen consumption rate (OCR). Decreased OCR with EIPA is not associated with changes in pathways that fuel oxidative phosphorylation or with mitochondrial membrane potential but occurs with a change in mitochondrial dynamics that includes a significant increase in elongated mitochondrial networks, suggesting increased fusion. These findings conflict with current paradigms on increased pHi inhibiting oxidative phosphorylation and increased oxidative phosphorylation being associated with mitochondrial fusion. Moreover, these findings raise questions on the suggested use of EIPA-like compounds to limit metabolic reprogramming in cancer cells.

cancer metabolism; intracellular pH; lactate; mitochondria; NHE1; oxidative phosphorylation

INTRODUCTION

Metabolic reprogramming is considered a hallmark of cancer cells that often includes increased glycolysis and decreased mitochondrial oxidative phosphorylation (1, 2) to generate biomass for fueling rapid proliferation. Although it is widely accepted that cancer cells predominantly convert glucose to lactate, either due to increased expression of the converting enzyme lactate dehydrogenase A (LDHA) (3, 4) or an impaired mitochondrial pyruvate import carrier (5), the functional status of mitochondria in cancer cells remains controversial. Cancer cells are reported to have dysfunctional mitochondria (6–8) but in contrast, the TCA cycle in mitochondria often remains a major source for ATP and functional mitochondria are essential for cancer cells to survive during tumor progression (2, 9, 10).

Another distinctive feature of most cancer cells is a constitutively higher intracellular pH (pHi) compared with untransformed cells (11–14). Although initially considered a conundrum based on metabolic acids produced by rapidly proliferating cancer cells, the higher pHi of cancer cells is now known to be in-part determined by increased activity or expression of acid extruding plasma membrane ion transporters, including the Na-H exchanger, NHE1, monocarboxylate transporters (MCTs), Na^+/HCO_3^- co-transporters, and V-ATPases (11, 12, 15, 16). The higher pHi of cancer cells is suggested to enable metabolic reprogramming and a shift from reliance on oxidative phosphorylation to glycolysis or glutaminolysis (11–14); however, this has not been conclusively determined. In addition, metabolic (17–19) and pHi (20, 21) heterogeneity occurs in cancers but whether or how these parameters might be linked in determining their heterogeneity has received limited attention (20, 22). These considerations are important because tumor heterogeneity is a challenge for effective cancer therapies.

We addressed a number of questions on pHi dynamics and cancer cell metabolism in studies using human clonal pancreatic cancer BxPC3 cells and breast cancer MDA-MB-157 cells. We focused on these cell types because our initial studies indicated that BxPC3 but not MDA-MB-157 cells show a metabolic reprogramming of increased glycolysis and decreased oxidative phosphorylation compared with untransformed tissue-matched clonal epithelial cells, which give us models with contrasting metabolic profiles.

Correspondence: D. L. Barber (diane.barber@ucsf.edu).
Submitted 13 January 2021 / Revised 20 May 2021 / Accepted 20 May 2021

CHAPTER 6: CONCLUDING REMARKS

Summary

Determining the molecular mechanisms of how pHi dynamic regulates cell behaviors through pH-sensitive proteins contributes new insights for our understanding of developmental processes and also diseases with dysregulated pHi. Although several endogenous pH sensors have been previously identified, our understanding of how pHi directly regulates gene expression and metabolism, and how we can target pH-sensors in cancer, is incomplete. In Chapter 2, we show how pH-dynamics can regulate DNA-binding specificity of transcription factors with a nucleotide-binding histidine in the DNA binding domain. I confirm that three FOX family proteins, FOXC2, FOXM1 and FOXN1, bind to the canonical FkhP DNA consensus sequence with high affinity at lower pH and for FOXC2, pH-regulated binding is conferred by a conserved His122. Our data also indicate FOXC2 activity at FkhP sequences in cancer cells is greater at lower pH by using approaches to pharmacologically or genetically lower pHi. Further, using an unbiased screen we find that FOXC2 prefers to bind known FHL-like sequences at the high pH of 7.8.

In addition to showing transcription factors as a previously unrecognized class of pH-sensors, in Chapter 3 we determined the molecular mechanism of pH-sensing by the known pH-sensor PFKM. While pH-dependent relief of allosteric ATP inhibition by PFKM was known for over 50 years, recent advancements in determining the PFKM crystal structure and a system for expression and purification of tetrameric, post-translationally modified PFK allowed us to resolve this longstanding question in molecular detail. Our data suggest an inhibitory ATP coordinating His242 residue is necessary for pH-dependent relief of allosteric ATP inhibition of PFKM but when substituted in the cognate site of PFKL it is not sufficient to confer pH sensing.

In Chapter 4 we explored the feasibility of targeting charge-changing somatic mutations with small molecules to confer predicted protein and cell behaviors. Using three libraries, we screened 3.5×10^6 bioactive compounds *in silico* to filter to 48 compounds predicted to rescue pH-independent binding of the highly recurrent p53-R273H mutant to DNA. Our *in vitro* data and

our preliminary data in cells indicate two of these compounds, K788-8393 and F2636-0583, significantly increase binding of p53-R273H to DNA at pH 7.6. Further studies are needed to determine the therapeutic promise of these compounds to retore tumor suppressor activity of mutant p53-R273H. Importantly, our findings in Chapter 4 may serve as proof-of-principle for broader applications of histidine-drugging and restoring the function of proteins with charge-changing mutations that affect diseases other than cancer. Taken together, findings from my thesis research further our understanding of how pHi dynamics regulates protein functions to affect cell behaviors and mechanisms that can be targeted in disease.

Future Directions

My thesis research generates new insights on how pHi dynamics regulates diverse pH sensors to drive myriad cell behaviors. Importantly, my findings open new directions for future studies. While my findings in Chapter 2 confirm that selective FOX family proteins have high affinity and activity for a canonical FkhP consensus motif *in vitro* and in cells, my results also generate new questions to investigate. First, *which endogenous target genes have pH-dependent binding of FOX family proteins for regulating gene expression*? Second, *do other transcription factors with a conserved histidine in the DBD such as in the SOX and MITF/MYC/MAX families also have pH-regulated binding to selective DNA consensus sequences?* Third, *how does pH-dependent binding of transcription factors to target genes regulate cell behaviors driven by pHi dynamics?*

My findings in Chapter 3 resolved the long-standing unknown of how increased pH relieves allosteric ATP inhibition specifically in the PFKM but not in PFKL or PFKP isoforms. Our data suggest the inhibitory ATP coordinating His242 residue in PFKM is required for relief of allosteric inhibition, but is not sufficient for a gain of pH-sensing in PFKL. Taken together, these findings highlight new questions necessary for a more complete understanding of how pH regulates ATP-inhibited PFKM activity. First, *is His242 sufficient for pH-dependent relief of ATP inhibition in the other PFK-1 isoform, PFKP?* Second, *is lack of sufficiency for a gain in pH-sensing in PFKL due to a required electrostatic network exclusive to PFKM where Arg245 may upshift the pKa of His242?* Resolving these questions is significant to understanding how dysregulated pHi in cancers can enable metabolic reprogramming and how an increase in pHi might promote the established shift in reliance on glycolysis for stem cell differentiation.

Although pHi dynamics are necessary for normal cell behaviors, constitutively increased pHi in cancers can enable tumorigenic functions of charge changing somatic mutations to drive cancer cell behaviors. My Chapter 4 explored using small molecules targeting the pH-dependent charge changing p53-R273H mutation to rescue WT function. While my findings suggest K788-8393 and F2636-0583 partially rescue p53-R273H high affinity binding to DNA at

high pH both *in vitro* and in p53-reporter assays in cells, these data highlight several important questions to resolve. First, *what is the efficacy of these drugs to elicit a functional response such as rescue of apoptosis in cells?* Second, *can we determine the crystal structure for p53-R273H in complex with these compounds and do they structurally align with our predictions?* Third, *do these compounds have therapeutic potential in vivo for reducing cancer progression?* Fourth, *what is the broader significance of our small molecule approach based on charge-changing mutations driving diseases in addition to cancers?*

REFERENCES

Adams, G. R., Foley, J. M., & Meyer, R. A. (1990). Muscle buffer capacity estimated from pH changes during rest-to-work transitions. *J Appl Physiol*, *69*(3), 968–972.

Ahmad, S., & Sarai, A. (2004). Moment-based prediction of DNA-binding proteins. *Journal of Molecular Biology*, *341*(1), 65–71. https://doi.org/10.1016/j.jmb.2004.05.058

Akinlalu, A. O., Chamundi, A., Yakumbur, D. T., Afolayan, F. I. D., Duru, I. A., Arowosegbe, M. A., & Enejoh, O. A. (2021). Repurposing FDA-approved drugs against multiple proteins of SARS-CoV-2: An in silico study. *Scientific African*, *13*. https://doi.org/10.1016/j.sciaf.2021.e00845

Alexandrov, L. B., Kim, J., Haradhvala, N. J., Huang, M. N., Tian Ng, A. W., Wu, Y., Boot, A., Covington, K. R., Gordenin, D. A., Bergstrom, E. N., Islam, S. M. A., Lopez-Bigas, N., Klimczak, L. J., McPherson, J. R., Morganella, S., Sabarinathan, R., Wheeler, D. A., Mustonen, V., Boutros, P., … Yu, W. (2020). The repertoire of mutational signatures in human cancer. *Nature*, *578*(7793), 94–101. https://doi.org/10.1038/s41586-020-1943-3

Amith, S. R., Wilkinson, J. M., & Fliegel, L. (2016). *Na + /H + exchanger NHE1 regulation modulates metastatic potential and epithelial-mesenchymal transition of triple-negative breast cancer cells* (Vol. 7, Issue 16). www.impactjournals.com/oncotarget

Ang, H. C., Joerger, A. C., Mayer, S., & Fersht, A. R. (2006). Effects of common cancer mutations on stability and DNA binding of full-length p53 compared with isolated core domains. *Journal of Biological Chemistry*, *281*(31), 21934–21941. https://doi.org/10.1074/jbc.M604209200

Anoosha, P., Sakthivel, R., & Michael Gromiha, M. (2016). Exploring preferred amino acid mutations in cancer genes: Applications to identify potential drug targets. *Biochimica et Biophysica Acta - Molecular Basis of Disease*, *1862*(2), 155–165. https://doi.org/10.1016/j.bbadis.2015.11.006

Baker, C. M., & Grant, G. H. (2007). Role of aromatic amino acids in protein–nucleic acid recognition. *Biopolymers*, *85*(4), 392–406. https://doi.org/10.1002/bip

Banaszak, K., Mechin, I., Obmolova, G., Oldham, M., Chang, S. H., Ruiz, T., Radermacher, M., Kopperschläger, G., & Rypniewski, W. (2011). The crystal structures of eukaryotic phosphofructokinases from Baker's yeast and rabbit skeletal muscle. *Journal of Molecular Biology*, *407*(2), 284–297. https://doi.org/10.1016/j.jmb.2011.01.019

Benitez, M., Tatapudy, S., Liu, Y., Barber, D. L., & Nystul, T. G. (2019). Drosophila anion exchanger 2 is required for proper ovary development and oogenesis. *Developmental Biology*, *452*(2), 127–133. https://doi.org/10.1016/j.ydbio.2019.04.018

Blane, A., & Fanucchi, S. (2015). Effect of pH on the Structure and DNA Binding of the FOXP2 Forkhead Domain. *Biochemistry*, *54*(25), 4001–4007. https://doi.org/10.1021/acs.biochem.5b00155

Brooks, E. A., Galarza, S., Gencoglu, M. F., Chase Cornelison, R., Munson, J. M., & Peyton, S. R. (2019). Applicability of drug response metrics for cancer studies using biomaterials. In *Philosophical Transactions of the Royal Society B: Biological Sciences* (Vol. 374, Issue 1779). Royal Society Publishing. https://doi.org/10.1098/rstb.2018.0226

Brüser, A., Kirchberger, J., Kloos, M., Sträter, N., & Schöneberg, T. (2012). Functional linkage of adenine nucleotide binding sites in mammalian muscle 6-phosphofructokinase. *Journal of Biological Chemistry*, *287*(21), 17546–17553. https://doi.org/10.1074/jbc.M112.347153

Carpenter' And, J. F., & Hand3, S. C. (1986). Comparison of pH-Dependent Allostery and Dissociation for Phosphofructokinases from Artemia Embryos and Rabbit Muscle: Nature of the Enzymes Acylated with Diethylpyrocarbonate'. In *ARCHIVES OF BIOCHEMISTRY AND BIOPHYSICS* (Vol. 248, Issue 1).

Casey, J. R., Grinstein, S., & Orlowski, J. (2010). Sensors and regulators of intracellular pH. In *Nature Reviews Molecular Cell Biology* (Vol. 11, Issue 1, pp. 50–61). https://doi.org/10.1038/nrm2820

Chen, S., Wu, Y., Gao, Y., Wu, C., Wang, Y., Hou, C., Ren, M., Zhang, S., Zhu, Q., Zhang, J., Yao, Y., Huang, M., Qi, Y. B., Liu, X. S., Horng, T., Wang, H., Ye, D., Zhu, Z., Zhao, S., &

Fan, G. (2023). Allosterically inhibited PFKL via prostaglandin E2 withholds glucose metabolism and ovarian cancer invasiveness. *Cell Reports*, *42*(10). https://doi.org/10.1016/j.celrep.2023.113246

Choi, C. H., Webb, B. A., Chimenti, M. S., Jacobson, M. P., & Barber, D. L. (2013). Ph sensing by FAK-His58 regulates focal adhesion remodeling. *Journal of Cell Biology*, *202*(6), 849–859. https://doi.org/10.1083/jcb.201302131

Clement, D. L., Mally, S., Stock, C., Lethan, M., Satir, P., Schwab, A., Pedersen, S. F., & Christensen, S. T. (2013). PDGFRα signaling in the primary cilium regulates NHE1-dependent fibroblast migration via coordinated differential activity of MEK1/2-ERK1/2-p90RSK and AKT signaling pathways. *Journal of Cell Science*, *126*(4), 953–965. https://doi.org/10.1242/jcs.116426

Colombo, G., Tate, P. W., Giro~i, A. W., & Kemp, R. G. (1975). *Interaction of Inhibitors with Muscle Phosphofructokinase** (Vol. 250, Issue 24).

Counillon, L., Bouret, Y., Marchiq, I., & Pouysségur, J. (2016). Na+/H+ antiporter (NHE1) and lactate/H+ symporters (MCTs) in pH homeostasis and cancer metabolism. *Biochimica et Biophysica Acta - Molecular Cell Research*, *1863*(10), 2465–2480. https://doi.org/10.1016/j.bbamcr.2016.02.018

De Oliveira, V. M., Dias, M. M. G., Avelino, T. M., Videira, N. B., Da Silva, F. B., Doratioto, T. R., Whitford, P. C., Leite, V. B. P., & Figueira, A. C. M. (2022). PH and the Breast Cancer Recurrent Mutation D538G Affect the Process of Activation of Estrogen Receptor α. *Biochemistry*, *61*(6), 455–463. https://doi.org/10.1021/acs.biochem.1c00806

Denker, S. P., & Barber, D. L. (2002). Cell migration requires both ion translocation and cytoskeletal anchoring by the Na-H exchanger NHE1. *Journal of Cell Biology*, *159*(6), 1087–1096. https://doi.org/10.1083/jcb.200208050

Depre, C., Rider, M. H., Veitch, K., & Hue, L. (1993). Role of fructose 2,6-bisphosphate in the control of heart glycolysis. *Journal of Biological Chemistry*, *268*(18), 13274–13279. https://doi.org/10.1016/s0021-9258(19)38648-x

Designed Research; A, J. N. K. (2021). *OCT4 induces embryonic pluripotency via STAT3 signaling and metabolic mechanisms*. *118*(3). https://doi.org/10.1073/pnas.2008890118/-/DCSupplemental

Eberhardt, J., Santos-Martins, D., Tillack, A. F., & Forli, S. (2021). AutoDock Vina 1.2.0: New Docking Methods, Expanded Force Field, and Python Bindings. *Journal of Chemical Information and Modeling*, *61*(8), 3891–3898. https://doi.org/10.1021/acs.jcim.1c00203

El-Deiry, W. S., Tokino, T., Velculescu, V. E., Levy, D. B., Parsons, R., Trent, J. M., Lin, D., Edward Mercer, W., Kinzler, K. W., & Vogelstein, B. (1993). WAR, a Potential Mediator of ~53 Tumor Suppression. *Cell*, *75*, 817–825.

Flinck, M., Kramer, S. H., Schnipper, J., Andersen, A. P., & Pedersen, S. F. (2018a). The acid-base transport proteins NHE1 and NBCn1 regulate cell cycle progression in human breast cancer cells. *Cell Cycle*, *17*(9), 1056–1067. https://doi.org/10.1080/15384101.2018.1464850

Flinck, M., Kramer, S. H., Schnipper, J., Andersen, A. P., & Pedersen, S. F. (2018b). The acid-base transport proteins NHE1 and NBCn1 regulate cell cycle progression in human breast cancer cells. *Cell Cycle*, *17*(9), 1056–1067. https://doi.org/10.1080/15384101.2018.1464850

Forbes, S. A., Beare, D., Boutselakis, H., Bamford, S., Bindal, N., Tate, J., Cole, C. G., Ward, S., Dawson, E., Ponting, L., Stefancsik, R., Harsha, B., YinKok, C., Jia, M., Jubb, H., Sondka, Z., Thompson, S., De, T., & Campbell, P. J. (2017a). COSMIC: Somatic cancer genetics at high-resolution. *Nucleic Acids Research*, *45*(D1), D777–D783. https://doi.org/10.1093/nar/gkw1121

Forbes, S. A., Beare, D., Boutselakis, H., Bamford, S., Bindal, N., Tate, J., Cole, C. G., Ward, S., Dawson, E., Ponting, L., Stefancsik, R., Harsha, B., YinKok, C., Jia, M., Jubb, H., Sondka, Z., Thompson, S., De, T., & Campbell, P. J. (2017b). COSMIC: Somatic cancer genetics at high-resolution. *Nucleic Acids Research*, *45*(D1), D777–D783. https://doi.org/10.1093/nar/gkw1121

Frantz, C., Barreiro, G., Dominguez, L., Chen, X., Eddy, R., Condeelis, J., Kelly, M. J. S., Jacobson, M. P., & Barber, D. L. (2008). Cofilin is a pH sensor for actin free barbed end formation: role of phosphoinositide binding. *Journal of Cell Biology*, *183*(5), 865–879. https://doi.org/10.1083/jcb.200804161

Frantz, C., Karydis, A., Nalbant, P., Hahn, K. M., & Barber, D. L. (2007). Positive feedback between Cdc42 activity and H+ efflux by the Na-H exchanger NHE1 for polarity of migrating cells. *Journal of Cell Biology*, *179*(3), 403–410. https://doi.org/10.1083/jcb.200704169

Gao, W., Zhang, H., Chang, G., Xie, Z., Wang, H., Ma, L., Han, Z., Li, Q., & Pang, T. (2014). Decreased intracellular pH induced by cariporide differentially contributes to human umbilical cord-derived mesenchymal stem cells differentiation. *Cellular Physiology and Biochemistry*, *33*(1), 185–194. https://doi.org/10.1159/000356661

Gillies, R. J., Pilot, C., Marunaka, Y., & Fais, S. (2019). Targeting acidity in cancer and diabetes. In *Biochimica et Biophysica Acta - Reviews on Cancer* (Vol. 1871, Issue 2, pp. 273–280). Elsevier B.V. https://doi.org/10.1016/j.bbcan.2019.01.003

Grillo-Hill, B. K., Choi, C., Jimenez-Vidal, M., & Barber, D. L. (2015). Increased H+ efflux is sufficient to induce dysplasia and necessary for viability with oncogene expression. *ELife*, *2015*(4), 1–31. https://doi.org/10.7554/eLife.03270

Grillo-Hill, B. K., Webb, B. A., & Barber, D. L. (2014). Ratiometric Imaging of pH Probes. In *Methods in Cell Biology* (Vol. 123, pp. 429–448). Academic Press Inc. https://doi.org/10.1016/B978-0-12-420138-5.00023-9

Guiley, K. Z., & Shokat, K. M. (2023). A Small Molecule Reacts with the p53 Somatic Mutant Y220C to Rescue Wild-type Thermal Stability. *Cancer Discovery*, *13*(1), 56–69. https://doi.org/10.1158/2159-8290.CD-22-0381

Hardonnière, K., Saunier, E., Lemarié, A., Fernier, M., Gallais, I., Héliès-Toussaint, C., Mograbi, B., Antonio, S., Bénit, P., Rustin, P., Janin, M., Habarou, F., Ottolenghi, C., Lavault, M. T., Benelli, C., Sergent, O., Huc, L., Bortoli, S., & Lagadic-Gossmann, D. (2016). The environmental carcinogen benzo[a]pyrene induces a Warburg-like metabolic reprogramming dependent on NHE1 and associated with cell survival. *Scientific Reports*, *6*. https://doi.org/10.1038/srep30776

Harguindey, S., Stanciu, D., Devesa, J., Alfarouk, K., Cardone, R. A., Polo Orozco, J. D., Devesa, P., Rauch, C., Orive, G., Anitua, E., Roger, S., & Reshkin, S. J. (2017). Cellular acidification as a new approach to cancer treatment and to the understanding and therapeutics of neurodegenerative diseases. In *Seminars in Cancer Biology* (Vol. 43, pp. 157–179). Academic Press. https://doi.org/10.1016/j.semcancer.2017.02.003

Hayata, H., Miyazaki, H., Niisato, N., Yokoyama, N., & Marunaka, Y. (2014). Lowered extracellular pH is involved in the pathogenesis of skeletal muscle insulin resistance. *Biochemical and Biophysical Research Communications*, *445*(1), 170–174. https://doi.org/10.1016/j.bbrc.2014.01.162

Icard, P., Poulain, L., & Lincet, H. (2012). Understanding the central role of citrate in the metabolism of cancer cells. In *Biochimica et Biophysica Acta - Reviews on Cancer* (Vol. 1825, Issue 1, pp. 111–116). https://doi.org/10.1016/j.bbcan.2011.10.007

Inaishi, T., Shibata, M., Ichikawa, T., Kanda, M., Hayashi, M., Soeda, I., Takeuchi, D., Takano, Y., Tsunoda, N., Kodera, Y., & Kikumori, T. (2022). Platelet isoform of phosphofructokinase accelerates malignant features in breast cancer. *Oncology Reports*, *47*(1). https://doi.org/10.3892/or.2021.8220

Ishfaq, M., Bashir, N., Riaz, S. K., Manzoor, S., Khan, J. S., Bibi, Y., Sami, R., Aljahani, A. H., Alharthy, S. A., & Shahid, R. (2022). Expression of HK2, PKM2, and PFKM Is Associated with Metastasis and Late Disease Onset in Breast Cancer Patients. *Genes*, *13*(3). https://doi.org/10.3390/genes13030549

Isom, D. G., Castañeda, C. A., Cannon, B. R., & García-Moreno, B. (2011). Large shifts in pK a values of lysine residues buried inside a protein. *PNAS*, *108*(13), 5620–5265. https://doi.org/10.1073/pnas.1010750108/-/DCSupplemental

Jensen, H. H., Pedersen, G. A., Morgen, J. J., Parsons, M., Pedersen, S. F., & Nejsum, L. N. (2019). The Na + /H + exchanger NHE1 localizes as clusters to cryptic lamellipodia and accelerates collective epithelial cell migration. *Journal of Physiology*, *597*(3), 849–867. https://doi.org/10.1113/JP277383

Joerger, A. C., Allen, M. D., & Fersht, A. R. (2004). Crystal structure of a superstable mutant of human p53 core domain: Insights into the mechanism of rescuing oncogenic mutations. *Journal of Biological Chemistry*, *279*(2), 1291–1296. https://doi.org/10.1074/jbc.M309732200

Johnston, R. J., Su, L. J., Pinckney, J., Critton, D., Boyer, E., Krishnakumar, A., Corbett, M., Rankin, A. L., Dibella, R., Campbell, L., Martin, G. H., Lemar, H., Cayton, T., Huang, R. Y. C., Deng, X., Nayeem, A., Chen, H., Ergel, B., Rizzo, J. M., … Korman, A. J. (2019). VISTA is an acidic pH-selective ligand for PSGL-1. *Nature*, *574*(7779), 565–570. https://doi.org/10.1038/s41586-019-1674-5

Kaplan, F. S., Chakkalakal, S. A., & Shore, E. M. (2012). Fibrodysplasia ossificans progressiva: Mechanisms and models of skeletal metamorphosis. In *DMM Disease Models and Mechanisms* (Vol. 5, Issue 6, pp. 756–762). https://doi.org/10.1242/dmm.010280

Karp, D. A., Stahley, M. R., & García-Moreno E., B. (2010). Conformational Consequences of Ionization of Lys, Asp, and Glu Buried at Position 66 in Staphylococcal Nuclease. *Biochemistry*, *49*(19), 4138–4146. https://doi.org/10.1021/bi902114m

Katoh, M., Igarashi, M., Fukuda, H., Nakagama, H., & Katoh, M. (2013). Cancer genetics and genomics of human FOX family genes. In *Cancer Letters* (Vol. 328, Issue 2, pp. 198–206). Elsevier Ireland Ltd. https://doi.org/10.1016/j.canlet.2012.09.017

Kazyken, D., Lentz, S. I., Wadley, M., & Fingar, D. C. (2023). Alkaline intracellular pH (pHi) increases PI3K activity to promote mTORC1 and mTORC2 signaling and function during growth factor limitation. *Journal of Biological Chemistry*, *299*(9), 105097. https://doi.org/10.1016/j.jbc.2023.105097

Lambert, S. A., Jolma, A., Campitelli, L. F., Das, P. K., Yin, Y., Albu, M., Chen, X., Taipale, J., Hughes, T. R., & Weirauch, M. T. (2018). The Human Transcription Factors. *Cell*, *172*(4), 650–665. https://doi.org/10.1016/j.cell.2018.01.029

Li, J., Rodriguez, J. P., Niu, F., Pu, M., Wang, J., Hung, L. W., Shao, Q., Zhu, Y., Ding, W., Liu, Y., Da, Y., Yao, Z., Yang, J., Zhao, Y., Wei, G. H., Cheng, G., Liu, Z. J., & Ouyang, S. (2016). Structural basis for DNA recognition by STAT6. *Proceedings of the National Academy of Sciences of the United States of America*, *113*(46), 13015–13020. https://doi.org/10.1073/pnas.1611228113

Li, X., & Fliegel, L. (2022). Permissive role of Na+/H+ exchanger isoform 1 in migration and invasion of triple-negative basal-like breast cancer cells. *Molecular and Cellular Biochemistry*, *477*(4), 1207–1216. https://doi.org/10.1007/s11010-022-04370-y

Li, X., Karki, P., Lei, L., Wang, H., Fliegel, L., & Michalak, M. (2009). Na /H exchanger isoform 1 facilitates cardiomyocyte embryonic stem cell differentiation The mouse stem cell line (CGR8) was kindly provided. *Am J Physiol Heart Circ Physiol*, *296*, 159–170. https://doi.org/10.1152/ajpheart.00375.2008.-Em

Lim, J. S., Shi, Y. J., Park, S. H., Jeon, S. M., Zhang, C., Park, Y. Y., Liu, R., Li, J., Cho, W. S., Du, L., & Lee, J. H. (2022). Mutual regulation between phosphofructokinase 1 platelet isoform and VEGF promotes glioblastoma tumor growth. *Cell Death and Disease*, *13*(11). https://doi.org/10.1038/s41419-022-05449-6

Liu, Y., Reyes, E., Castillo-Azofeifa, D., Klein, O. D., Nystul, T., & Barber, D. L. (2023). Intracellular pH dynamics regulates intestinal stem cell lineage specification. *Nature Communications*, *14*(1). https://doi.org/10.1038/s41467-023-39312-9

Lu, Y., Zuo, P., Chen, H., Shan, H., Wang, W., Dai, Z., Xu, H., Chen, Y., Liang, L., Ding, D., Jin, Y., & Yin, Y. (2023). Structural insights into the conformational changes of BTR1/SLC4A11 in complex with PIP2. *Nature Communications*, *14*(1). https://doi.org/10.1038/s41467-023-41924-0

Luna, L. A., Lesecq, Z., White, K. A., Hoang, A., Scott, D. A., Zagnitko, O., Bobkov, A. A., Barber, D. L., Schiffer, J. M., Isom, D. G., & Sohl, C. D. (2020). An acidic residue buried in the dimer interface of isocitrate dehydrogenase 1 (IDH1) helps regulate catalysis and pH sensitivity. *Biochemical Journal*, *477*(16), 2999–3018. https://doi.org/10.1042/BCJ20200311

Magalhaes, M. A. O., Larson, D. R., Mader, C. C., Bravo-Cordero, J. J., Gil-Henn, H., Oser, M., Chen, X., Koleske, A. J., & Condeelis, J. (2011). Cortactin phosphorylation regulates cell invasion through a pH-dependent pathway. *Journal of Cell Biology*, *195*(5), 903–920. https://doi.org/10.1083/jcb.201103045

Mahmoud, A. I. (2023). Metabolic switches during development and regeneration. *Development (Cambridge, England)*, *150*(20). https://doi.org/10.1242/dev.202008

Majdi, A., Mahmoudi, J., Sadigh-Eteghad, S., Golzari, S. E. J., Sabermarouf, B., & Reyhani-Rad, S. (2016). Permissive role of cytosolic pH acidification in neurodegeneration: A closer look at its causes and consequences. In *Journal of Neuroscience Research* (Vol. 94, Issue 10, pp. 879–887). John Wiley and Sons Inc. https://doi.org/10.1002/jnr.23757

Malevanets, A., Chong, P. A., Hansen, D. F., Rizk, P., Sun, Y., Lin, H., Muhandiram, R., Chakrabartty, A., Kay, L. E., Forman-Kay, J. D., & Wodak, S. J. (2017). Interplay of buried histidine protonation and protein stability in prion misfolding. *Scientific Reports*, *7*(1). https://doi.org/10.1038/s41598-017-00954-7

Man, C. H., Mercier, F. E., Liu, N., Dong, W., Stephanopoulos, G., Jiang, L., Jung, Y., Lin, C. P., Leung, A. Y. H., & Scadden, D. T. (2022). Proton export alkalinizes intracellular pH and reprograms carbon metabolism to drive normal and malignant cell growth. *Blood*, *139*(4), 502–522. https://doi.org/10.1182/BLOOD.2019000962

Mani, S. A., Yang, J., Brooks, M., Schwaninger, G., Zhou, A., Miura, N., Kutok, J. L., Hartwell, K., Richardson, A. L., & Weinberg, R. A. (2007). *Mesenchyme Forkhead 1 (FOXC2) plays a key role in metastasis and is associated with aggressive basal-like breast cancers*. www.pnas.org/cgi/content/full/

Manoli, S. S., Kisor, K., Webb, B. A., & Barber, D. L. (2021). Ethyl isopropyl amiloride decreases oxidative phosphorylation and increases mitochondrial fusion in clonal untransformed and cancer cells. *American Journal of Physiology - Cell Physiology*, *321*(1), C147–C157. https://doi.org/10.1152/ajpcell.00001.2021

Martin, C., Pedersen, S. F., Schwab, A., & Stock, C. (2011). Intracellular pH gradients in migrating cells. *American Journal of Physiology - Cell Physiology*, *300*(3). https://doi.org/10.1152/ajpcell.00280.2010

Mathieu, J., & Ruohola-Baker, H. (2017). Metabolic remodeling during the loss and acquisition of pluripotency. *Development*, *144*(4), 541–551. https://doi.org/10.1242/dev.128389

Matsson, P., & Kihlberg, J. (2017). How Big Is Too Big for Cell Permeability? In *Journal of Medicinal Chemistry* (Vol. 60, Issue 5, pp. 1662–1664). American Chemical Society. https://doi.org/10.1021/acs.jmedchem.7b00237

McBrian, M. A., Behbahan, I. S., Ferrari, R., Su, T., Huang, T. W., Li, K., Hong, C. S., Christofk, H. R., Vogelauer, M., Seligson, D. B., & Kurdistani, S. K. (2013). Histone Acetylation Regulates Intracellular pH. *Molecular Cell*, *49*(2), 310–321. https://doi.org/10.1016/j.molcel.2012.10.025

Medina, E., Villalobos, P., Coñuecar, R., Ramírez-Sarmiento, C. A., & Babul, J. (2019). The protonation state of an evolutionarily conserved histidine modulates domainswapping stability of FoxP1. *Scientific Reports*, *9*(1). https://doi.org/10.1038/s41598-019-41819-5

Meima, M. E., Webb, B. A., Witkowska, H. E., & Barber, D. L. (2009). The sodium-hydrogen exchanger NHE1 is an akt substrate necessary for actin filament reorganization by growth factors. *Journal of Biological Chemistry*, *284*(39), 26666–26675. https://doi.org/10.1074/jbc.M109.019448

Moerke, N. J. (2009). Fluorescence Polarization (FP) Assays for Monitoring Peptide-Protein or Nucleic Acid-Protein Binding. *Current Protocols in Chemical Biology*, *1*(1), 1–15. https://doi.org/10.1002/9780470559277.ch090102

Moon, J. S., Kim, H. E., Koh, E., Park, S. H., Jin, W. J., Park, B. W., Park, S. W., & Kim, K. S. (2011). Krüppel-like Factor 4 (KLF4) activates the transcription of the gene for the platelet isoform of phosphofructokinase (PFKP) in breast cancer. *Journal of Biological Chemistry*, *286*(27), 23808–23816. https://doi.org/10.1074/jbc.M111.236737

Moparthi, L., & Koch, S. (2020). A uniform expression library for the exploration of FOX transcription factor biology. *Differentiation*, *115*, 30–36. https://doi.org/10.1016/j.diff.2020.08.002

Mor, I., Cheung, E. C., & Vousden, K. H. (2011). Control of glycolysis through regulation of PFK1: Old friends and recent additions. *Cold Spring Harbor Symposia on Quantitative Biology*, *76*, 211–216. https://doi.org/10.1101/sqb.2011.76.010868

Morales Rodríguez, L. M., Crilly, S. E., Rowe, J. B., Isom, D. G., & Puthenveedu, M. A. (2023). Location-biased activation of the proton-sensor GPR65 is uncoupled from receptor trafficking. *Proceedings of the National Academy of Sciences*, *120*(39). https://doi.org/10.1073/pnas.2302823120

Mortazavi, F., An, J., Dubinett, S., & Rettig, M. (2010). p120-Catenin is transcriptionally downregulated by FOXC2 in non-small cell lung cancer cells. *Molecular Cancer Research*, *8*(5), 762–774. https://doi.org/10.1158/1541-7786.MCR-10-0004

Nakagawa, S., Gisselbrecht, S. S., Rogers, J. M., Hartl, D. L., & Bulyk, M. L. (2013). DNA-binding specificity changes in the evolution of forkhead transcription factors. *Proceedings of the National Academy of Sciences of the United States of America*, *110*(30), 12349–12354. https://doi.org/10.1073/pnas.1310430110

Newman, J. A., Aitkenhead, H., Gavard, A. E., Rota, I. A., Handel, A. E., Hollander, G. A., & Gileadi, O. (2020). The crystal structure of human forkhead box N1 in complex with DNA reveals the structural basis for forkhead box family specificity. *Journal of Biological Chemistry*, *295*(10), 2948–2958. https://doi.org/10.1074/jbc.RA119.010365

Nikolova, P. V, Henckel, J., Lane, D. P., & Fersht, A. R. (1998). Semirational design of active tumor suppressor p53 DNA binding domain with enhanced stability (protein designthermodynamic stability). In *Biochemistry* (Vol. 95). www.iarc.fr

Nikolovska, K., Cao, L., Hensel, I., Di Stefano, G., Seidler, A. E., Zhou, K., Qian, J., Singh, A. K., Riederer, B., & Seidler, U. (2022). Sodium/hydrogen-exchanger-2 modulates colonocyte lineage differentiation. *Acta Physiologica*, *234*(3). https://doi.org/10.1111/apha.13774

Oginuma, M., Harima, Y., Tarazona, O. A., Diaz-Cuadros, M., Michaut, A., Ishitani, T., Xiong, F., & Pourquié, O. (2020). Intracellular pH controls WNT downstream of glycolysis in amniote embryos. *Nature*, *584*(7819), 98–101. https://doi.org/10.1038/s41586-020-2428-0

Onufriev, A. V., & Alexov, E. (2013). Protonation and pK changes in protein-ligand binding. In *Quarterly Reviews of Biophysics* (Vol. 46, Issue 2, pp. 181–209). https://doi.org/10.1017/S0033583513000024

Parks, S. K., Chiche, J., & Pouysségur, J. (2013). Disrupting proton dynamics and energy metabolism for cancer therapy. In *Nature Reviews Cancer* (Vol. 13, Issue 9, pp. 611–623). https://doi.org/10.1038/nrc3579

Parks, S. K., Cormerais, Y., Durivault, J., & Pouyssegur, J. (2017). Genetic disruption of the pH i-regulating proteins Na + /H + exchanger 1 (SLC9A1) and carbonic anhydrase 9 severely reduces growth of colon cancer cells. *Oncotarget*, *7*(8), 10225–10237. www.impactjournals.com/oncotarget

Pedersen, S. F., & Stock, C. (2013). Ion channels and transporters in cancer: Pathophysiology, regulation, and clinical potential. *Cancer Research*, *73*(6), 1658–1661. https://doi.org/10.1158/0008-5472.CAN-12-4188

Pettigrew, D. W., & Frieden, C. (1979). Binding of Regulatory Ligands to Rabbit Muscle Phosphofructokinase A MODEL FOR NUCLEOTIDE BINDING AS A FUNCTION OF TEMPERATURE AND pH. In *THE JOURNAL OF BUX.OG~CAL CHEM~~Y* (Vol. 254, Issue 6).

Putney, L. K., & Barber, D. L. (2003). Na-H Exchange-dependent Increase in Intracellular pH Times G2/M Entry and Transition. *Journal of Biological Chemistry*, *278*(45), 44645–44649. https://doi.org/10.1074/jbc.M308099200

Putney, L. K., & Barber, D. L. (2004). Expression profile of genes regulated by activity of the Na-H exchanger NHE1. *BMC Genomics*, *5*. https://doi.org/10.1186/1471-2164-5-46

Putney, L. K., Denker, S. P., & Barber, D. L. (2002). The Changing Face of the Na+/H+ Exchanger, NHE1: Structure, Regulation, and Cellular Actions. *Annu. Rev. Pharmacol. Toxicol.*, *42*, 527–552. www.annualreviews.org

Rani, Y., Kaur, K., Sharma, M., & Kalia, N. (2020). In silico analysis of SNPs in human phosphofructokinase, muscle (PFKM) gene: An apparent therapeutic target of aerobic glycolysis and cancer. *Gene Reports*, *21*. https://doi.org/10.1016/j.genrep.2020.100920

Ren, Y.-H., Liu, K.-J., Wang, M., Yu, Y.-N., Yang, K., Chen, Q., Yu, B., Wang, W., Li, Q.-W., Wang, J., Hou, Z.-Y., Fang, J.-Y., Yeh, E. T., Yang, J., & Yi, J. (2014). De-SUMOylation of FOXC2 by SENP3 promotes the epithelial-mesenchymal transition in gastric cancer cells. *Oncotarget*, *5*(16), 7093–7104. www.impactjournals.com/oncotarget/

Reshkin, S. J., Bellizzi, A., Caldeira, S., Albarani, V., Malanchi, I., Poignee, M., Alunni-Fabbroni, M., Casavola, V., & Tommasino, M. (2000). Na + /H + exchanger-dependent intracellular alkalinization is an early event in malignant transformation and plays an essential role in the development of subsequent transformation-associated phenotypes. *The FASEB Journal*, *14*(14), 2185–2197. https://doi.org/10.1096/fj.00-0029com

Respuela, P., Nikolić, M., Tan, M., Frommolt, P., Zhao, Y., Wysocka, J., & Rada-Iglesias, A. (2016). Foxd3 Promotes Exit from Naive Pluripotency through Enhancer Decommissioning and Inhibits Germline Specification. *Cell Stem Cell*, *18*(1), 118–133. https://doi.org/10.1016/j.stem.2015.09.010

Riley, T. R., Slattery, M., Abe, N., Rastogi, C., Liu, D., Mann, R. S., & Bussemaker, H. J. (2014). SELEX-seq: A method for characterizing the complete repertoire of binding site preferences for transcription factor complexes. *Methods in Molecular Biology*, *1196*, 255–278. https://doi.org/10.1007/978-1-4939-1242-1_16

Robergs, R. A., Ghiasvand, F., & Parker, D. (2004). Biochemistry of exercise-induced metabolic acidosis. *Am J Physiol Regul Integr Comp Physiol*, *287*, R502–R516. https://doi.org/10.1152/ajpregu.00114.2004.-The

Rogers, J. M., Waters, C. T., Seegar, T. C. M., Jarrett, S. M., Hallworth, A. N., Blacklow, S. C., Bulyk, M. L., Rogers, J. M., Waters, C. T., Seegar, T. C. M., Jarrett, S. M., & Hallworth, A. N. (2019). Bispecific Forkhead Transcription Factor FoxN3 Recognizes Two Distinct Motifs with Different DNA Shapes. *Molecular Cell*, *74*(2), 245-253.e6. https://doi.org/10.1016/j.molcel.2019.01.019

Romano, R., Palamaro, L., Fusco, A., Giardino, G., Gallo, V., Del Vecchio, L., & Pignata, C. (2013). FOXN1: A master regulator gene of thymic epithelial development program. *Frontiers in Immunology*, *4*. https://doi.org/10.3389/fimmu.2013.00187

Schöneberg, T., Kloos, M., Brüser, A., Kirchberger, J., & Sträter, N. (2013). Structure and allosteric regulation of eukaryotic 6-phosphofructokinases. In *Biological Chemistry* (Vol. 394, Issue 8, pp. 977–993). Walter de Gruyter GmbH. https://doi.org/10.1515/hsz-2013-0130

Schönichen, A., Webb, B. A., Jacobson, M. P., & Barber, D. L. (2013a). Considering Protonation as a Posttranslational Modification Regulating Protein Structure and Function. *Annual Review of Biophysics*, *42*(1), 289–314. https://doi.org/10.1146/annurev-biophys-050511-102349

Schönichen, A., Webb, B. A., Jacobson, M. P., & Barber, D. L. (2013b). Considering Protonation as a Posttranslational Modification Regulating Protein Structure and Function. *Annual Review of Biophysics*, *42*(1), 289–314. https://doi.org/10.1146/annurev-biophys-050511-102349

Schulte, K. W., Green, E., Wilz, A., Platten, M., & Daumke, O. (2017). Structural Basis for Aryl Hydrocarbon Receptor-Mediated Gene Activation. *Structure*, *25*(7), 1025-1033.e3. https://doi.org/10.1016/j.str.2017.05.008

Shyh-Chang, N., & Ng, H. H. (2017). The metabolic programming of stem cells. *Genes and Development*, *31*(4), 336–346. https://doi.org/10.1101/gad.293167.116

Spear, J. S., & White, K. A. (2023). Single-cell intracellular pH dynamics regulate the cell cycle by timing the G1 exit and G2 transition. *Journal of Cell Science*, *136*(10). https://doi.org/10.1242/jcs.260458

Srivastava, J., Barreiro, G., Groscurth, S., Gingras, A. R., Goult, B. T., Critchley, D. R., Kelly, M. J. S., Jacobson, M. P., & Barber, D. L. (2008). Structural model and functional significance of pH-dependent talin-actin binding for focal adhesion remodeling. *Proceedings of the*

National Academy of Sciences, *105*(38), 14436–14441. https://doi.org/10.1073/pnas.0805163105

Sun, S., Poudel, P., Alexov, E., & Li, L. (2022). Electrostatics in Computational Biophysics and Its Implications for Disease Effects. In *International Journal of Molecular Sciences* (Vol. 23, Issue 18). MDPI. https://doi.org/10.3390/ijms231810347

Swietach, P., Boedtkjer, E., & Pedersen, S. F. (2023). How protons pave the way to aggressive cancers. In *Nature Reviews Cancer*. Nature Research. https://doi.org/10.1038/s41568-023-00628-9

Szpiech, Z. A., Strauli, N. B., White, K. A., Ruiz, D. G., Jacobson, M. P., Barber, D. L., & Hernandez, R. D. (2017). Prominent features of the amino acid mutation landscape in cancer. *PLoS ONE*, *12*(8). https://doi.org/10.1371/journal.pone.0183273

Tencer, A. H., Gatchalian, J., Klein, B. J., Khan, A., Zhang, Y., Strahl, B. D., van Wely, K. H. M., & Kutateladze, T. G. (2017). A Unique pH-Dependent Recognition of Methylated Histone H3K4 by PPS and DIDO. *Structure*, *25*(10), 1530-1539.e3. https://doi.org/10.1016/j.str.2017.08.009

Toft, N. J., Axelsen, T. V., Pedersen, H. L., Mele, M., Burton, M., Balling, E., Johansen, T., Thomassen, M., Christiansen, P. M., & Boedtkjer, E. (2021). Acid-base transporters and ph dynamics in human breast carcinomas predict proliferative activity, metastasis, and survival. *ELife*, *10*. https://doi.org/10.7554/eLife.68447

Tominaga, T., Ishizaki, T., Narumiya, S., & Barber, D. L. (1998). p160ROCK mediates RhoA activation of Na-H exchange. *EMBO Journal*, *17*(16), 4712–4722. https://doi.org/10.1093/emboj/17.16.4712

Trivedi, B., & Danforth, W. H. (1966). Effect of pH on the Kinetics of Frog Muscle Phosphofructokinase. *Journal of Biological Chemistry*, *17*, 4110–4113.

Trott, O., & Olson, A. J. (2009). AutoDock Vina: Improving the speed and accuracy of docking with a new scoring function, efficient optimization, and multithreading. *Journal of Computational Chemistry*, NA-NA. https://doi.org/10.1002/jcc.21334

Tsogtbaatar, E., Landin, C., Minter-Dykhouse, K., & Folmes, C. D. L. (2020). Energy Metabolism Regulates Stem Cell Pluripotency. In *Frontiers in Cell and Developmental Biology* (Vol. 8). Frontiers Media S.A. https://doi.org/10.3389/fcell.2020.00087

Tsuber, V., Kadamov, Y., Brautigam, L., Berglund, U. W., & Helleday, T. (2017). Mutations in cancer cause gain of cysteine, histidine, and tryptophan at the expense of a net loss of arginine on the proteome level. *Biomolecules*, *7*(3). https://doi.org/10.3390/biom7030049

Ulmschneider, B., Benitez, M., Azimova, D. R., Nystul, T. G., Grillo-Hill, B. K., & Barber, D. L. (2016). Increased intracellular pH is necessary for adult epithelial and embryonic stem cell differentiation. *Journal of Cell Biology*, *215*(3), 345–355. https://doi.org/10.1083/jcb.201606042

Vo, T., Wang, S., Poon, G. M. K., & David Wilson, W. (2017). Electrostatic control of DNA intersegmental translocation by the ETS transcription factor ETV6. *Journal of Biological Chemistry*, *292*(32), 13187–13196. https://doi.org/10.1074/jbc.M117.792887

Wang, W., Xi, L., Xiong, X., Li, X., Zhang, Q., Yang, W., & Du, L. (2019). Insight into the structural stability of wild-type and histidine mutants in Pin1 by experimental and computational methods. *Scientific Reports*, *9*(1). https://doi.org/10.1038/s41598-019-44926-5

Webb, B. A., Chimenti, M., Jacobson, M. P., & Barber, D. L. (2011). Dysregulated pH: A perfect storm for cancer progression. *Nature Reviews Cancer*, *11*(9), 671–677. https://doi.org/10.1038/nrc3110

Webb, B. A., Dosey, A. M., Wittmann, T., Kollman, J. M., & Barber, D. L. (2017a). The glycolytic enzyme phosphofructokinase-1 assembles into filaments. *Journal of Cell Biology*, *216*(8), 2305–2313. https://doi.org/10.1083/jcb.201701084

Webb, B. A., Dosey, A. M., Wittmann, T., Kollman, J. M., & Barber, D. L. (2017b). *The glycolytic enzyme phosphofructokinase-1 assembles into filaments*. *216*(8), 2305–2313.

Webb, B. A., Forouhar, F., Szu, F. E., Seetharaman, J., Tong, L., & Barber, D. L. (2015a). Structures of human phosphofructokinase-1 and atomic basis of cancer-associated mutations. *Nature*, *523*(7558), 111–114. https://doi.org/10.1038/nature14405

Webb, B. A., Forouhar, F., Szu, F. E., Seetharaman, J., Tong, L., & Barber, D. L. (2015b). Structures of human phosphofructokinase-1 and atomic basis of cancer-associated mutations. *Nature*, *523*(7558), 111–114. https://doi.org/10.1038/nature14405

Webb, B. A., White, K. A., Grillo-Hill, B. K., Schönichen, A., Choi, C., & Barber, D. L. (2016). A histidine cluster in the cytoplasmic domain of the Na-H exchanger NHE1 confers pH-sensitive phospholipid binding and regulates transporter activity. *Journal of Biological Chemistry*, *291*(46), 24096–24104. https://doi.org/10.1074/jbc.M116.736215

Westermark, P., Andersson, A., & Westermark, G. T. (2011). Islet amyloid polypeptide, islet amyloid, and diabetes mellitus. In *Physiological Reviews* (Vol. 91, Issue 3, pp. 795–826). https://doi.org/10.1152/physrev.00042.2009

Whalen, S., Héron, D., Gaillon, T., Moldovan, O., Rossi, M., Devillard, F., Giuliano, F., Soares, G., Mathieu-Dramard, M., Afenjar, A., Charles, P., Mignot, C., Burglen, L., Van Maldergem, L., Piard, J., Aftimos, S., Mancini, G., Dias, P., Philip, N., … Giurgea, I. (2012). Novel comprehensive diagnostic strategy in Pitt-Hopkins syndrome: Clinical score and further delineation of the TCF4 mutational spectrum. *Human Mutation*, *33*(1), 64–72. https://doi.org/10.1002/humu.21639

White, K. A., Esquivel, M., Barber, D. L., Grillo-Hill, B. K., Peralta, J., Bui, V. N., & Chire, I. (2018). β-Catenin is a pH sensor with decreased stability at higher intracellular pH. *Journal of Cell Biology*, *217*(11), 3965–3976. https://doi.org/10.1083/jcb.201712041

White, K. A., Grillo-hill, B. K., & Barber, D. L. (2017). Cancer cell behaviors mediated by dysregulated pH dynamics at a glance. *Journal of Cell Science*, 663–669. https://doi.org/10.1242/jcs.195297

White, K. A., Kisor, K., & Barber, D. L. (2019). Intracellular pH dynamics and charge-changing somatic mutations in cancer. *Cancer and Metastasis Reviews*, *38*(1–2), 17–24. https://doi.org/10.1007/s10555-019-09791-8

White, K. A., Ruiz, D. G., Szpiech, Z. A., Strauli, N. B., Hernandez, R. D., Jacobson, M. P., & Barber, D. L. (2017). Cancer-associated arginine-to-histidine mutations confer a gain in pH sensing to mutant proteins. *Science Signaling*, *10*(495), 1–10. https://doi.org/10.1126/scisignal.aam9931

Wierstra, I. (2013). The transcription factor FOXM1 (Forkhead box M1): Proliferation-specific expression, transcription factor function, target genes, mouse models, and normal biological roles. In *Advances in Cancer Research* (Vol. 118, pp. 97–398). Academic Press Inc. https://doi.org/10.1016/B978-0-12-407173-5.00004-2

Wu, D., Potluri, N., Lu, J., Kim, Y., & Rastinejad, F. (2015). Structural integration in hypoxia-inducible factors. *Nature*, *524*(7565), 303–308. https://doi.org/10.1038/nature14883

Xi, Y. B., Zhang, K., Dai, A. B., Ji, S. R., Yao, K., & Yan, Y. Bin. (2014). Cataract-linked mutation R188H promotes βb2-crystallin aggregation and fibrillization during acid denaturation. *Biochemical and Biophysical Research Communications*, *447*(2), 244–249. https://doi.org/10.1016/j.bbrc.2014.03.119

Xiang, W., Menges, S., Schlachetzki, J. C. M., Meixner, H., Hoffmann, A. C., Schlötzer-Schrehardt, U., Becker, C. M., Winkler, J., & Klucken, J. (2015). Posttranslational modification and mutation of histidine 50 trigger alpha synuclein aggregation and toxicity. *Molecular Neurodegeneration*, *10*(1). https://doi.org/10.1186/s13024-015-0004-0

Yan, W., Nehrke, K., Choi, J., & Barber, D. L. (2001). The Nck-interacting Kinase (NIK) Phosphorylates the Na+-H + Exchanger NHE1 and Regulates NHE1 Activation by Platelet-

derived Growth Factor. *Journal of Biological Chemistry*, *276*(33), 31349–31356. https://doi.org/10.1074/jbc.M102679200

Yu, Y. C., Sohma, Y., & Hwang, T. C. (2016). On the mechanism of gating defects caused by the R117H mutation in cystic fibrosis transmembrane conductance regulator. *Journal of Physiology*, *594*(12), 3227–3244. https://doi.org/10.1113/JP271723

Zhang, Y., Li, Y., Thompson, K. N., Stoletov, K., Yuan, Q., Bera, K., Lee, S. J., Zhao, R., Kiepas, A., Wang, Y., Mistriotis, P., Serra, S. A., Lewis, J. D., Valverde, M. A., Martin, S. S., Sun, S. X., & Konstantopoulos, K. (2022). Polarized NHE1 and SWELL1 regulate migration direction, efficiency and metastasis. *Nature Communications*, *13*(1). https://doi.org/10.1038/s41467-022-33683-1

Zheng, R., & Kemps, G. (1992). *The Mechanism of ATP Inhibition of Wild Type and Mutant Phosphofructo- 1-kinase from Escherichia coli *. 8*(9), 23640–23645.

Zhou, W., Choi, M., Margineantu, D., Margaretha, L., Hesson, J., Cavanaugh, C., Blau, C. A., Horwitz, M. S., Hockenbery, D., Ware, C., & Ruohola-Baker, H. (2012). HIF1α induced switch from bivalent to exclusively glycolytic metabolism during ESC-to-EpiSC/hESC transition. *EMBO Journal*, *31*(9), 2103–2116. https://doi.org/10.1038/emboj.2012.71

Zhu, X., Chen, C., Wei, D., Xu, Y., Liang, S., Jia, W., Li, J., Qu, Y., Zhai, J., Zhang, Y., Wu, P., Hao, Q., Zhang, L., Zhang, W., Yang, X., Pan, L., Qi, R., Li, Y., Wang, F., … Zhao, Y. (2023). FOXP2 confers oncogenic effects in prostate cancer. *ELife*, *12*. https://doi.org/10.7554/ELIFE.81258

Publishing Agreement

It is the policy of the University to encourage open access and broad distribution of all theses, dissertations, and manuscripts. The Graduate Division will facilitate the distribution of UCSF theses, dissertations, and manuscripts to the UCSF Library for open access and distribution. UCSF will make such theses, dissertations, and manuscripts accessible to the public and will take reasonable steps to preserve these works in perpetuity.

I hereby grant the non-exclusive, perpetual right to The Regents of the University of California to reproduce, publicly display, distribute, preserve, and publish copies of my thesis, dissertation, or manuscript in any form or media, now existing or later derived, including access online for teaching, research, and public service purposes.

DocuSigned by:
Kyle Kisor
253EE6FB83934E1...
Author Signature

12/13/2023
Date